

LYMAN-BREAK GALAXIES

Mauro Giavalisco

*Space Telescope Science Institute, 3700 San Martin Drive, Baltimore, Maryland 21218;
email: mauro@stsci.edu*

Key Words cosmology, galaxy observations, galaxy formation, galaxy evolution, distances, redshifts

■ **Abstract** In this paper we review the properties of Lyman-break galaxies, namely starburst galaxies at high redshifts, approximately in the range $2.5 < z < 5$, identified by the colors of their far ultraviolet spectral energy distribution around the 912 Å Lyman continuum discontinuity. The properties of forming galaxies in the young universe are very important to constrain the history of galaxy evolution and the formation of the Hubble sequence, and until recently, they have remained largely unexplored. The Lyman-break technique has broken an impasse in the exploration of galaxies at high redshift that lasted for about two decades, and within a few years has yielded large and well-controlled samples of star-forming, but otherwise normal, galaxies at $z > 2.5$, including ~ 1000 spectroscopic redshifts and another few thousands of robust candidates. This dataset has allowed us an unprecedented look at fundamental properties of galaxies at 20% of the Hubble time or less. In this paper, we discuss the nature of the Lyman-break galaxies and their properties, including star-formation rate, stellar and total mass, chemical abundance, morphology, and interstellar medium (ISM) kinematics, and outline their contribution to the stellar content of the universe and their connection to the galaxies observed in the present-day universe. We also discuss what the properties of these galaxies, in particular their spatial clustering, imply about the mechanisms of galaxy formation and about the relationship between the underlying distribution of dark matter and the activity of star formation.

INTRODUCTION

The formation and evolution of galaxies, namely the sequence of events that led from the first stars that formed some time ago at very high redshifts to the diversity of the galaxy population observed in the present-day universe and to the assembly of the Hubble sequence, are among astronomy's grand questions that still await complete explanation. In part this is due to the fact that we do not know much about the nature of the dominant forms of mass and energy in the universe, other than that mass interacts with the radiation primarily through gravity and that the energy that currently would accelerate the cosmic expansion has an unknown equation of state and an unknown origin. These two primary cosmological components affect the formation of the large-scale structure of the universe and the timescale of its

evolution, including galaxies and their properties. In addition, galaxies also evolve as astrophysical systems through the conversion of gas into stars and the subsequent release of chemically enriched material by supernovae, and because we observe the cosmic structures primarily through the light of the stars that have formed in them, and because we do not understand star formation very well, we are often incapable of interpreting evidence of evolution as due to cosmology or astrophysics, with the result that we cannot constrain either. To complicate this state of affairs even further, we have long been missing empirical information on galaxies' properties at crucial epochs, primarily at high redshifts during the formation of the first structures, but also at later times when the Hubble sequence formed and galaxies diversified into their present variety.

On the bright side is the fact that we have identified gravitational instability as the most likely candidate for the primary physical process responsible for the formation of structure in the universe, at least on the scale of galaxies and clusters (Eggen et al. 1962, Sandage, et al. 1970, Peebles 1971, Press & Schechter 1974, White & Rees 1978). As a result, we have a theoretical framework that guides our investigation: Galaxies form when density perturbations in the dark matter distribution collapse under gravitational instability and when gas condenses and cools at the bottom of the potential wells of these "halos" and forms stars (White & Rees 1978). Although we do not know the nature of the mass that dominates the universe, the physics of gravity is sufficiently general that we are able to predict in simple terms for all plausible dark matter candidates how cosmic structures form, their mass spectrum, dynamics, spatial abundance, and clustering properties.

Where the major conceptual problem with galaxy formation resides is in the physics of star formation, namely how the baryonic matter formed the stars within the dark matter halos and how the properties of the latter, primarily mass, central density, and angular momentum, have affected the evolution of the former. The hydrodynamics of the gas, the role of magnetic fields, the action of feedback by the supernovae and stellar winds, the role of merging and interactions with other galaxies are the physical processes that deeply affect the activity of star formation and that are very difficult to model. Even simple models of galaxy formation and evolution generally require too large a number of free parameters and uncontrolled assumptions to result in useful predictions that can be compared with the observations.

Given that theoretical guidance is so uncertain, direct empirical information is essential in guiding the investigation, and this was recognized early (e.g., Eggen et al. 1962; Tinsley 1973a,b; Quirk & Tinsley 1973). In particular, the identification of the first galaxies that appeared in the universe was quickly identified as a fundamental step to achieve before progress could be made (Partridge & Peebles 1967a,b; Tinsley 1972a,b, 1973b; Davis & Wilkinson 1974; Meier 1976a,b). These early works promoted a searching campaign for the most distant and youngest galaxies, or primeval galaxies as they came to be generically called by the mid-1970s, which came to occupy a central role in observational extragalactic research during the following three decades, and that is still driving much of the effort at the present.

Toward the end of 1995, the frontier of galaxy redshift surveys was abruptly moved forward from $z \sim 1$ to $z \sim 4$, opening to the empirical investigation about 90% of cosmic time, and more importantly, the early phases of galaxy evolution. The observational breakthrough that made this possible was the relatively new technique (actually, a rejuvenated old idea, as we shall see later) of selecting target galaxies by means of their observed colors rather than by the more conventional flux selection. This simple method not only turned out to be very effective in targeting sources in preassigned redshift ranges, but it also proved to be surprisingly efficient, yielding large and well-controlled samples with a relatively modest investment of observing time. As a result, a wealth of high quality information on the properties of galaxies at redshifts $z > 2$, including their star-formation activity, morphology, luminosity function, spatial clustering, stellar population, and chemical enrichment was rapidly piled up, breaking an observational impasse that lasted for two decades. This progress took place over a relatively short period of time—we went from knowing of no “normal” galaxies with $z > 1$ by the end of 1995 to having samples approaching 10^3 galaxies with redshifts that reach up to $z \sim 6$ (and a plausible candidate to $z \sim 11$) by the end of the millennium. As a consequence, the full impact of the new discoveries will require additional time and work before being understood in the context of an evolutionary history of galaxies, particularly because a comparatively large gap in the observations still exists in the crucial redshift range $1 \lesssim z \lesssim 2$, where only sparse samples are available, and where the Hubble sequence likely assembled. Nevertheless, the redshift range and the region of the parameter space that the high-redshift surveys have opened are somewhat disjointed from those of previous works that it seems appropriate, now that the initial excitement of the discovery has settled down a little, to review what has been accomplished in the attempt to identify general trends and provide guidelines for future works.

In this paper we review the properties of Lyman-break galaxies (LBGs), namely of starburst, but otherwise normal, galaxies identified at high redshifts ($z > 2$) by means of the colors of their ultraviolet spectral energy distribution in proximity of the 912 Å Lyman continuum discontinuity. Thanks to the high efficiency of this Lyman-break technique (LBT), these galaxies provide the richest source of information on galaxies’ properties in the high redshift universe. This review expands those by Stern & Spinrad (1999) who discussed high-redshift galaxy searches in general, and by Ferguson et al. (2000) who discussed the Hubble Deep Field survey. It also complements the reviews by McCarthy (1993) on high-redshift radio galaxies, and by Ellis (1997) on the general “faint blue galaxy” populations. This last work in particular summarizes the status of the many faint redshift surveys that studied the evolution of galaxy populations over the redshift range $z \lesssim 1$, covering approximately the past two thirds of the age of the universe, and largely complements this paper.

Two important results emerged from the surveys around $z \sim 1$. On the one hand, they have shown that bright galaxies (e.g., $L \gtrsim 0.3L^*$) of the early and middle types of the Hubble sequence were largely in place by those epochs, with the same

structural components that characterize them today, and have moderately evolved from then to the present time (Brinchmann & Ellis 2000, McCarthy et al. 2001, Cimatti et al. 2002). The luminosity function of these galaxies was consistently found to have evolved by only a modest amount during this time, dimming by about ≈ 0.7 – 1 mag from $z \sim 1$ to the present (Steidel et al. 1994; Lilly et al. 1995; Ellis et al. 1996; Brinchmann et al. 1998; Schade et al. 1999; Cohen et al. 1999, 2000). At the same time, imaging taken by the Hubble Space Telescope (HST) confirmed that the counts of galaxies morphologically selected to be of early through mid types are characterized by modest evolution relative to the extrapolation of the present luminosity function (Schade et al. 1995, 1999; Abraham et al. 1996, 1999; Driver et al. 1995a,b; Lilly et al. 1998; Brinchmann et al. 1998). On the other hand, deep imaging with HST and spectroscopic surveys of field galaxies have provided convincing evidence that the substantial amount of evolution that is observed to have taken place in the overall galaxy population over the same cosmic time is primarily contributed by faint blue galaxies that have been identified as irregular galaxies, very similar to the later types of the Hubble sequence (Tyson 1988; Broadhurst et al. 1988; Lilly et al. 1991; Cowie et al. 1994, 1995a,b; Colless et al. 1994; Lilly et al. 1995, 1996; Glazebrook et al. 1995b; Abraham et al. 1996; Driver et al. 1995a,b, 1998; Heyl et al. 1997; Glazebrook et al. 1998; Ellis 1998; Hogg et al. 1998; Brinchmann et al. 1998; Cohen et al. 1999; Brinchmann & Ellis 2000).

Initially, it was thought that the faint blue galaxies included a population of high-redshift galaxies (e.g., $z > 2$) made very luminous, and hence easily detectable, by enhanced activity of star formation (e.g., Tyson 1988, Colless et al. 1993, Ellis 1997 and references therein). However, when the first spectroscopic surveys were carried out, it became clear that the bulk of these sources is placed at relatively modest redshifts, e.g., $\langle z \rangle \sim 0.5$ for $B \leq 24$ (Broadhurst et al. 1988, Colless et al. 1991, Lilly et al. 1991). Spectroscopic incompleteness was initially put forward as an explanation for the lack of detection of a high-redshift tail in the redshift distribution, but deeper surveys with a high degree of completeness essentially ruled out this possibility (Cowie et al. 1994, 1995a; Glazebrook et al. 1995a). Whereas the nature and evolutionary fate of the rapidly evolving faint blue population still remains unclear (Ellis 1997), the important conclusion that emerged from the observations at $z \approx 1$ is that they do not seem to be primarily responsible for the formation of the brighter and earlier members of the Hubble sequence, namely the E/S0 galaxies and the early-type spirals, because these were already formed during the same epoch when the blue galaxies were evolving very rapidly (McCarthy et al. 2001, Brinchmann & Ellis 2000, Cimatti et al. 2002). The structure and the bulk of the stellar populations of the bright galaxies, and with them the Hubble sequence, must have formed prior to $z \sim 1$, and by the mid-1990s it became clear that in order to understand how and when these systems formed, it was necessary to push the investigation to earlier epochs.

This review is organized as follows. The section titled “The Search for Primeval Galaxies” contains an historical review of the searches of star-forming galaxies at very high redshift and the ideas behind the techniques used to carry out the observations. In the section titled “The Lyman-Break Galaxy Surveys,” we illustrate

the first two major successful surveys for such sources, which have identified the largest samples to date by exploiting the information on the colors of the rest-frame UV spectral energy distribution of the candidates. In the section titled “Other UV-Selected Star-Forming Galaxies at High Redshift,” we compare the observations of these Lyman-break galaxies to those from other surveys at even higher redshift and to galaxies identified by means of their $Ly\alpha$ emission line. In the section titled “The Nature of Lyman-Break Galaxies,” we review the primary astrophysical properties of these galaxies as deduced from the current data, while in the sections “Star Formation Rates,” and “Other Starburst Galaxies at High Redshift,” we discuss the important issue of the relative contribution of Lyman-break galaxies and other early star-forming galaxies to the cosmic stellar budget. The first, still rather crude attempts to estimate elemental abundances, stellar mass and age of Lyman-break galaxies are discussed in the sections “Chemical Abundances,” and “Stellar Mass and Age,” while in the section titled “Morphology,” we review the results of the observations at high angular resolution of these sources made with the Hubble Space Telescope. In the two sections “Clustering and Large Scale Structure,” and “The Mass Spectrum,” we discuss the implications that the observed spatial clustering of Lyman-break galaxies has regarding the relationship between the visible structure and the underlying mass distribution, and the evolution of the galaxy mass spectrum. In the last section of the paper, titled “Looking at the Big Picture,” we attempt to put our current understanding of the properties of Lyman-break galaxies and other galaxies at similarly high redshift in the more general context of galaxy formation and evolution. When we need to specify a cosmological model to transform observed quantities into physical quantities we will use the cosmological model specified by $\Omega_m = 0.3$, $\Omega_\Lambda = 0.7$, $H_0 = 65 \text{ km}^{-1} \text{ Mpc}^{-1}$, which seems in good agreement with the recent observations of the cosmic microwave background fluctuations and distant supernovae (Tegmark & Zaldarriaga 2000, Turner 2001). We will point out when this assumption is critical to some conclusion. At other times, to facilitate the comparison with other works, the dependence of some derived quantities on the Hubble constant is expressed as a function of $h = H_0/(100 \text{ km s}^{-1} \text{ Mpc}^{-1})$, and it will be obvious when this occurs. Throughout the paper magnitudes are expressed in the AB scale of Oke & Gunn (1983).

THE SEARCH FOR PRIMEVAL GALAXIES

Targeted observational efforts to search for primeval galaxies started in the mid-1970s. Most of the initial work consisted of either imaging or spectroscopy at optical wavelengths that attempted to identify forming galaxies at high redshifts from their UV spectroscopic features. From the observational standpoint, two considerations provided the ground for the development of these observing strategies, namely (a) that the interstellar medium of these galaxies did not contain significant amounts of dust (as expected from very young systems), implying that their UV spectrum was characterized by little or no reddening and by an intense $Ly\alpha$ -emission line; and (b) that the same spectrum also had a very pronounced 912 Å Lyman continuum discontinuity, which is produced both in the stellar atmospheres

of massive stars and also by photoelectric absorption by neutral hydrogen in the interstellar medium.

The conceptual idea that motivated much of these works was that if the total mass of what are today bright galaxies had already assembled (although not necessarily collapsed) by the time they started to form their stars at high redshifts, then there should be a range of cosmic times when a whole population of young galaxies could be observed because of its pronounced activity of star formation. The most obvious candidates for these nascent galaxies were identified in the progenitors of the present-day spheroids, i.e., elliptical galaxies and bulges of spirals. The red spectral energy distribution and narrow dispersion of colors of these systems have been interpreted as evidence that their stellar populations are very old and, therefore, must have formed at high redshifts during a relatively short period of time and, hence, almost coevally (Baade 1958, Tinsley & Gunn 1976, Ellis et al. 1997; see also Wyse et al. 1997). One possibility is that this happened during the monolithic gravitational collapse of the whole structure, when a large fraction of the gas was converted into stars within a few free-fall timescales (Eggen et al. 1962). For systems with total mass comparable to local bright galaxies ($M \sim 10^{12} M_{\odot}$) passbands this time is of the order of $\sim 10^8$ yr, and if their whole stellar mass, $M \sim 10^{11} M_{\odot}$, formed during such a short burst, then the star-formation rates must have been very high, of the order of $\sim 10^3 M_{\odot} \text{ yr}^{-1}$. Even if observed at redshifts $z \gtrsim 3$, the nascent spheroids would appear rather luminous to optical and near-infrared (near-IR) observations, where the UV radiation is redshifted. For example, an unreddened galaxy with a star-formation rate of $10^3 M_{\odot} \text{ yr}^{-1}$ would have magnitude $\mathcal{R} = 5 \log(h) + 20.7$ in the adopted cosmology.

Partridge & Peebles (1967a,b) placed the formation of the bulk of the spheroids at very high redshifts ($10 < z < 30$), but because they assumed that the star formation occurred before they collapsed in a dissipationless “violent relaxation,” they concluded that the objects would probably appear at too low a surface brightness to be detectable with the (then) available instrumentation. The authors, however, predicted a strong Ly α emission to be present in the spectra of the galaxies, and also suggested the existence of the Lyman peak in the spectrum of these primeval galaxies as an additional possible feature to identify them. In an unpublished 1966 paper, Weymann (R. J. Weymann, unpublished manuscript) suggested that the bulk of the star formation could also take place during or after the gravitational collapse, in which case the objects would appear much more compact—even stellar—than what was initially proposed by Partridge & Peebles and therefore would have correspondingly higher surface brightness.

Meier (1976a,b) used population synthesis models to compute the expected spectra of forming galaxies, and predicted their positions in color-color diagrams (e.g., $U - B$ vs. $B - V$) at various redshifts. His models differed from the earlier ones in that they included the effects of dissipation and postulated that star formation occurs at all stages in the early assembly of a galaxy. He pointed out that by looking at their colors, one can select primeval galaxy candidates among those objects whose redshifted Lyman limit is bracketed by the two shorter wavelengths, which appear red in that color but remain blue in the other one. He also proposed

that, because primeval galaxies may occupy an extended range of redshifts, three or more filters and more than one color-color diagram are necessary if one is interested in covering the corresponding period of cosmic epochs. Although Meier's models did not include the effects of the cosmic opacity in the observed colors of distant galaxies [the paper appeared before the works by Sargent & Young on quasistellar object (QSO) absorption systems of the next decade, e.g., Sargent et al. (1980) and Young et al. (1982)], they were remarkably foreseeing, predicting redshifts, sizes, and apparent magnitudes that agree reasonably well with what was discovered 20 years later using essentially the same technique.

The first observational searches for primeval galaxies (and the first time that such a terminology was used) were conducted by Partridge (1974) and Davis & Wilkinson (1974) who, following the initial theoretical predictions by Partridge & Peebles (1967a,b), used photoelectric and photographic *BVR* photometry to look for red, extended sources with low surface brightness as young galaxy candidates, reporting no identifications. Both papers explicitly mention the possibility of a Lyman break in the spectrum of the galaxies caused by stellar atmosphere as a possible, additional identifying feature. Following these pioneering works, Koo & Kron (1980) used a charge-coupled device (CCD) and photographic slitless spectroscopy to look for Lyman-break and Ly α candidates at $z \sim 5$, also reporting no detections. It is interesting that despite the fact the idea behind the Lyman-break technique was essentially developed in its broad lines by the mid-1970s, the strategy behind the observations that began in the mid-1980s, well after these pioneering works, and lasted for a decade focused mainly on the search for redshifted Ly α emission.

The first galaxies discovered at significant redshifts were radio galaxies at $1.5 \lesssim z \lesssim 1.8$ (see the review by McCarthy 1993). These were actually found because of their strong radio luminosity, although redshift identifications were made with optical telescopes thanks to the intense UV emission lines, including the Ly α one, redshifted into the optical window (Spinrad & Djorgovski 1984a,b; Spinrad et al. 1985). After these initial discoveries, the number of radio sources identified as high-redshift galaxies steadily increased, as improved instrumentation and larger telescopes became available, and radio galaxies were identified up to redshifts as high as $z = 5.19$ (Lilly 1988; Spinrad 1989; Chambers et al. 1988, 1990; McCarthy 1991; McCarthy et al. 1990, 1991, 1992; Rawlings et al. 1990; Windhorst et al. 1991, 1992; Miley et al. 1992; Eales et al. 1993a,b; Eales & Rawlings 1993; Lacy et al. 1994; Spinrad et al. 1995; Van Breugel et al. 1999). Whereas high-redshift radio galaxies may very well be special cases of primeval galaxies, their UV-spectral energy distribution is dominated by features that are commonly observed in other types of active nuclei, such as high ionization emission lines and Ly α emission with very large equivalent width, but not in normal (i.e., without a dominant or detectable AGN activity) star-forming galaxies (Meier & Terlevich 1981, Eales & Rawlings 1990, McCarthy 1993, Dey et al. 1997, Ivison et al. 1998). Furthermore, they are very rare, with surface densities of $\sim 2 \times 10^{-3}$ radio sources per square arcmin at $S_{1.4 \text{ GHz}} = 10 \text{ mJy}$. Because the relationship between their properties and those expected from normal star-forming galaxies has not yet been clarified,

in particular including the role played by the central nucleus in the star-formation activity and how to separate its contribution from the observed spectral energy distribution (McCarthy 1993), high-redshift radio galaxies came to be regarded by most as not representative of the general case of primeval galaxies.

Searches for high-redshift galaxies with narrowband imaging tuned to redshifted Ly α emission were first carried out by Djorgovski et al. (1985). These authors targeted fields around known distant QSOs, looking for companion galaxies at the same redshift of the quasar. The idea behind this technique is that, because galaxies are clustered in space, the probability of detection is enhanced in the volumes nearby a known high-redshift galaxy, in this case, the host to the QSO. These observations indeed yielded a successful detection of a Ly α -emitting source at $z = 3.215$ around the quasar PKS1614 + 051. Another detection of a Ly α emitter at $z = 3.27$ around the gravitational lens MG 2016 + 112 was reported a year later by Schneider et al. (1986). In the following years, a few more similar detections were reported by other groups (Steidel et al. 1991, Hu & Cowie 1987). Other detections of galaxy-like objects include low surface brightness diffuse nebulosity around QSOs, which are thought to be part of the host galaxies (Heckman et al. 1991a,b). However, additional searches around 26 other QSOs by Djorgovski et al. (1987) and Hu & Cowie (1987) reported negative results, casting doubts on the effectiveness of this technique. The same strategy has also been adopted to look for companions of QSO-damped Ly α -absorption systems at high redshifts, which are thought to be caused by protogalactic disks (Wolfe et al. 1993, Wolfe & Prochaska 2000a,b). Except for a handful of detections (Macchetto et al. 1993, Giavalisco et al. 1994, Moller & Warren 1993, Francis et al. 1996, Djorgovski et al. 1996, Warren & Moller 1996, Fynbo et al. 1999, Francis et al. 2001), the results have been generally negative (Foltz et al. 1986, Smith et al. 1989, Wolfe 1989, Deharveng et al. 1990) or contradictory (Hunstead et al. 1990, Wolfe et al. 1992), or they have yielded cases where the emission has been attributed to the QSO itself more than to independent star-formation activity (Moller & Warren 1993).

Until very recently, the search for a population of Ly α -emitting star-forming galaxies at high redshifts in the field, namely conducted in inconspicuous “blank” regions of the sky as opposed to the targeted search described above, has been generally unsuccessful. A number of groups have carried out searches in the redshift interval $2 \lesssim z \lesssim 6$ by means of narrowband and long-slit spectroscopy (Pritchet & Hartwick 1990, Lowenthal et al. 1990, Djorgovski & Thompson 1992, De Propriis et al. 1993, Thompson & Djorgovski 1995, Thompson et al. 1995), reporting no detections. Selective dust obscuration has been proposed as a possible explanation for the dearth of detections, since Ly α is a resonant line and hence the optical path of the photons in IGM is largely increased by resonant scattering (Neufeld 1991). Even a modest amount of dust is sufficient, in this case, to significantly extinguish the Ly α emission (Charlot & Fall 1991, 1993). This problem does not affect searches conducted using the Balmer lines or other optical nebular lines such as [OII] and [OIII], which at the redshifts of interest are shifted to near-IR wavelengths (Thompson et al. 1994). Interestingly, however, direct near-IR searches did not result in a higher rate of detections than their optical counterparts (Pahre

& Djorgovski 1995, Thompson et al. 1996, Teplitz et al. 1998), and only a small number of candidates have been selected, a few of which are confirmed at high redshifts (Teplitz et al. 1999, Beckwith et al. 1998).

Only recently, thanks to the sensitivity afforded by the 8-m class telescopes and the large area of modern CCD arrays, deep optical narrowband surveys routinely return Ly α emitters at high redshifts, both around QSOs and in the field (Hu & McMahon 1996; Hu et al. 1996, 1998; Cowie & Hu 1998; Steidel et al. 2000; Kudritzki et al. 2000; Rhoads et al. 2000; Rhoads & Malhotra 2001; Malhotra & Rhoads 2002; Stiavelli et al. 2002). Because of their double sensitivity thresholds of flux level and equivalent width (only galaxies with a relatively large equivalent width can be detected in these surveys, no matter how bright the continuum is) and the very narrow redshift range that each filter can probe at a given time, these surveys are generally less efficient than surveys based on continuum emission. However, they nicely complement the continuum surveys in that they can reach sources with much fainter continuum luminosity, which is particularly useful to constrain the faint end of the luminosity function, which would not be otherwise accessible, and also to study large concentrations of galaxies at the same redshifts, e.g., high-redshift clusters (Steidel et al. 2000).

The Lyman-Break Technique

Another important feature in the UV spectrum of star-forming galaxies is the Lyman continuum discontinuity at 912 Å or Lyman break. The feature forms in the stellar atmosphere of massive stars as a result of the hydrogen ionization edge and is quite pronounced, with a discontinuity of an order of magnitude in the luminosity density. The break in the stellar continuum is made more pronounced by the photoelectric absorption of the interstellar HI gas, which is abundant in young galaxies (Heckman 2000), and also by intervening HI gas (Steidel et al. 1995, 1999; Madau 1995). Spectroscopy of the rest-frame far-UV continuum found direct evidence of a break in local (Leitherer et al. 1995; see also Hurwitz et al. 1997) as well as distant star-forming galaxies (Steidel et al. 2001). Finally, the UV spectrum of sources at high redshifts is also subject to additional opacity owing to line blanketing by the intervening Ly α forest that dims the continuum between 912 Å and 1216 Å by an amount that depends on redshifts, and it is a factor of ≈ 2 at $z = 3$ (e.g., Madau 1995). This effectively creates another spectroscopic feature that helps in the identification of high-redshift galaxies from color photometry.

An additional effect that contributes to shape the UV spectrum emerging from star-forming galaxies is the presence of dust, since this often accompanies intense star formation. Dust attenuates and reddens the UV-spectral energy distribution, and to make quantitative predictions of the expected colors of galaxies at high redshifts it is necessary to calculate its effects. Different from the opacity created by neutral hydrogen, reddening by dust randomly varies by large amounts from galaxy to galaxy owing to varying amounts of dust and, in general, a varying reddening curve. Interestingly, however, the integrated UV and optical light of local starburst galaxies seems characterized by its own specific reddening curve (Calzetti 1997),

which has a relatively weak dependence on wavelength, implying that only moderate reddening occurs even in relatively highly obscured galaxies. In practice, dust does not seem to introduce significant confusion between the colors of high-redshift star-forming galaxies and those of other foreground sources (e.g., elliptical galaxies). Also, the number of distant galaxies missed by commonly adopted color selection criteria because too reddened by dust is apparently small (Steidel et al. 1999, Adelberger & Steidel 2000).

The far-UV spectrum of star-forming galaxies at redshift $z > 2$ is observed at optical wavelengths, allowing surveys with ground-based telescopes and sensitive CCD detectors. Figure 1 graphically illustrates the idea behind the Lyman-break technique using a set of two colors based on three optical passbands applied to the case of galaxies at $z \sim 3$ and $z \sim 4$. The bluest filter, U and G in the two cases respectively, samples blueward of the Lyman break, the intermediate filter, G and \mathcal{R} respectively, the $\text{Ly}\alpha$ -forest region, and the reddest filter, \mathcal{R} and I respectively, the opacity-free spectrum.

It is clear that the choice of the passbands determines the redshift selection function of the survey, namely the redshift range of sensitivity. In practice, this is primarily determined by the bluest passband, which for ground-based surveys is the U one. This filter, coupled to filters such as the G and the \mathcal{R} bands, yields a redshift selection function peaked at $z \sim 3$ and approximately covering the range $2.5 \lesssim z \lesssim 3.5$. This also is the range where the technique is most sensitive, as a result of the fortuitous combination of the color distribution of foreground galaxies, (which represent the noise), the luminosity function of the targets, and the sensitivity afforded by current technology at optical wavelengths. Galaxy candidates in this redshift range, dubbed “ U -band dropouts” because they obviously appear very faint in this passband,¹ are culled from the faints counts with a yield (i.e., the rate of successfully spectroscopically confirmed high-redshift galaxies) that approaches 90% at $\mathcal{R} \sim 25.5$, and essentially no contamination by interlopers. Redder passbands return galaxies at correspondingly higher redshifts, for example B - or G -band dropouts at $z \sim 4$ and V -band dropouts at $z \sim 5$, although the efficiency decreases with redshifts and the contamination increases, e.g., $\approx 50\%$ and $\sim 20\%$, respectively for G -band dropouts at $z \sim 4$ (Steidel et al. 1999).

The first modern search for galaxies at high redshift using the Lyman-break technique was carried out by Guhathakurta et al. (1990), who took deep CCD imaging in UB_jR to identify U -band dropouts in the color-color diagram ($U - B_j$) vs. $(B_j - R)$. They identified candidates down to $B_j \sim 27$, none of which received follow-up spectroscopic observations for redshift confirmation. Based on the luminosity distribution of the candidates, they estimated that the upper limits to the fraction of the deep counts with $B_j < 26$ that is at $z > 2.5$ is $< 7\%$.

¹It has become customary to refer to Lyman-break galaxy candidates as dropouts, and specify the passband that they effectively drop out from when compared to redder bands, because of the Lyman discontinuity. Thus, $z \sim 3$ candidates are frequently cited as U -band dropouts, $z \sim 4$ candidates as B -band (or G -band) dropouts, and so on.

Steidel & Hamilton (1992, 1993) used the same technique to identify the galaxies responsible for QSO absorption systems at high redshifts. The idea behind this strategy was that if optically thick QSO absorption systems (i.e., damped systems and Lyman-limit systems) at high redshifts are caused by relatively massive galaxies (Wolfe et al. 1986, Turnshek et al. 1989, Lanzetta et al. 1991), as is the case at $z \sim 1$ (Steidel et al. 1994), once detected these can be used as templates to fine-tune a more general search. Furthermore, galaxy clustering could enhance the probability of finding galaxies in proximity to known ones. For their search they used a filter system optimized to construct colors with maximized signal-to-noise ratio, the U_nGR set shown in Figure 1, and defined a set of color selection criteria based on predictions from spectral population synthesis, including the effects of the intervening photoelectric and line blanketing absorption by neutral hydrogen (estimated from the spectra of high-redshifts QSOs). For example, they calculated that a relatively unreddened star-forming galaxy at $z \sim 3$ would be observed with colors $(U_n - G) \geq 1.6$ and $(G - R) \leq 1.2$. They applied these criteria to deep CCD imaging around two QSOs with damped Ly α absorption systems, at $z \sim 3.4$ and 3.0, and despite the very poor seeing conditions, identified a sample of 23 objects with $R \leq 25$, including the candidate damped systems, identified after subtracting the QSO PSF from the G and R images.

One of the candidates was spectroscopically confirmed at $z = 3.428$ by Giavalisco, Macchetto & Sparks et al. (1994) during the spectroscopic follow-up of a sample of Ly α -emitting candidates at $z = 3.4$ from narrowband imaging around the same QSO (Q0000-263), confirming the effectiveness of color selection in identifying galaxies at high redshift. Unfortunately, spectroscopic observations from 4-m telescopes of the other candidates were inconclusive. Giavalisco et al. (1994, unpublished manuscript) obtained significantly deeper U_nGR imaging in the same QSO field in good seeing conditions using the NTT telescope. Using the same selection criteria of Steidel & Hamilton, they obtained a new, higher quality sample of candidates (including again the confirmed galaxy and the candidate damped Ly α absorber of the QSO). Steidel et al. (1996b) expanded this sample with additional candidates obtained with the 5-m Hale telescope on Mount Palomar and followed them up with spectroscopy taken at the 10-m Keck telescope with the LRIS spectrograph (Oke et al. 1995), confirming that U -band dropouts include star-forming but otherwise normal galaxies (i.e., with no detectable AGN activity) with redshifts in the range $2.2 \lesssim z \lesssim 3.6$.

LYMAN-BREAK GALAXY SURVEYS

The Color Selection

Two major and largely complementary surveys for Lyman-break galaxies (LBGs) were started after the successful spectroscopic identification of the initial candidates by Steidel et al. (1996a,b), one conducted from the ground and the other from HST. The ground-based survey is the continuation of the discovery works

described above, which has also been expanded to galaxies at $z \sim 4$, and today it includes ~ 1000 spectroscopic redshifts and several thousands of other candidates (Steidel et al. 1999). In the following we shall refer to it as the ground-based survey. The HST survey is the Hubble Deep Field (HDF), which has been conducted during two separate observing campaigns, targeting one field in the Northern sky and the other in the Southern (Williams et al. 1996, 2000; Casertano et al. 2000), achieving the deepest multicolor images of the sky at optical wavelengths with the highest angular resolution. Designed to be sensitive to LBGs, the survey returned a sample with flux limit $V \sim 27.5$ (Madau et al. 1996, Dickinson 1998, Cristiani et al. 2000), extending the reach of the ground-based one about 2.5 mag fainter, while at the same time providing information on the morphology of the galaxies. Ferguson et al. (2000) discuss in greater detail the HDF survey and the samples of LBGs derived from it. Spectroscopic confirmation of the brightest LBG candidates of the HDF sample have been obtained by Steidel et al. (1996a) and Lowenthal et al. (1997) with the Keck telescope soon after the HDF North observations. Cristiani et al. (2000) obtained spectra of candidates from the HDF South sample with the European Southern Observatory (ESO) 8-m Very Large Telescope (VLT).

The selection of galaxies in a preassigned redshift interval by means of their broadband colors is essentially equivalent to very low resolution spectroscopy, with a resolving power $\lambda/\Delta\lambda \approx 4$. The technique, therefore, is not useful to measure the redshifts of the galaxies, which is the goal of the conceptually similar but significantly more sophisticated technique of photometric redshifts (e.g., Connolly et al. 1997, Fernandez-Soto et al. 1999), but rather to identify large numbers of candidates, distributed in the targeted redshift range according to a characteristic probability distribution function. The technique is very efficient when strong spectral features are present in the spectra of the candidates, such as in the case of the LBGs.

The candidates are selected according to their position in a color-color plane, as illustrated in Figure 1 for the cases of $z \sim 3$ and $z \sim 4$. The expected colors in a given passband set can be calculated from templates or population synthesis models of star-forming galaxies (Bruzual & Charlot 1993), under assumptions of star-formation history and dust reddening. To first approximation, young burst with no dust has a relatively steep UV spectrum, with spectral index approximately $\alpha \sim -0.5$, if the spectrum is modeled as $f_\nu \propto \lambda^{-\alpha}$, which corresponds to colors that are bluer than the flat spectrum ($\alpha = 0$). Continuous star formation has $\alpha \sim 0$, whereas a decaying burst can be very red, depending on its age. The effect of dust in the interstellar medium (ISM) of the galaxies is commonly modeled as

$$F_a(\lambda) = F_i(\lambda) \times 10^{-0.4 \times A_\lambda \times E(B-V)}, \quad (1)$$

(Calzetti 2001) where F_a and F_i are the attenuated and intrinsic spectra, respectively, the color excess $E(B-V)$ parametrizes the amount of dust, and the attenuation function A_λ describes the reddening as a wavelength-dependent attenuation. Because this function generally increases with decreasing wavelength, shorter wavelengths are selectively more attenuated than longer wavelengths. To calculate

the reddened spectrum for an assigned value of $E(B - V)$, the function A_λ is required. This is generally not known for galaxies at high redshifts and, unfortunately, rather different results are obtained using local reddening curves, such as the Galactic, the Small Magellan Cloud (SMC), the Large Magellan Cloud (LMC) ones, or the starburst attenuation function that describes the integrated extinction properties of local starburst galaxies (Calzetti 1997). Luckily, there is some evidence that the Calzetti law might also apply to starbursts at higher redshifts, including LBGs (Meurer et al. 1997, 1999; Adelberger & Steidel 2000, Pettini et al. 2000, Calzetti & Giavalisco 2001), and thus this is generally adopted for them as well, although a final test of the robustness of this assumption is still lacking. Finally, the calculation of the expected colors also includes the cosmic opacity, namely line blanketing and the photoelectric absorption of ionizing radiation by local and intervening HI gas, since the column density of the intervening gas (cosmic opacity) depends on the redshift, and it has a nonnegligible effect on the observed spectra $z \gtrsim 2$ (Madau 1995).

The dispersion of intrinsic spectral shape and dust reddening of LBGs is not known, and sets a limit to one's ability to accurately define a region of the color-color plane that selects all cases of star-forming galaxies. Furthermore, photometric errors scatter the observed colors around their intrinsic values by an amount that depends on the quality of the data and mixes them with the colors of interlopers at lower redshifts. Thus, the definition of a region to use in practice for candidate selection is somewhat arbitrary, and reflects the compromise between one's desire to include as many diverse galaxies as possible while keeping the contamination by interlopers to a minimum (Steidel et al. 1995, 1999; Madau et al. 1996; Dickinson 1998). With different passbands, the optimal color selection criteria will be different, and no definitive method has yet been established. The criteria adopted for the ground-based survey have been fine-tuned for the U_nGR and GRI photometric systems, and have also been optimized by taking advantage of the availability of large samples of spectroscopic redshifts. For candidates at $z \sim 3$ and ~ 4 (U - and G -band dropouts) of the ground-based survey, these color criteria are

$$(U_n - G) \geq 1 + (G - R); \quad (U_n - G) \geq 1.6; \quad (G - R) \leq 1.2, \quad (2)$$

and

$$(G - R) \geq 2.0; \quad (G - R) \geq 2 \times (R - I) + 1.5; \quad (R - I) \leq 0.6, \quad (3)$$

respectively. Figure 1 shows the corresponding regions in the color-color diagrams as shaded areas together with the tracks of star-forming galaxies (the UV spectrum of continuous star formation with age $T=0.1$ Gyr has been assumed) for selected amounts of dust reddening as they are placed at progressively higher redshifts. The triangles correspond to no reddening, i.e., $E(B - V) = 0$, the squares to $E(B - V) = 0.15$, the pentagons to $E(B - V) = 0.3$, and the hexagons to $E(B - V) = 0.45$. The figure also shows the colors of galactic stars, from early to late types, and for the case of G -band dropouts only, of elliptical galaxies in the

redshift range $0.5 < z < 1.6$ (no evolution assumed). Stars of the G and K types contaminate the U -band dropouts (by about 3.4% at $\mathcal{R} = 25.5$), whereas for the G -band dropouts the predominant contamination comes from early-type galaxies at intermediate redshifts ($\approx 20\%$ down to $I = 24$).

Dickinson (1998) has discussed the case of the HDF survey, for which the WFPC2 four-band photometric system U_{300} , B_{450} , V_{606} , and I_{814} has been adopted. The number of LBG candidates that have been selected by various groups varies from sample to sample depending on the adopted criteria. For example, Madau et al. (1996) defined conservative criteria in order to select $z > 2$ galaxies while avoiding significant risk of contamination from objects at lower redshifts. These criteria, however, miss some of the HDF galaxies that have been spectroscopically confirmed to have $z \gtrsim 2$ by other groups (e.g., Lowenthal et al. 1997). Using the redshift information currently available in the HDF (Steidel et al. 1996a, Lowenthal et al. 1997, Cohen et al. 1996, Cowie et al. 1996) to fine-tune the selection, Dickinson (1998) built a sample of LBGs from the HDF-N by applying criteria similar to the ground-based ones discussed above, which for the HDF filters are written as

$$(U_{300} - B_{450}) \geq 1.0 + (B_{450} - V_{606}); \quad (B_{450} - V_{606}) \leq 1.2; \quad V_{606} \leq 27 \quad (4)$$

and

$$\begin{aligned} (B_{450} - V_{606}) &> 1.5; \quad (B_{450} - V_{606}) > 1.7 \times (V_{606} - I_{814}) + 0.7 \\ (B_{450} - V_{606}) &< 3.5 \times (V_{606} - I_{814}) + 1.5; \quad (V_{606} - I_{814}) < 1.5; \quad V_{606} \leq 27.7 \end{aligned} \quad (5)$$

for the U_{300} - and B_{450} -dropouts, respectively. The first selection window successfully recovers all 25 spectroscopically confirmed LBGs in the HDF at $2 < z < 3.5$, whereas the second includes the only spectroscopically confirmed B_{450} -dropout (Dickinson 1998; see also Ferguson et al. 2000). As is the case for the ground-based samples, the dominant source of contaminants is a very small number of galactic stars, but these are easily recognized in the WFPC2 images and excluded (all obvious stars with the above colors have also already been observed spectroscopically, as it turns out).

The extensive program of spectroscopy of the LBG candidates carried out during the ground-based survey has demonstrated that the Lyman-break technique is highly efficient. Multiband imaging from 4-m class telescopes returns photometry of sufficient accuracy for color selection of candidates down to flux limits where follow-up spectroscopy with 8-m class telescopes is still practical, namely $\mathcal{R} \sim 25.5$ for U -band dropouts and $I \sim 25$ for G -band dropouts. Down to these limits the ground-based survey currently includes about 2000 U -band dropout candidates from nine different pointings in the sky with approximately 1000 secured redshifts, and about 200 G -band dropout candidates with ~ 50 secured redshifts. The surface density of candidates that satisfy Equation 2 and Equation 3 down to

these flux limits is

$$\Sigma_{U_n}(25.5) = 1.21 \pm 0.06 \text{ galaxies/arcsec}^{-2} \quad (6)$$

for the U -band dropouts and

$$\Sigma_G(25) = 0.47 \pm 0.02 \text{ galaxies/arcsec}^{-2}, \quad (7)$$

where, in both cases, the error bars reflect both the Poisson counting and the observed field-to-field variations (Steidel et al. 1999, Giavalisco & Dickinson 2001). At the flux limits reached by the HDF survey, namely $V \sim 27$ for the U -band dropouts and $I \sim$ for the B -band ones, the surface densities are

$$\Sigma_{U_{300}}(27) = 29.4 \pm 3.5 \text{ galaxies/arcsec}^{-2} \quad (8)$$

and

$$\Sigma_{B_{450}}(25) = 8.7 \pm 5 \text{ galaxies/arcsec}^{-2}, \quad (9)$$

respectively (Dickinson 1998, Giavalisco & Dickinson 2001). Of course, most of the HDF candidates are too faint for spectroscopic observations, even with the largest telescopes available.

The surface density of the ground-based samples is relatively high and well matched to the field of view and multiplexing capabilities of modern multi-object spectrographs, which makes the compilation of large samples of LBGs relatively economical in terms of telescope time. For example, by covering 1 square degree of sky, which is a relatively easy task with today's large CCD arrays, one secures ~ 4400 U -band dropouts and ~ 1700 G -band dropouts. These can be followed-up with spectroscopy in less than two dozen nights. The spectroscopic yield, namely the fraction of spectroscopic targets that are confirmed in the expected redshift range, is also high. For U -band dropouts the observed yield is $\approx 85\%$, with a $\sim 3.4\%$ contamination by galactic stars (Steidel et al. 1999) and the remainder of the targets unidentified. However, the true yield is certainly higher, because the missed identifications are invariably due to lack of S/N, very likely as the result of observational accidents such as slit misalignments or insufficient exposure time (in no case has a spectroscopically confirmed U -band dropout turned out to be an interloper). The yield of G -band dropouts is about 45%, and this is the combined result of the fact that the targets are fainter and securing the redshifts is more difficult because the relevant spectral features have now moved from the range 4500–6000 Å to 6500–7500 Å, where the sky is 1.5 to 2 times brighter. Furthermore, early-type galaxies at intermediate redshifts provide a contamination of $\approx 20\%$. Taken together with the lower surface density of candidates, this highlights the difficulty of extending the Lyman-break surveys to higher redshift intervals.

The Redshift Distribution

Figure 2 shows the redshift distribution of the spectroscopically confirmed galaxies of the ground-based survey together with the redshift distribution function

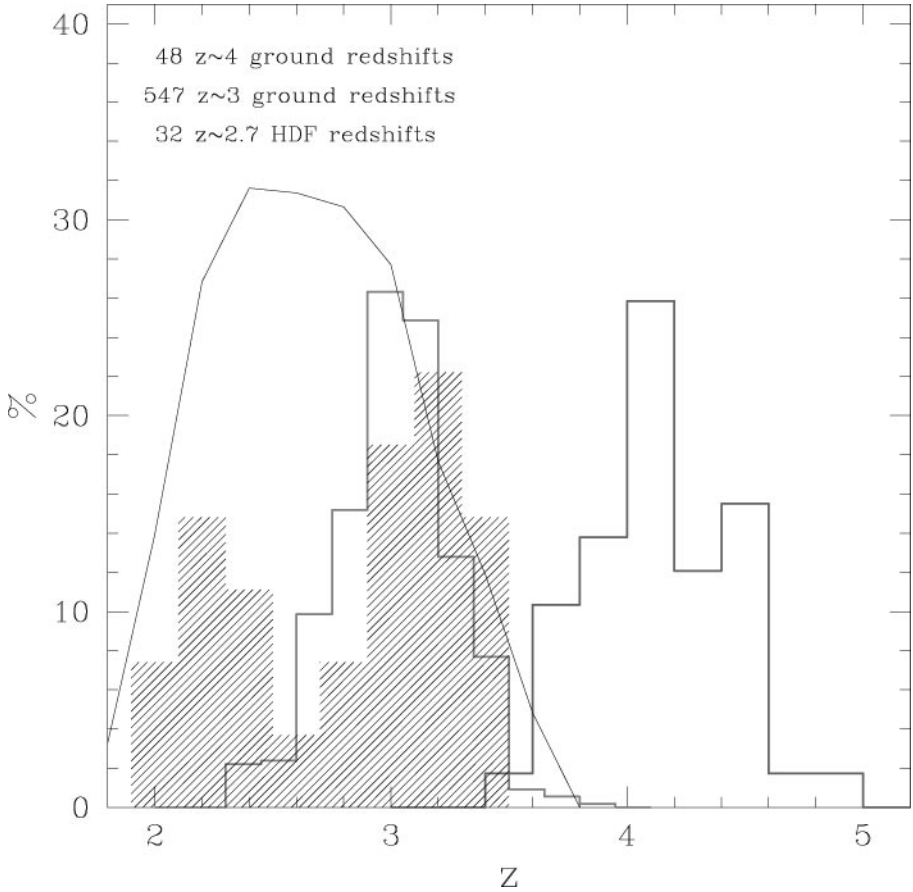


Figure 2 Histograms of the spectroscopic redshifts of U -band ($z \sim 3$) and G -band ($z \sim 4$) dropouts. The thick histograms represent galaxies from the ground-based survey, the shaded histogram galaxies from the HDF (U -band dropouts only). The thin continuous line is the expected redshift distribution function of the HDF. Only 32 redshifts of HDF U -band dropouts have been measured so far, and the histogram is clearly affected by small number statistics; nonetheless there is good agreement with the predictions. Note the wider- and lower-redshift distribution of the HDF U -band dropouts compared to their ground-based counterparts, due to the bluer and wider F300W passband compared to the U_n one.

calculated from Monte Carlo simulations of the color selection. The cutoff at low redshift of the bell-shaped curve occurs because most galaxies in that redshift region are not red enough in the bluest color [either ($U_n - G$) or ($G - \mathcal{R}$) at $z \sim 3$ or ~ 4 , respectively] to satisfy the color selection, because the Lyman break is still within in the bluest passband. The cutoff at higher redshifts occurs because

there galaxies appear redder because of the stronger line blanketing of the Lyman continuum and eventually fail to satisfy the color criteria. Figure 2 also shows the predicted redshift selection function of the HDF U -band dropouts (thin continuous curve) together with the histogram of the observed 32 spectroscopic redshifts (shaded area). As expected, because the effective wavelength of the U_{300} filter is $\approx 600 \text{ \AA}$ shorter than that of the U_n filter, the HDF redshift distribution is broader and extends to lower redshifts than the ground-based counterpart. For the B -band dropouts of the HDF sample, there is only tentative spectroscopic confirmation of only one candidate (Dickinson 1998), an object with a single line emission, which is asymmetric and has absorption on the blue side, similar to what was observed in LBGs at $z \sim 3$ and 4. This strongly suggests that the line is indeed redshifted $\text{Ly}\alpha$ emission, placing the galaxy at $z = 4.02$.

Throughout the sampled redshift windows, galaxies with excessively red UV colors remain undetected by the Lyman-break color selection criteria. This occurs preferentially at the high-redshift end because the stronger line blanketing and the fact that the galaxies appear fainter both reduce the useful color dynamic range. In other words, the distribution of the intrinsic colors of the detected galaxies is bluer at the higher end of the redshift distribution. Red UV colors are the result of either reddening by dust or of an aging burst or both, and it is of great interest to estimate how many of such red galaxies are being missed by the surveys. Steidel et al. (1999) and Adelberger & Steidel (2000) used Monte Carlo simulations to estimate the magnitude of the selection effect against red LBGs as a function of redshift in the ground-based survey, and they concluded that such galaxies are actually intrinsically rare. For example, star-forming galaxies with dust reddening as large as $0.3 < E(B - V) < 0.45$ could be detected by the survey if they were present, but they have never been observed. Galaxies with very red colors have been detected by near-IR surveys (McCarthy et al. 2001), but their redshift distribution is not yet constrained, although at bright magnitudes it does not seem to overlap with that of the LBGs. For example, Cimatti et al. 2002 showed that about half of spectroscopically identified galaxies with $R - K < 5$ down to $K \sim 19.5$ are very dusty star-forming galaxies at $0.6 < z < 1.6$, with the other half being elliptical galaxies at the same redshifts. However, because no rest-frame UV spectra of these dusty starbursts have been recorded, it is not clear whether they would be observed as LBGs if they were placed at $z \sim 3$.

With large spectroscopic samples available, Steidel et al. (1999) estimated the luminosity functions of LBGs at $z \sim 3$ and ~ 4 from the ground-based survey, and found that they agree very well, both in shape and in normalization, over the common range of absolute luminosity. This is shown in Figure 3, where for simplicity the luminosity functions are computed in the Einstein de Sitter cosmology (with $H_0 = 50 \text{ km}^{-1} \text{ Mpc}^{-1}$), although the agreement is insensitive to the choice of the world model. This shows that, at least at the relatively bright luminosity probed from the ground, there is no evidence of evolution in the LBG population over this redshift interval contrary to claims based on the fainter and much smaller HDF sample alone (Madau et al. 1996, 1998; Pozzetti et al. 1998).

Unfortunately, because of the limited number of spectroscopic redshifts available for the HDF sample, it is not possible to estimate its luminosity function in the same way as it is done from the ground. Note that, to first approximation, the distribution of apparent magnitude of LBGs can be used as a proxy for the luminosity function because the redshift distribution function is rather peaked around the average redshift of the survey (both at $z \sim 3$ and ~ 4), and thus the dispersion of luminosity distance of galaxies with given apparent magnitude is relatively small. Thus, in a given bin of apparent magnitude, the difference in absolute luminosity between a galaxy placed at either end of the redshift distribution function and one placed at the average redshift is $\sim 50\%$, and the apparent magnitude can be used to trace the absolute magnitude.

A luminosity function constructed in this way (for simplicity, plotted as a function of apparent magnitude) and including both the ground-based and HDF data, is plotted in Figure 3, *right*. The top panel shows the U -band dropouts;² there is very good consistency between the ground-based and the HDF data in the range of overlapping luminosity, and a Schechter function (Schechter 1976) provides a good model of the data (the best fit and its parameters are also shown in the figure). The faint end slope is significantly steeper than that of the optical luminosity function of the local mix of galaxies, and similar to that of the luminosity function of local and moderate redshift late-type and irregular galaxies (Folkes et al. 1999), UV-selected galaxies (Sullivan et al. 2000), and $H\alpha$ -selected galaxies (Sullivan et al. 2000, Tresse & Maddox 1998, Gallego et al. 1995). This is consistent with the general trend that star-forming galaxies and galaxies of later types (at any redshift) have a steeper slope. The characteristic luminosity m^* , $\mathcal{R} = 24.5$, is a relatively faint apparent magnitude, but at $z=3$ it corresponds to an absolute luminosity at $\lambda = 1700$ of $M = -21.2$. The characteristic volume density $\phi^* = 1.6 \times 10^{-2} h^3 \text{ Mpc}^{-3}$ directly compares with that of the K -band local luminosity function, $\phi_K^* = 1.08 \times 10^{-2}$ (Cole et al. 2001), showing that the volume density of LBGs is similar to that of present-day galaxies. Note that the cosmic volume probed by the $z=3$ and $z=4$ surveys is very large. For example, at $z=3$ the width of the redshift distribution function corresponds to $2600 h^{-3} \text{ Mpc}^3$ per square arcmin, and a survey that covers 1 square degree of sky probes a volume of $9.4 \times 10^6 h^{-3} \text{ Mpc}^3$, namely $1.5 \times 10^5 (\phi^*)^{-1}$.

The luminosity function of the G - and B -band dropouts at $z \sim 4$ is shown in the bottom panel. In this case, it is difficult to assess the consistency between the ground-based data and the HDF because there is very little overlap between the ranges of luminosities spanned by the two samples (only a single HDF B -band dropout is bright enough to be included in the ground-based sample); however, the data suggest at least a broad consistency. The $z = 4$ data are not good enough for a meaningful fit to the Schechter function; however, it is possible to compare them

²The U_{300} sample from the HDF has been put onto the same magnitude scale of the U_n sample using the approximation $\mathcal{R} \sim (V_{606} + I_{814})/2$ (Steidel et al. 1996a), and all the HDF magnitudes have been made fainter by the amount $\Delta m = 0.25$ to account for its smaller mean redshift ($\bar{z} \sim 2.6$ vs. $\bar{z} \sim 3$).

to the $z = 3$ fit by redshifting m^* by the relative distance modulus and by adjusting ϕ^* to take into account the slight difference in the cosmic volume probed by the $z = 3$ and $z = 4$ selection criteria. This “redshifted” luminosity function matches the $z = 4$ data points at the bright end fairly well, although it seems to overpredict the number of fainter HDF galaxies by about a factor of two, apparently implying a luminosity function with a shallower slope than at $z \sim 3$. Steidel et al. (1999) suggest that this likely is an effect of the small size of the HDF sample, and consequently, of the large sample variance due to strong spatial clustering (more on this later). In conclusion, there is no evidence of evolution between $z \sim 3$ and $z \sim 4$, and in fact, the null hypothesis that there is no evolution cannot be rejected with confidence with the current data.

OTHER UV-SELECTED STAR-FORMING GALAXIES AT HIGH REDSHIFT

Lyman-Break Galaxies at $z > 4$

A number of groups have identified LBGs at redshifts $z > 4$, mostly selecting them from the HDF, but the numbers are too small to study them with the same detail as was done at $z = 3$ and 4. For some candidates there are tentative spectroscopic confirmations, although almost all spectra have either low S/N or show only one emission line to securely confirm the redshifts.

Spinrad et al. (1998) obtained Keck spectra for two faint V -band dropouts selected from the HDF with $V_{606} = 28.1$ and $I_{814} = 25.6$. The galaxies had been previously identified by Fernandez-Soto et al. (1999), who measured photometric redshifts $z_{ph} = 5.28$ for both of them. The Keck spectra show a relatively sharp and pronounced discontinuity in otherwise blue, featureless continua, similar to what was observed in other LBGs at $z \sim 3$ and 4, consistent with both galaxies being at $z = 5.34 \pm 0.01$.

Weymann et al. (1998) obtained a Keck spectrum of another V -band dropout from the HDF. As in the other case, the object had been previously selected by Lanzetta et al. (1998) as a candidate, with an estimated photometric redshift of $z_{ph} = 6.8$. The Keck spectrum shows a single emission line that, if interpreted as $\text{Ly}\alpha$, places the galaxy at $z = 5.60$. As is often the case, the line profile is asymmetric, with clear evidence of absorption on the blue side, supporting the redshift interpretation.

Combining their deep HST Near Infrared Camera and Multi-Object Spectrometer (NICMOS) photometry of the HDF in J and H with the existing WFPC2 optical data, Dickinson et al. (2000) reported the detection of a J -band dropout. The optical through near-IR colors of this object (in the observed frame) can be matched by those of a dusty galaxy at $z \gtrsim 2$, by those of an old elliptical galaxy at $z \gtrsim 3$, or by an object at $z \gtrsim 10$ where the cosmic opacity has suppressed the light observed shortward of $1.1 \mu\text{m}$.

A number of other spectroscopic observations of dropout candidates at $z > 4$, selected either from the HDF or other ground-based surveys, have been reported

in the past few years, although most remain unpublished at the time of this writing (see Stern & Spinrad 1999).

Other galaxies or galaxy candidates at $z > 4$ have been identified from the putative Ly α emission by means of narrowband imaging (Hu et al. 1998, 1999; Thommes et al. 1998), serendipitous long-slit spectroscopy (Dey et al. 1998, Hu et al. 1998) or slitless spectroscopy from HST (Chen et al. 1999). If confirmed, the latter discovery would hold the record of the most distant galaxy, with a probable redshift of $z = 6.68$ (based on a spectrum with a single emission line), although recent observations cast doubt on this identification (Chen et al. 2000).

Ly α Galaxies

High-redshift galaxies identified by the strength of their Ly α emission are currently routinely detected thanks to the combination of telescopes with larger aperture and wide-field detector arrays, including cases with redshift as high as $z \sim 5.7$. The recent surveys mostly consist of narrow-band imaging (Cowie & Hu 1998; Hu et al. 1998, 1999; Thommes et al. 1998; Kudritzki et al. 2000; Steidel et al. 2000; Rhoads et al. 2000; Rhoads & Malhotra 2001; Malhotra & Rhoads 2002; Stiavelli et al. 2002), but serendipitous detections with long-slit spectroscopy (Pascarelle et al. 1996a, 1998; Dey et al. 1998, Hu et al. 1998) have also been reported. These galaxies are similar to the LBGs in that they also are characterized by a high UV luminosity that is relatively unobscured by dust, although the proportions of Ly α and continuum emission might differ. The selection function of narrow-band surveys, which cover a much narrower redshift range than continuum-selected surveys, results from a relatively complex combination of equivalent width sensitivity and flux sensitivity, and only the fraction of galaxies with a relatively large equivalent width, e.g., rest-frame $W_\alpha \gtrsim 20 \text{ \AA}$, can be detected and included in the samples. The distribution of Ly α equivalent width of LBGs (Steidel et al. 2000, Shapley et al. 2001), which are selected independently of their Ly α emission, shows that down to the flux limit of the ground-based survey this fraction is small. Therefore, narrow-band surveys miss a large fraction of the galaxies that are identified by the continuum emission. However, they are sensitive to galaxies with fainter continua than LBGs, provided that they have large enough Ly α emission, and in this sense, they provide a nice complement to continuum-selected surveys. Furthermore, they become competitive with continuum-selected ones at very high redshifts (e.g., $z > 5$), where the galaxies are faint and the continuum selection is inefficient. Even at lower redshifts, they are also very useful to map the spatial distribution of galaxies in narrow redshift intervals, e.g., where large concentrations of galaxies have already been identified. In such cases, the Ly α selection allows one to build large samples that would be much more expensive (in terms of telescope time) or even impossible to collect with the Lyman-break technique.

Pascarelle et al. (1996a, 1998), Francis et al. (1997), and Campos et al. (1999) discovered large concentrations of Ly α emitters at $z \sim 2.4$, possibly protogroups or clusters, with narrowband imaging. Steidel et al. (2000) carried out deep Ly α narrow-band imaging of a large concentration of LBGs at $z \sim 3.1$ discovered along

the line of sight of one of the ground-based survey fields (Steidel et al. 1998), possibly a protocluster or supercluster. The Ly α selection returned both galaxies that were previously identified as LBGs as well as galaxies that were not, because their continuum is too faint. Based on the luminosity distribution of the Ly α sample, they suggested LBGs and Ly α galaxies belong to a similar population, although it is possible that at fainter continuum magnitudes the Ly α emission is intrinsically larger than that observed in LBGs. Kudritzki et al. (2000) probed similar redshifts, and Cowie & Hu (1998), and Hu et al. (1998) also extended the search to $z \sim 4.5$. Both these teams observed that the Ly α emitters seem to contribute comparable amounts to the cosmic star formation at their redshifts as LBGs, and concluded that Ly α searches are better suited to study faint, young, and relatively dust-free star-forming galaxies at $z \gtrsim 4$, where color selection becomes progressively more difficult.

Hu et al. (1998) report the detection of galaxies with very large equivalent width ($W_\alpha \gg 100 \text{ \AA}$ rest-frame) and continua too faint to be detected by current continuum searches (except the HDF, which, however, covers too little an area to be effective). Rhoads et al. (2000) and Rhoads & Malhotra (2001) also find large numbers of similar objects. These Ly α galaxies with large equivalent width are very rare in LBG samples at $z \sim 3$ (e.g., Steidel et al. 2000, Shapley et al. 2001) and perhaps even at $z \sim 4$ (Steidel et al. 1999), possibly because their continua are too faint. The Ly α samples, however, seem to include too few galaxies with small W_α , i.e., in the 50–100 \AA range (rest-frame), which represent a considerable fraction of the equivalent width distribution of LBGs (Steidel et al. 2000, Shapley et al. 2001), even if current narrowband surveys are sensitive to these objects. Malhotra & Rhoads (2002) suggest that these very large Ly α equivalent widths occur during the early stages of evolution of starburst galaxies, when the first generations of massive stars have, essentially, null metal content and, possibly, also a top-heavy Initial Mass Function (IMF). Unfortunately, there is currently too little spectroscopy of narrow-band-selected galaxies to constrain their nature with confidence and in particular, to estimate the contribution of AGN. This situation should improve very rapidly, however.

THE NATURE OF LYMAN-BREAK GALAXIES

Starburst Galaxies at $\sim 10\%$ of the Hubble Time

Since the first spectroscopic identifications, it became immediately clear that the sources identified by the color selection criteria discussed above are starburst galaxies (Steidel et al. 1996a,b; Lowenthal et al. 1997; Trager et al. 1997). At the redshifts of the LBGs, $z \geq 2$, the far-UV spectrum is observed at optical wavelengths, and sensitive CCD ground-based spectroscopy from large-aperture telescopes reveals a great deal about the nature of these galaxies, even at the relatively low spectral resolution used for redshift identification. This is illustrated in Figure 4, where examples of spectra of U -band dropouts obtained with the Keck telescope and the Low Resolution Imaging Spectrometer (LRIS) instrument (Oke et al. 1995)

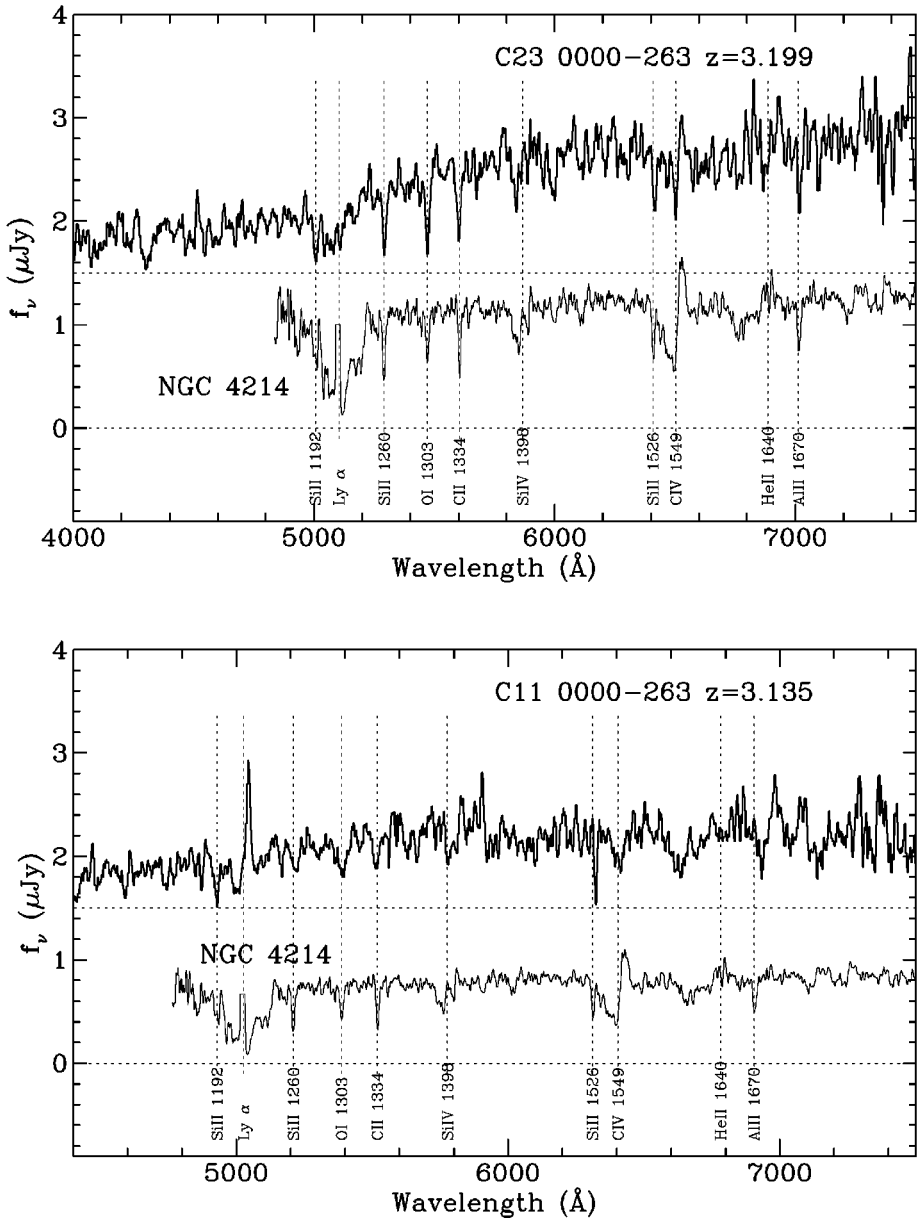


Figure 4 Examples of spectra of Lyman-break galaxies compared to the starburst galaxy NGC 4214. The high-redshift spectra have been obtained with the Keck telescope and the LRIS spectrograph; the spectrum of NGC 4214 has been recorded by Leitherer et al. (1996) with HST and the GHRS. The spectra are shown in the observer's frame, at the indicated redshift. The figure illustrates the similarity of the spectra of Lyman-break galaxies with that of local starburst galaxies, but also the diversity found among the LBG spectra (reproduced from Steidel et al. 1996b).

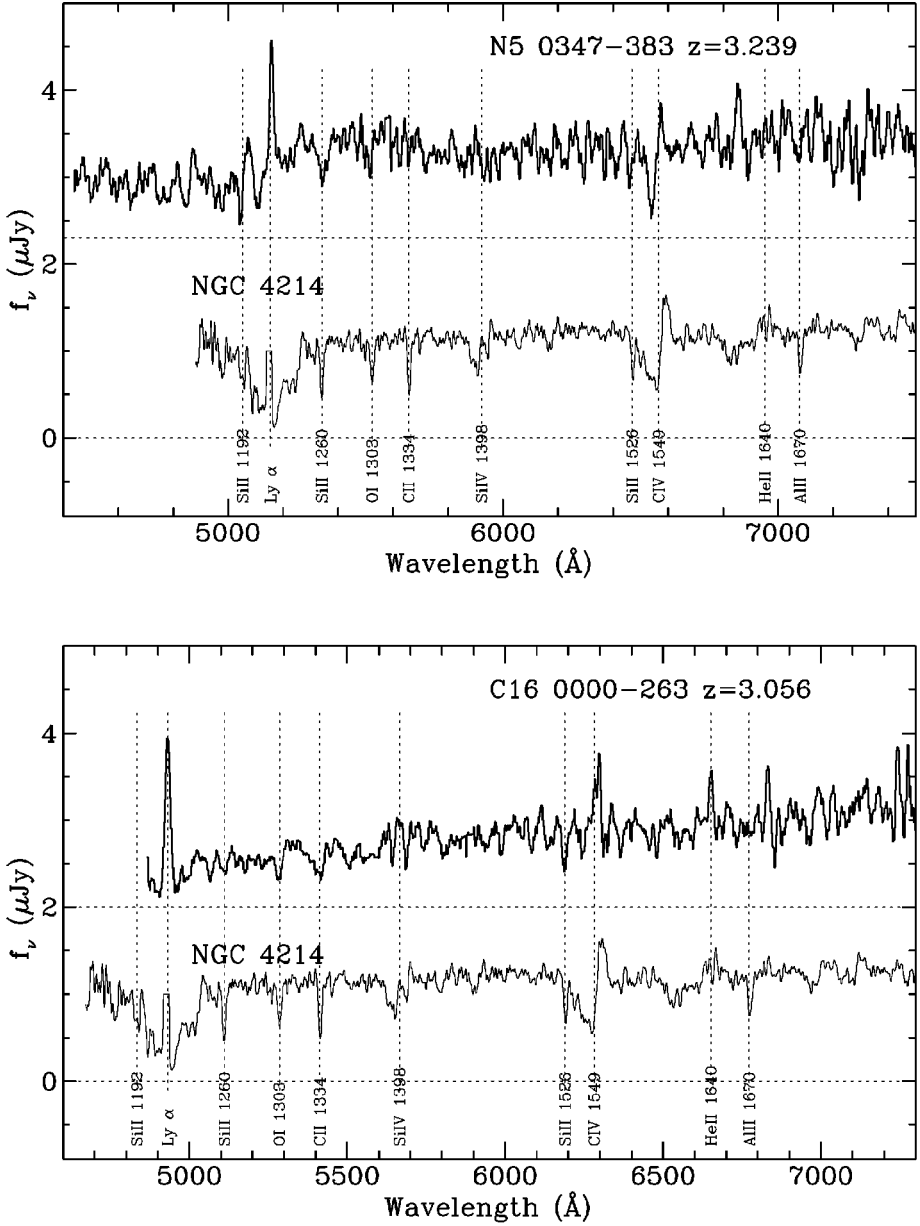


Figure 4 (Continued)

are compared to the local starburst galaxy NGC 4214 observed with HST and the GHRS spectrograph (Leitherer et al. 1996).

The similarity between the spectra of the LBGs and that of local galaxies is striking. Both have strong blue continua, denoting production of massive young stars of the O and B types. Similar to their local counterparts, the LBG spectra generally are redder than the predictions for dust-free spectral energy distributions of star formation from stellar population synthesis (Bruzual & Charlot 1993, Leitherer & Heckman 1995), with no obvious indications that the high-redshift galaxies are characterized by bluer spectra. Despite the copious production of ionizing photons, the Ly α properties of LBGs (Steidel et al. 2000) are also rather similar to those of nearby star-forming galaxies (e.g., Giavalisco et al. 1996a), and the distribution of rest-frame equivalent width is symmetrical around the median value $W_{\alpha,median} = 0$ (Steidel et al. 2000, Shapley et al. 2001). When the line is observed in emission, the equivalent width is typically much weaker (usually by factors of more than 10) than the ionization-bound, dust-free expectations, $W_{\alpha} \sim 150 \text{ \AA}$, for continuous star formation (Charlot & Fall 1991, 1993). Only a rather small fraction of the galaxies have large equivalent widths, e.g., larger than 20 \AA , even if the color selection introduces no bias against objects with large equivalent width, which generally also have unobscured UV continua. If such objects exist in large numbers, they must have continua significantly fainter than the flux limit of the LBG samples, $\mathcal{R} = 25.5$.

Another characteristic of the LBGs' UV spectra in common with local starbursts is the presence of strong interstellar absorption lines due to low-ionization stages of C, O, Si, and Al, and of prominent high-ionization stellar lines of He II, C IV, Si IV, and N V. These stellar and interstellar lines are actually the most distinctive spectral features, which make confirmation of LBG candidates with optical spectroscopy relatively easy and economical in terms of telescope time, given the sensitivity and multiplexing capability of current instrumentation, even in the absence of strong emission lines such as Ly α . The interstellar lines, which can have rest-frame equivalent widths as large as $W_0 \simeq 2\text{--}3.5 \text{ \AA}$, are evidence that the interstellar medium of these galaxies has obviously undergone some degree of chemical enrichment. However, they cannot be used, at least in these low-resolution spectra, to measure the metallicity, because they are undoubtedly heavily saturated, and hence are much more sensitive to the kinematics of the gas than to its column density. The velocity widths are generally large, with FWHM in the range $\geq 400\text{--}700 \text{ km s}^{-1}$, implying velocity fields of the order of $\sigma_v = 200\text{--}400 \text{ km s}^{-1}$, very likely large-scale outflows driven by the release of mechanical energy of supernovae and winds from massive stars (Pettini et al. 2001). Evidence of such large outflows, which are common in starburst galaxies (Heckman 1996), also comes from the relative kinematics of interstellar absorption lines, Ly α emission lines, and optical nebular emission lines of the HII gas (observed with near-IR spectroscopy), which suggests the presence of large-scale gas shells expanding with velocity as high as $\sim 600 \text{ km s}^{-1}$ (Pettini et al. 2001, Frye et al. 2002).

Despite the morphological similarity of the spectra, the UV emission of the LBGs is much more intense than that of the local star-forming regions. For example,

an L^* LBG at $z \sim 3$, observed with apparent magnitude $\mathcal{R} = 24.5$, has $M_{1700} \sim -21.2$ (Steidel et al. 1999). This corresponds to a continuum specific luminosity at 1700 Å of $L_{1700} = 5.5 \times 10^{40} h^{-2} \text{ erg s}^{-1} \text{ Å}^{-1}$, approximately 1500 times higher than the knot of star formation in NGC 4214 and ≈ 100 times higher than the brightest such knots seen in nearby starburst galaxies. Assuming an initial mass function (IMF) with a Salpeter index $x = 1.33$ and extending from $0.1 M_{\odot}$ to $100 M_{\odot}$, the far-UV continuum of the typical LBG is produced by the equivalent of $\approx 6 \times 10^5$ O5 stars. Despite this difference in scale, however, the dominant characteristics of the far-UV spectra in common with both low-redshift and high-redshift starbursts seem to point to a similarity of physical conditions in the regions of star formation.

Figure 4 is also illustrative of the diversity of properties encountered in the LBG spectra (Steidel et al. 1999; see also Pettini et al. 2000), most noticeably the strength and morphology of the Ly α line, of the interstellar absorption lines of Si II, O I, and C II, and of the P-Cygn C IV features. For example, the spectrum on the top panel does not have Ly α in emission and shows a broad absorption feature around the wavelength of the line. It also has relatively narrow interstellar absorption lines of Si II, O I, and C II, and a relatively well detected C IV feature. The spectrum in the bottom of the figure has Ly α in emission together with much broader interstellar lines, and a different morphology of the absorption component of the C IV feature. In general, while there is a large variety in the strengths of the lines that are predominantly of stellar origin (C IV $\lambda 1549$, Si IV $\lambda\lambda 1393, 1402$, and He II $\lambda 1640$), these features seem to be weaker than in present-day starbursts. Steidel et al. (1996b) suggest that this is probably an abundance effect; these lines are formed predominantly in the winds of massive stars, where both mass-loss rates and wind terminal velocities are known to depend sensitively on metallicity (e.g., Walborn et al. 1995).

The optical spectra of LBGs have recently been studied with near-IR spectroscopy (Pettini et al. 1998, 2000; Kobulnicky & Koo; Teplitz et al. 2000a,b). The observations targeted the optical nebular emission lines of [OII] $\lambda 3727$, H β , and [OIII] $\lambda\lambda 4959, 5007$, because the continuum emission generally is too faint to be detected with useful signal-to-noise ratio. As expected from starburst galaxies, these features are generally strong and although narrow, they have been resolved in every case, raising the possibility of deriving dynamical information on the galaxies. Despite the still relatively modest signal-to-noise ratios, these features provide a wealth of information on the activity of star formation, extinction, metallicity, and kinematics of the gas in LBGs, as we discuss in the next sections.

STAR-FORMATION RATES

An obvious important issue in understanding both the evolution of the individual galaxies and their contribution to the cosmic stellar mass budget is the star-formation activity of the LBGs. In the absence of dust obscuration, the far-UV

luminosity of star-forming galaxies, which is dominated by the integrated light of the short-lived massive stars (O and early B types) formed in the burst, is simply proportional to the instantaneous rate of star formation (Kennicutt 1998). The conversion between UV luminosity density and star-formation rate can be computed from population synthesis models (e.g., Bruzual & Charlot 1993), and the optimal wavelength range to derive the constant of proportionality is $1250 \lesssim \lambda \lesssim 2500$, most of which is covered by the LBG surveys. Calibrations have been derived by several authors (Buat 1989, Deharveng et al. 1994, Leitherer & Heckman 1995, Meurer et al. 1995, Cowie et al. 1997, Madau et al. 1998), and the results agree with each other within a factor of ≈ 2 , when converted to a common reference wavelength and initial mass function. The difference between the various derivations reflects differences in the used stellar libraries and/or different assumptions about the timescale of the star formation, namely if longer or comparable to the lifetime of O and B stars. Assuming Salpeter's (1955) IMF with mass limits between 0.1 and $100 M_{\odot}$, and that the duration of the star-formation activity is significantly longer than the lifetime of the stars, i.e., $T > 5 \times 10^7$ yr (continuous star-formation approximation), Madau et al. (1998) derived the relationship:

$$\text{SFR } M_{\odot} \text{ yr}^{-1} = 1.4 \times 10^{-28} L_{\nu}(\lambda_{1500}), \quad (10)$$

where L_{ν} is the luminosity density in units of $\text{erg s}^{-1} \text{ Hz}^{-1}$. The luminosity of an instantaneous burst is larger, and use of this relationship in such cases would overestimate the star-formation rate.

Unfortunately, the direct UV emission from the forming stars is seldom observed, because they are often embedded in an ISM rich in dust, which reprocesses the UV radiation and re-radiates it over a huge wavelength range, from the UV itself to radio wavelengths (Calzetti 2001, Adelberger & Steidel 2000). For example, in virtually all starburst galaxies in the local universe, most of the energy powered by star formation emerges at far-IR wavelengths as thermal emission by dust. Thus, to measure the star-formation rate one is left with the options of either carrying out the observations in the far-IR or correcting the UV data for dust obscuration. The former is a very hard task, because far-IR observations are comparatively much more difficult and less sensitive than optical ones. Adelberger & Steidel (2000) suggest that as far as the detection of the galaxies is concerned, targeting the UV emission from star-forming galaxies is still the most economical and efficient way to detect them, despite the large fraction of energy destroyed by dust and the uncertainty involved in estimating it.

In general, it is very difficult to infer the amount of dust obscuration from the observed UV-spectral energy distribution, because different geometries of the dust spatial distribution result in different observed colors for the same amount of dust and the same intrinsic spectrum. Luckily, the case of UV-bright starburst galaxies is simpler because these systems show a tight correlation between the slope of the UV continuum and the total dust obscuration as traced by the ratio of the far-IR to bolometric luminosity (Calzetti 1997, Meurer et al. 1999). This property allows one

to calibrate the observed UV colors in terms of dust obscuration and hence estimate the intrinsic UV luminosity and the star-formation rate. However, Ultra Luminous Infrared Galaxies (ULIRGs) markedly deviate from such a relationship (Goldader et al. 2002), whereas galaxies with infrared properties intermediate between the ULIRGs, and the UV-bright ones (Alonso-Herrero et al. 2001, Forster et al. 2001) exhibit a less pronounced deviation. The behavior of LBGs is not currently known.

The simple behavior of the dust opacity in starburst galaxies is very likely due to the combined effects of the specific geometry of the dust that forms in the starburst environment and of the duration of the burst. The diffuse nature of the starbursts in UV-bright galaxies favors the onset of large-scale galactic winds that are conducive to the formation of a foreground screen of dust, which apparently is the main factor behind the proportionality between UV-spectral index and dust obscuration (Calzetti 1997, 2001) observed in these systems. Diffuse starbursts also seem to last significantly longer than the lifetime of O and B stars (Calzetti 1997, Tremonti et al. 2001), implying a relatively narrow dispersion of intrinsic UV-spectral energy distribution, namely that of continuous star formation. These conditions are not verified in the case of the ULIRGs, where the high concentration of gas and dust required to fuel large nuclear starbursts favors a combination of a clumpy mixed and foreground distribution of dust and stars as well as intense bursts of short duration (Genzel et al. 1998).

The UV and optical spectral energy distribution and far-IR emission (Barger et al. 1999b, Chapman et al. 2000, Van der Werf et al. 2001) of LBGs suggest that their dust obscuration properties are similar to those of UV-bright starburst galaxies (Adelberger & Steidel 2000, Calzetti 2001). In this case, the starburst attenuation law can be used to infer the reddening and obscuration correction. Figure 5 shows the $G - \mathcal{R}$ colors of LBGs as a function of redshift together with the predicted colors for continuous star formation ($\tau = 0.1$ Gyr) for selected values of $E(B - V)$ and for an unreddened burst of star formation ($\tau = 0.001$ Gyr). For a given redshift, almost all LBGs are redder than the unobscured burst, which represents the blue envelope of the distribution, and most of them are redder than the unobscured continuous star formation, with the median value in the range $0.15 \lesssim E(B - V) \lesssim 0.2$. For reference, using the starburst attenuation law, this corresponds to an attenuation at 1700 \AA (the rest-frame wavelength that corresponds to the \mathcal{R} band at $z = 3$) in the range $4 < C(1700) < 7$, where $C(\lambda) = 10^{0.4 \times A_\lambda \times E(B - V)}$. Note that a number of galaxies have colors that appear artificially bluer because of the presence of Ly α emission with large equivalent width. Also, selection effects bias the color distribution toward bluer values, implying that the fraction of redder galaxies, either because intrinsically redder or because at higher redshift, is higher than observed, although this effect is probably small (Steidel et al. 1999).

Figure 6 compares the star-formation rates derived from the observed UV fluxes (heavily shaded histogram) with those corrected from dust obscuration in two cases. In the first case (medium-shaded histogram), the correction is calculated from the observed UV colors under the assumption of the starburst attenuation law and that the unattenuated spectrum is that of continuous

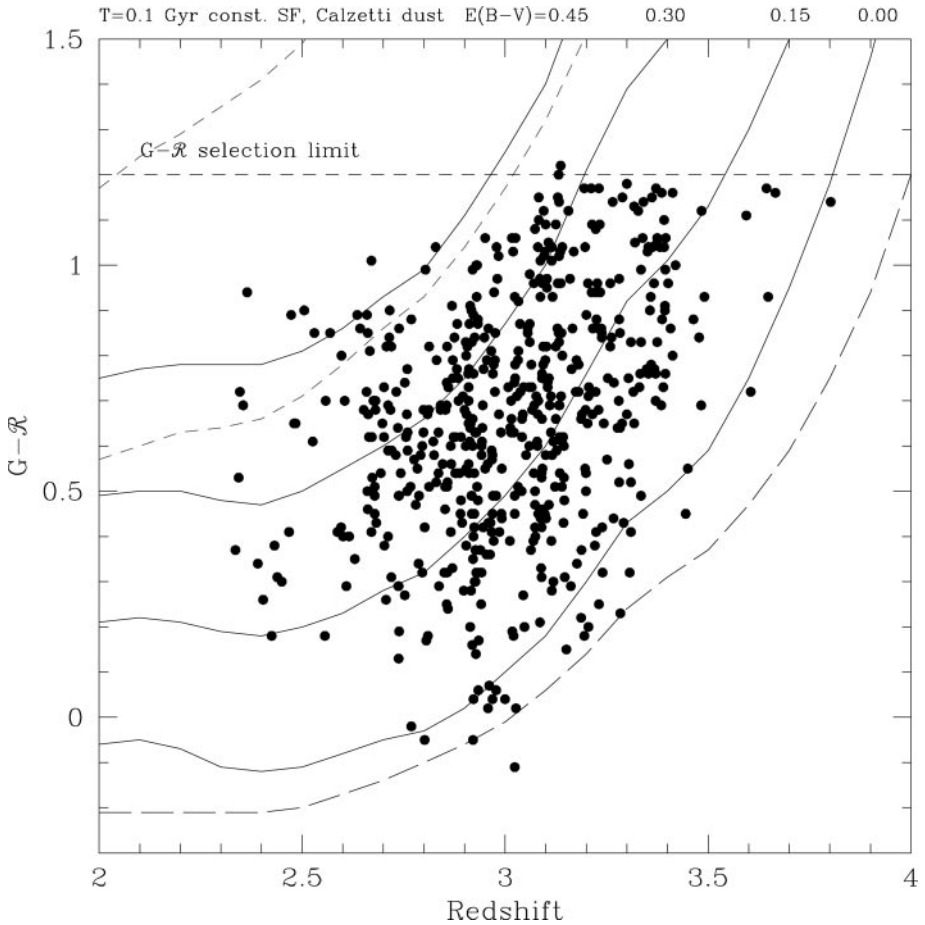


Figure 5 Scatter plot of the $G - R$ color versus redshift of U -band dropouts. The curves show the predicted colors for various choices of star formation history and dust obscuration. The continuous and dashed curves show the case of continuous star formation with Salpeter IMF and age $T=0.1$ Gyr with the starburst attenuation law (*continuous curves*) and SMC extinction law (*dashed curves*). The amount of obscuration is parameterized by the $E(B - V)$ color excess, as labeled. For the SMC curves only the first three cases from $E(B - V)=0$ through $E(B - V)=0.3$ (*the curve to the upper left*) can be seen. The dotted curve shows a burst with $T=0.001$ Gyr with no dust obscuration, which defines the blue envelope of the color distribution. Some galaxies have bluer colors because of the strong Ly α emission in the G band. The median color excess is $E(B - V) \approx 0.17$ and most galaxies are between $E(B - V) \sim 0.1$ and $E(B - V) \sim 0.35$. The cosmic opacity is calculated as prescribed by Madau (1995).

star formation. In the second case (lightly shaded histogram), the unobscured UV luminosity (and hence the star-formation rate) is calculated from fitting broadband photometry covering from the rest UV to the optical to population-synthesis models (Papovich et al. 2001, Shapley et al. 2001) to derive the best fitting intrinsic spectral energy distribution, extinction, age, and stellar mass, under the assumption of initial mass function, metallicity, star-formation history, and extinction law (we describe this procedure in more detail later). It is interesting that there is a broad agreement between the results from the two techniques, given the large uncertainties involved. After the correction, most rates exceed $10^2 M_{\odot} \text{ yr}^{-1}$, with some reaching as high as $\sim 10^3 M_{\odot} \text{ yr}^{-1}$. At these rates, $\sim 10^{11} M_{\odot}$ worth of stars, the value observed today in $L > L^*$ galaxies, can be assembled in ~ 1 Gyr. Shapley et al. (2001) suggest that there is a statistically significant correlation between the star-formation rate and age of the star-formation activity, where younger bursts have higher rates and larger dust obscuration.

Independent information on the star-formation rate and extinction can be obtained from the optical nebular emission lines, in particular $H\beta$ and $H\alpha$, where the effect of extinction is less pronounced than in the UV. Teplitz et al. (2000b) obtained high S/N near-IR spectra of the lensed LBG MS1512–cB58, and measured the flux of optical nebular lines, from $[\text{O II}]\lambda 3727$ to $H\alpha$ and $[\text{N II}]\lambda 6583$. They report that the star-formation rate derived from $H\alpha$ is ≈ 4 times smaller than that derived from the UV continuum, despite an extinction of $E(B - V) \sim 0.27$ measured from the Balmer decrement. They suggest that this discrepancy is probably due to the different calibrations of star-formation rates used for the $H\alpha$ and the UV continuum, (e.g., Kennicutt 1998), implying that the magnitude of this uncertainty is comparable to the relative effects of reddening at optical and UV wavelengths. For comparison, with the same value of $E(B - V)$, the starburst law predicts that the extinction at 1700 \AA is ≈ 4 times larger than that at 6563 \AA , whereas the SMC extinction law predicts a factor ≈ 7 . Kobulnicky & Koo (2000) observed two galaxies, one $\text{Ly}\alpha$ -emitting galaxy at $z = 2.3$ and one LBG at 2.9, and reported the star-formation rates derived from the Balmer lines to be 2 to 3 times larger than those derived from the UV continuum, although no correction for extinction was made because it was not possible to measure the Balmer decrement. Moorwood et al. (2000) obtained spectra for six galaxies, selected from $H\alpha$ -emitting galaxies (not LBGs), at $z \sim 2.2$ and found that in two cases the star-formation rates derived from the line flux are ≈ 4 times larger than those obtained from the UV continuum, whereas in the other four cases the rates are approximately the same.

Pettini et al. (2000) observed a comparatively larger sample, including 14 galaxies selected from the ground-based survey. They find that the star-formation rates derived from the $H\beta$ flux are, on average, no larger than those derived from the UV continuum. Whereas a few galaxies can be found that have larger $H\beta$ rates than the UV ones, looking at the whole sample reveals that this is just an effect of the scatter of the data. Thus, both indicators uncorrected for dust extinction are equally affected by the systematics introduced by dust, and statistically yield the same star-formation rates. Also, the ratio of the two estimators does not show

any obvious tendency to correlate with the UV-spectral index derived from the observed UV color $G - \mathcal{R}$, which in local starburst galaxies is a good tracer of the dust extinction (Calzetti et al. 1994). This is consistent with the results from the other observations of the nebular lines of LBGs, and adds strong evidence that the attenuation law of LBGs is relatively gray, adding support to the notion that the starburst attenuation law provides a good description of the reddening properties of these galaxies, also.

Cosmic Star Formation

Madau et al. (1996) have summarized the available empirical information on the evolution of the cosmic activity of star formation with time in terms of the UV luminosity density as a function of redshifts (Madau diagram). Recalling that UV luminosity is a good tracer of the star-formation rate (modulo the obscuration by dust), this can also be expressed as star-formation density per unit of comoving volume. For LBGs, if the luminosity function remains approximately constant within the redshift interval targeted by a given set of color selection criteria, the star-formation density can be estimated as an average of the integral of the luminosity function over the probed cosmic volumes

$$\rho^*(z) = \int f^{-1}(z) dz \int S_\lambda L_\lambda \phi(L_\lambda, z) dL_\lambda, \quad (11)$$

where $f(z)$ is the redshift selection function and S_λ converts the luminosity L_λ into the star-formation rate. It is important to note that the observed UV luminosity function of the LBGs at $z \sim 3$ implies that $\gtrsim 50\%$ of the total contribution to the star-formation density by galaxies with $\mathcal{R} \leq 27$ is produced by galaxies with $\mathcal{R} \lesssim 25$.

The original compilation of data by Madau et al. (1996, 1998) covered the redshift range $0 < z < 5$ using the LBGs from the Hubble Deep Field in combination with galaxies from other spectroscopic and photometric surveys at lower redshifts. For the LBGs they assumed that the adopted color selection criteria for the U - and B -band dropouts uniformly probe the redshift intervals $2.0 < z < 3.5$ and $3.5 < z < 4.5$, respectively, estimated by convolving the WFPC2 photometric system with population synthesis spectra (i.e., $f(z) = 1$ in these intervals). They estimated the LBG luminosity functions from the magnitude distribution of the HDF sample (Dickinson 1998) and did not attempt any correction for dust extinction. The corresponding Madau plot shows a rapid increase of the star-formation activity from $z = 0$ to $z \sim 1$ (Lilly et al. 1995, 1996), where a broad peak seems to be present, followed by a decrease at higher redshifts (see Figure 7, triangles).

This peak, however, does not seem confirmed by the data of the ground-based survey (Steidel et al. 1999). The data points at $z \sim 3$ and $z \sim 4$ from the ground-based survey, which covers ~ 200 times more area than the HDF and benefits from

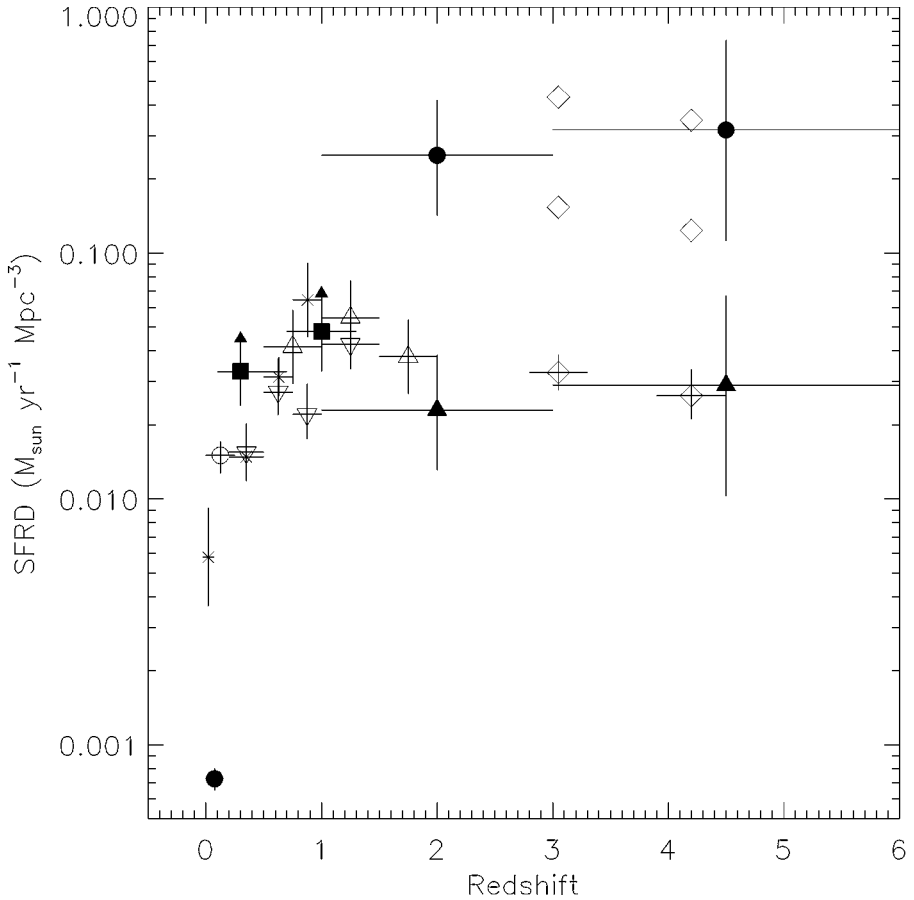


Figure 7 Star-formation density traced by a variety of star-forming galaxies at different redshifts (Madau diagram). The *open diamonds* with error bars are the data points at $z=3$ and 4 of LBGs from the ground-based survey with no dust correction included (Steidel et al. 1999). The *filled triangles* are SCUBA galaxies with flux >6 mJy, whereas the *filled circles* are SCUBA galaxies integrated down to 0.2 mJy. The two sets of *open diamonds* with no error bars represent two different estimates of the dust obscuration correction for the LBGs, as explained in the text (reproduced from Barger et al. 2000).

almost 1000 redshifts, are consistent with a constant star-formation density at least up to $z \sim 5$ (Steidel et al. 1999). The difference from the previous work includes (a) a proper measure of the volume density, which has been derived using the observed redshift distributions; (b) an estimate of the effects of incompleteness with Monte Carlo simulations performed on the data themselves; and (c) an attempt to include the effect of dust obscuration. For consistency, data points at all

redshifts have been corrected with the same technique, assuming the same mean $E(B-V) \sim 0.15$, the Calzetti (1997) starburst extinction law, and the implied correction at $z \sim 1$ is consistent with that derived by Glazebrook et al. (1998) from $H\alpha$ spectroscopy and with those derived by Tresse & Maddox (1998) from direct UV observations at $z \sim 0.3$.

It is important to observe that the ground-based data points at $z \sim 3$ and $z \sim 4$ do not support the peak at $z \sim 1$ even without corrections for dust obscuration. This result is particularly interesting, because it actually does not depend on the assumptions about the luminosity function. Even if the integral in Equation 10 is extended over the observed luminosity, as opposed to the extrapolated luminosity, the two data points would be the same within the errors. Steidel et al. (1999) calculated the star-formation density at each redshift by integrating the luminosity functions down to $0.1L^*$, which corresponds to $\mathcal{R} \sim 27$ at $z \sim 3$. Because of the small size of the HDF sample, the luminosity function at $z \sim 3$ and (especially) $z \sim 4$ have not been convincingly measured down to such faint luminosity. This is one of the major uncertainties that affect this type of comparison, although if the slope is not significantly steeper than $\alpha \sim -1.6$ (as the data at $z \sim 3$ seem to show), the contribution of galaxies with $m > m^*$ to the luminosity density is relatively small. Finally, note that Lanzetta et al. (2002) suggest that current estimates of the the star-formation density at high redshift have been underestimated because of the strong bias introduced by the $(1+z)^4$ surface brightness dimming, and that the cosmic star-formation density increases monotonically with redshift up to the highest observed redshifts.

OTHER STARBURST GALAXIES AT HIGH REDSHIFTS

In the past few years, faint surveys at wavelengths of 450 and 850 μm with the Submillimeter Common-User Bolometer Array (SCUBA) at the James Clerk Maxwell telescope (JCMT) have identified starburst galaxies at high redshifts by targeting their far-IR emission, which at redshift of a few is redshifted to the submillimeter spectral region (Smail et al. 1997; Barger et al. 1998, 1999a, 2000; Hughes et al. 1998; Blain et al. 1999a,b; Eales et al. 1999; Lilly et al. 1999). In the local universe, most of the UV luminosity produced by young, massive stars in starburst galaxies, which dominate the total bolometric luminosity, is absorbed by dust and re-radiated as far-IR wavelengths (Heckman et al. 1998; see also Calzetti 2001, Adelberger & Steidel 2000). The spectral energy distribution of the reprocessed radiation reaches a maximum in the range $60 \lesssim \lambda \lesssim 100 \mu\text{m}$ (Sellgren 1984, Helou 1986) due to the thermal emission of hot dust heated by stellar radiation at UV and optical wavelengths. If starbursts at high redshifts are similar to the local ones, observations at submillimeter wavelengths will detect them up to $z \lesssim 10$ thanks to the negative k-correction that results when the spectral region redward of the peak is redshifted to $\sim 850 \mu\text{m}$, which more than compensates for the dimming due to the luminosity distance. For example, a dusty star-forming galaxy observed

at $\sim 850 \mu\text{m}$ would require approximately constant sensitivity to be observed within the range $2 \lesssim z \lesssim 10$ (Blain et al. 1998). Such observations would be ideal to derive an accurate census of the star-formation activity of the universe at those epochs were it not for the fact that they reach limited sensitivity due to the generally high opacity of the atmosphere in most of those bands and the very low angular resolution of the instrumentation (at $850 \mu\text{m}$, SCUBA has a beam size of ~ 14 arcsec), which also hampers the secure identification of the sources with their optical and near-IR counterparts (e.g., Adelberger & Steidel 2000). In comparison, despite most of the luminosity being absorbed, UV observations are much more efficient at detecting and identifying the galaxies, except that reconstructing the bolometric luminosity is highly uncertain.

One of the most important questions is what is the nature of the SCUBA sources, namely if mostly starburst or mostly AGN, and what is their contribution to the cosmic star-formation activity at high redshift compared to that of the LBGs? Because the direct identification of SCUBA sources with optical and near-IR counterparts is generally very uncertain, the redshift distribution of the SCUBA sources is poorly constrained.³ In some cases, likely optical and near-IR candidate counterparts to SCUBA sources have been identified (Hughes et al. 1998, Lilly et al. 1999, Smail et al. 1999, Scott et al. 2000), and in a few cases, the additional detection of these counterparts in high-resolution radio images makes the identification more likely (Barger et al. 1999b, 2000), including bona fide LBGs at redshifts $z \sim 2.5$. Other likely identifications rely on the optical images alone, and the redshifts of most of these galaxies are significantly lower than those of the LBGs (Lilly et al. 1999, Scott et al. 2000).

Because the far-IR radiation does not suffer significant reprocessing, and it is an indicator of the star-formation rate (Kennicutt 1998, Adelberger & Steidel 2000, Calzetti 2001), a very useful upper limit to the total amount of star formation at high redshifts is set by the value of the diffuse background at $850 \mu\text{m}$ measured

³Note that if starburst galaxies at $z \gtrsim 6$ significantly contribute to the SCUBA population, they are unlikely to have detectable counterparts in current imaging or spectroscopic surveys, even if relatively unobscured. If such galaxies have a luminosity function similar to that of the LBGs at $z \sim 3$ and 4, they would appear extremely faint in even the deepest images and certainly beyond current spectroscopic capabilities. Regardless of the likelihood of the proposed identifications, another caveat to keep in mind is that there is neither evidence nor compelling reason to believe that in every case, the same energy output that powers a SCUBA source also powers its optical counterpart (rest-frame UV), even in the same galaxy. One could have, for example, galaxies hosting nuclear starburst regions heavily obscured by dust with no detectable UV radiation that are very bright in the far-IR, which also have circumnuclear UV-bright starburst regions with low dust obscuration (Kennicutt 1998). Such galaxies would be detected in both submillimetric and optical surveys, but in this case the observed UV and far-IR luminosity are not quantitatively related. In this regard, note that Blain et al. (1999a) suggested that violent, dust-obscured star formation might represent a transient phase (triggered, for example, by a close encounter or a merging event) in the life of an otherwise relatively more quiescent starburst galaxy.

by the Cosmic Background Explorer (COBE) (Puget et al. 1996, Hauser et al. 1998, Fixsen et al. 1998, Schlegel et al. 1998). At bright flux levels, e.g., >6 mJy, a fraction of the order of 75% of the SCUBA sources are powerful starbursts in the redshift range $2 < z < 5$, the high-redshift equivalent of ULIRGs, although they contribute only $\sim 5\%$ of the background (Barger et al. 2000). Down to the confusion limit of 2 mJy, discrete SCUBA sources contribute 20–30% of the background (Barger et al. 1999a), although it is difficult to understand their nature, because of the poor resolution. Of the handful of optical identifications that are based on extensive multiwavelength data sets, approximately one half are AGN, and a few have been associated with star-forming galaxies (Frayser et al. 1999, Dey et al. 1999, Chapman et al. 2000, Frayer et al. 2000, Ivison et al. 2000). Barger et al. (2000) have shown that bright sources with flux >6 mJy contribute as much star formation as LBGs down to $\mathcal{R} \sim 27$ uncorrected for dust obscuration (Steidel et al. 1999), whereas integrating along the SCUBA luminosity distribution down to ~ 0.5 mJy, the contribution is about one order of magnitude larger (Smail et al. 1998, Barger et al. 2000), even if LBGs are about one order of magnitude more abundant than SCUBA galaxies (e.g., Lilly et al. 1998). At these flux levels, the contribution to the background is estimated to be $\sim 90\%$ (Blain et al. 1999b), implying that the faint SCUBA sources host most of the star formation at high redshift. Correcting the UV luminosity of LBGs for dust obscuration yields a similar star-formation density to that of the SCUBA galaxies (see Figure 7).

To compare the contribution of the cosmic star-formation density of LBGs and SCUBA galaxies one needs to know the amount of overlap between the two classes of sources, i.e., the contribution of the LBGs to the SCUBA faint counts and to the submillimeter background. Empirically, the situation is very uncertain. Adelberger & Steidel (2000) suggest that LBGs should have fainter far-IR emission than ULIRGs, which are powered by huge nuclear starbursts (Sanders & Mirabel 1996) and have their UV emission largely obscured by vast amounts of dust. Indeed, only a small fraction of LBGs observed with SCUBA have been detected at flux levels of a few mJy (Barger et al. 1999b, Chapman et al. 2000, Sawicki 2001, Van der Werf et al. 2001). At these flux levels, the submillimeter counts are probably dominated by AGN and cosmologically distant ULIRGs with redshift comparable to that of LBGs (Hughes et al. 1998, Barger et al. 1998, Lilly et al. 1999, Smail et al. 1998, Ivison et al. 2000), supporting the notion that LBGs have properties closer to those of UV-bright starbursts (Aldeberger & Steidel 2000, Calzetti 2001) and that they significantly contribute to the SCUBA counts mostly at the faintest levels currently explored.

Modeling the contribution of LBGs to the SCUBA counts is also uncertain, because it requires essentially uncontrolled assumptions about the properties of starburst galaxies at high redshifts. Calzetti et al. (2000) estimate that the detectability with SCUBA of LBGs strongly depends on the far-IR Spectral Energy Distribution (FIR SED), in particular the submillimeter/total-FIR ratio, and suggest that metal-poor LBGs (e.g., $< 1/7$ solar) might not be detectable at all. Adelberger & Steidel (2000) noted that the contribution of starbursts to the submillimeter

background is produced in a large redshift range, approximately $1 < z < 5$, and calculated that if these galaxies have (a) far-IR SED in the same range as observed in the local universe; (b) obey to the same relationship between UV spectral index and bolometric dust luminosity (Meurer et al. 1999), then they are responsible for $\approx 75\%$ of the background and provide most of the faint SCUBA counts.

Barger et al. (2000) showed that SCUBA submillimeter sources brighter than 6 mJy at $1 < z < 3$ contribute as much as LBGs uncorrected for dust obscuration (see Figure 7), and that their contribution to the background is only $\sim 5\%$, indicating that these sources, which are all ULIRGS, do not host the bulk of star formation at high redshifts. By the same token, however, this shows that the contribution to the background by LBGs at $z > 2$ is significantly larger, because dust does obscure the UV luminosity of these sources. SCUBA sources brighter than ~ 2 mJy contribute to $\sim 40\%$ of the background, and they certainly include ULIRGS at $z > 1$ (Arp 220 at $z = 3$ would be observed with a $850 \mu\text{m}$ flux of 2 mJy). However, ULIRGS are not the only starbursts contributing to the submillimeter counts at these flux levels, because at least a few LBGs have also been detected (Barger et al. 1999b, 2000; Chapman et al. 2000; van der Werf et al. 2001), although a robust estimate of the fraction of LBGs that are also SCUBA sources at these flux level is not known. SCUBA sources down to the faintest $850 \mu\text{m}$ flux levels observed account for a major fraction, and possibly for all, of the submillimeter background (Blain et al. 1999, Barger et al. 2000), indicating that the galaxies that produced the bulk of the stars at $z > 2$ are to be searched among them.

The key question is, therefore, how many LBGs contribute to these faint SCUBA counts, and for this no direct empirical constraints exist. Peacock et al. (2000) show that the large fluctuations of diffuse light in deep SCUBA images are comparable to the strength of the spatial clustering of LBGs, arguing that faint SCUBA galaxies and LBGs largely coincide. Adelberger & Steidel (2000) and Papovitch et al. (2001) predict that if LBGs obey the same relationship of proportionality between the UV-spectral index β and the ratio of UV bolometric luminosity to dust bolometric luminosity and also have a similar far-IR spectral energy distribution as local starburst galaxies, then they dominate the faint SCUBA counts. The first assumption is a direct consequence of the spatial distribution of dust in the ISM of starburst galaxies (Calzetti 1997, 2001; Calzetti et al. 2000), and it seems reasonable to expect that it also is verified by LBGs (Adelberger & Steidel 2000); the validity of the second assumption, however, is much more difficult to assess, because it depends on the specific physical conditions of the ISM of the galaxies, primarily the temperature and composition of the dust (Kennicutt 1998, Calzetti 2001). These could be different in the high-redshift galaxies, which have a much larger star-formation rate per unit volume than their local counterparts (Meurer et al. 1997). The star-formation density of LBGs at $2 < z < 4$ corrected for dust obscuration is roughly comparable to that of the faint SCUBA galaxies. This is illustrated in Figure 7, which shows the star-formation density of LBGs at $z = 3$ and 4 after correction for dust obscuration. Two dust-corrected points are plotted in the figure at each redshift to illustrate the uncertainty that affects the

correction. The lower value corresponds to an average multiplicative correction of a factor 5 estimated from the observed distribution of UV colors, under the assumption of continuous star formation (Steidel et al. 1999, Adelberger & Steidel 2000); the upper value corresponds to a correction of a factor 13, and is derived from fitting multiwavelength photometry to stellar population synthesis models (Papovich et al. 2001, Shapley et al. 2001, see also Meurer et al. 1999).

CHEMICAL ABUNDANCES

Measuring the chemical abundances of LBGs is very important in understanding the evolutionary link to present-day galaxies. We have discussed earlier that although the presence of strong interstellar absorption lines is evidence that these galaxies have undergone chemical enrichment, the features cannot be used to measure it because they are heavily saturated. Under these circumstances, values of metallicity anywhere between 1/1000 of solar and solar are compatible with the line strengths, and observations at higher resolution—observations of intrinsically weaker lines are required to measure elemental abundances (Pettini & Lipman 1995). These have been attempted by Pettini et al. (2000) for the gravitationally lensed galaxy cB58, whose bright apparent magnitude allowed them to reach comparatively high S/N ratio. The resolution of the recorded spectrum of cB58, although ten times higher than that of the spectra obtained for redshift identification, is still an order of magnitude lower than that normally required to measure elemental abundances from interstellar lines. In this case, one can consider the weakest ($W_0 \leq 0.5 \text{ \AA}$) gaseous lines in the spectrum (Ni II, Si II, and S II), and derive metallicity by assuming that the saturation effects are unimportant to estimate the column density of the observed species. Similar to what is frequently observed in LBGs, the Ly α line in cB58 contains both an emission and an absorption component, the latter characterized by a damped profile. Thus, one can directly estimate the column density of HI and use it to compute the metal abundances in the interstellar gas. This yields values between one third and one fifth of solar, in qualitative agreement with the metallicity of the stars from the morphology of the C IV P-Cygni profile.

More recently, Pettini et al. (2002) obtained a spectrum of cB58 with a resolution of 58 km s^{-1} , and found that the ISM of the galaxy is already highly enriched in elements from Type II supernovae, such as O, Mg, Si, P, and S, which have abundances of $\sim 2/5$ their solar value. However, N and the Fe-peak elements Mn, Fe, and Ni are under-abundant by a factor of 3. This implies that the burst that has enriched the ISM of cB58 must be young, of the order of the timescale for release of N from intermediate mass stars, namely $\leq 300 \text{ Myr}$ and comparable with the dynamical timescale, suggesting that the galaxy is perhaps a young spheroid.

Direct measures of the metal enrichment of the nebular gas from optical line ratios have been presented by Pettini et al. (2001), Kobulnicky & Koo (2000), and Teplitz et al. (2000b), who obtained near-IR spectra of a sample of LBGs. They

used the ratio of $[\text{OII}] + [\text{OIII}]$ relative to $\text{H}\beta$, known as the R_{23} index (Pagel 1986, McGaugh 1991, Kobulnicky et al. 1999) to measure the oxygen abundance relative to hydrogen of the HII gas. The method is relatively easy and generally accurate within ~ 0.2 dex. Unfortunately, in the region of values of R_{23} occupied by the LBGs, the calibration of the index onto a scale of oxygen abundance is a double valued function, and for a given value of R_{23} , two values of the oxygen abundance are derived that bracket the true one, effectively defining an interval of uncertainty that is larger than the magnitude of the random error. This degeneracy can be broken with measures of $\text{H}\alpha$ and N [II] flux, which unfortunately are generally unavailable from ground-based observations at the redshifts of the LBGs. This is illustrated in Figure 8, which plots the calibration of the 4 LBGs from the paper by Pettini et al. The figure shows that for three galaxies the metallicity is constrained to within an order of magnitude, between $1/10$ solar and near solar. In one lucky case, the R_{23} index is located near the apex of the double valued function, yielding the measure $[\text{O}/\text{H}] = 0.3$ solar. A similar case has been reported by Kobulnicky & Koo (2000). Of course, whereas these measures are in general agreement with the measures of cB58 discussed above, given the very small sample size, they should not be used to conclude that all LBGs have a metallicity of about one third solar.

Also, note that no correction for dust obscuration has been made to the line fluxes discussed here, because no measure of the Balmer decrement could be made without the $\text{H}\alpha$ line. Dust obscuration, which in starbursts affects the line fluxes about two times more strongly than the continuum for a given amount of extinction (Calzetti et al. 1994), causes the measures of R_{23} to be overestimated. This means that the data point in Figure 8 should be moved to the left of the plot (by an unknown amount), toward a region of larger uncertainty for the final value of $[\text{O}/\text{H}]$. Thus, in conclusion, while it is probably fair to say that LBGs are more metal rich than damped $\text{Ly}\alpha$ absorbers at the same redshifts and more metal poor than luminous QSOs (Pettini et al. 2000, 2001), it is not possible to say much more about their metallicity other than constraining it between $\sim 1/10$ solar and solar value.

Finally, it is worth mentioning that Pettini et al. (2001) and Kobulnicky & Koo (2000) compared the position of LBGs relative to the well-known correlation between metallicity and B -band absolute luminosity observed for star-forming and late-type galaxies. This comparison shows that LBGs are either too luminous for their metallicity or too metal poor for their luminosity. Keeping the metallicity constant, a dimming of about 5 magnitudes is required to bring the LBGs in line with the other galaxies. This likely reflects the fact that LBGs have a rather low M/L ratio, due to their very high activity of star formation.

STELLAR MASS AND AGE

Measuring the stellar mass assembled in LBGs and the age of the stars at $z \sim 3$ and higher is very important in constraining the link to galaxies observed at later cosmic times. These measures require observations at rest-frame optical and preferably

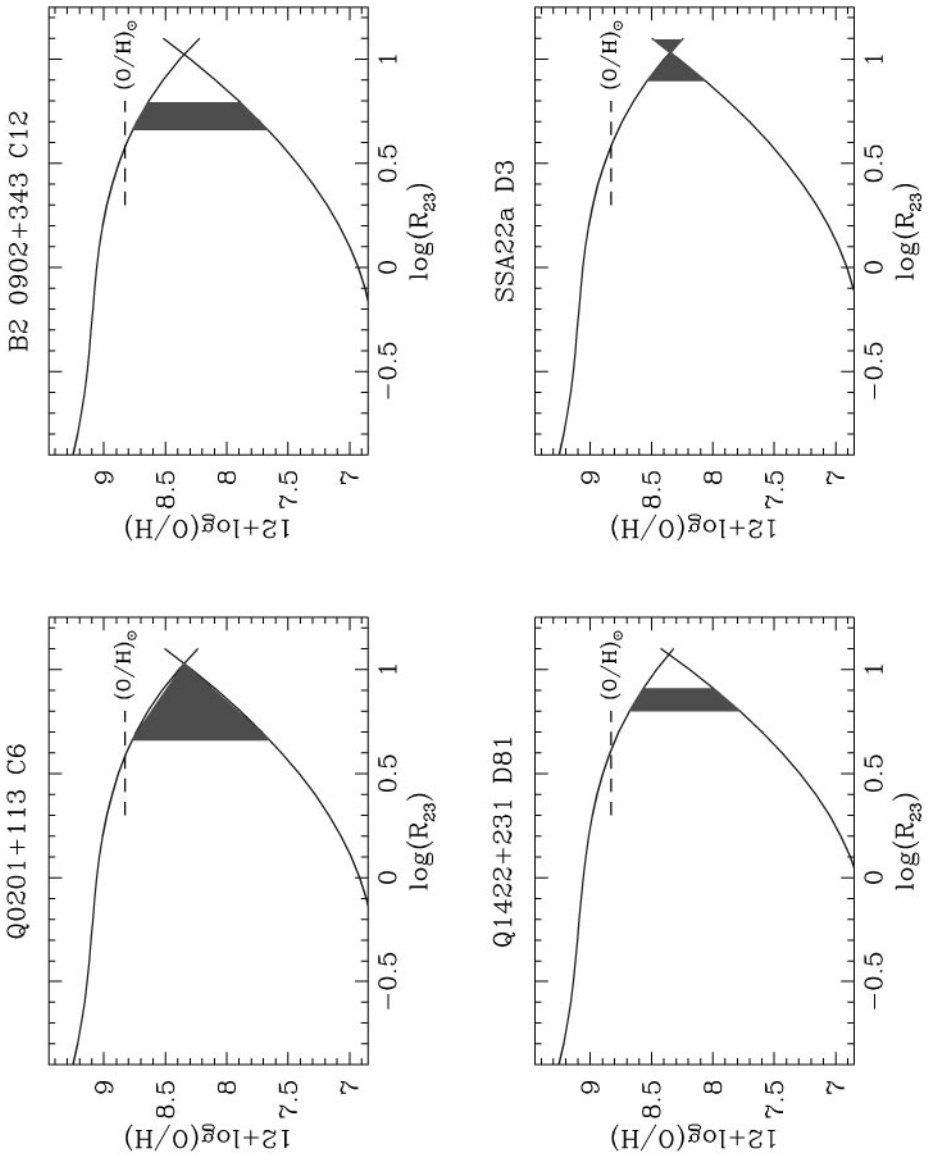


Figure 8 Calibration diagram of the Oxygen abundance (in solar units) in terms of the R_{23} index. The uncertainty in the measure of R_{23} is the width of the shaded band (see text). The value of the solar metallicity is marked by a *horizontal dashed line* [reproduced from Pettini et al. (2001)].

longer wavelengths, because the rest-frame UV spectrum alone provides information only on the young, massive stars of the newly formed stellar population. The current estimates come from fitting UV through optical broadband photometry to stellar population synthesis models to derive the intrinsic parameters of the forming and formed stellar populations, including the stellar mass. The details of the fitting procedure vary, but in general, the stellar populations are modeled with a set of parameters. Some of these parameters, such as the total length of the burst, the age of the burst, and the extinction are adjusted during the fit; others, such as the IMF, the metallicity, and the extinction law, remain fixed and their effect on the results is explored by varying them within preassigned intervals and repeating the fitting procedures.

Sawicki & Yee (1998) first applied this technique to a sample of 17 LBGs galaxies from the HDF-N (Williams et al. 1996) using the optical WFCP2 photometry augmented by ground-based near-IR *JHK* photometry of medium depth obtained by Dickinson et al. (compare Dickinson 1998). They concluded that on average these galaxies are young starbursts observed at an average age of ~ 25 Myr after the onset of star formation and highly reddened by dust, with mean $E(B - V) \sim 0.3$ and $A_{1700} \sim 3.5$ mag. This seems to indicate that the typical LBG of their sample could only produce a very small fraction, approximately 5%, of the total stellar mass of a present-day L^* galaxy. However, the LBGs from the HDF are rather faint, and the ground-based IR data, which were obtained from a 4-m class telescope, could only reach relatively modest flux levels. As a consequence, the fits by Sawicki & Yee are characterized by large uncertainty. The reason is that because the UV light of these galaxies is dominated by the short-lived massive stars of the forming populations, to constrain the mass in smaller stars one important requirement is to have high S/N rest-frame optical photometry. With most of the information in the UV alone, it is simply not possible to break the degeneracy between age, metallicity, and dust extinction.

Photometry of LBGs in *J* and *H* obtained with HST and NICMOS in the HDF (Papovich et al. 2001) and with Keck in *J* and *K* (Shapley et al. 2001) reach very deep flux levels and are better suited to estimate the contribution to the optical luminosity by formed—as opposed to forming—stellar populations. The fitting procedures and other details of these two works differ a little, but they both reach the same general conclusions. Papovich et al. derived both the total burst duration and its age (effectively, the star-formation history) from the fit, while Shapley et al. adopted the continuous star-formation approximation and fitted the age. Also, Papovich et al. restricted their analysis to LBGs with spectroscopic redshifts in the range $2 < z < 3.5$ to ensure adequate samples of the rest-frame optical wavelengths, and considered models with varying metallicity and IMF, while Shapley et al. adopted solar metallicity and the Salpeter function throughout their analysis.

The two teams consistently found that the stellar mass is generally well constrained by the fitting procedure, and the results are also relatively insensitive to the assumptions of IMF and metallicity, within a factor of ≈ 2 (recall that from direct

analysis of the spectrum of cB58 Pettini et al. (2000) found no evidence of IMF substantially different from the Salpeter one). Fitted values of the instantaneous rate of star formation have comparatively larger uncertainties, but they still provide useful information on the star-formation activity of the population. However, the technique does not seem to be useful to constrain the star-formation history of the individual galaxies, in particular the age, since the errors on this parameter are so large as to make the fitted value useless.

The top panel of Figure 9 shows the histogram of the fitted stellar mass from both the ground-based and HDF samples (shaded area). The dark gray histogram represents the ground-based sample alone, whereas the light gray one represents the HDF sample. It is important to keep in mind that the fitted stellar mass is that of the forming stellar population (i.e., of the current starburst), and hence, only a lower limit to that of the formed populations assembled in previous bursts. Using a two-population fit (the forming one plus a maximally old one), Papovich et al. (2001) estimate that one can miss, on average, four times the mass of the young population, and derive the mass of the old population for each galaxy of the HDF sample. The histogram of the sum of the mass of the young plus old populations of the HDF sample is shown with the light gray curve in the bottom panel of Figure 9. Unfortunately, no similar information is available for the ground-based sample; we hence have crudely estimated the old population mass for this sample by multiplying the young one by a factor of 4, the average value found in the HDF. The corresponding histogram is plotted with the dark gray curve, whereas the sum of the HDF plus ground-based samples is represented by the shaded histogram. Also plotted is the range of dynamical mass derived from the kinematics of the optical nebula emission lines. Notice that even the young masses alone span the range from the typical mass of an L^* galaxy today, $M^* = 10^{11} M_{\odot}$ (Cole et al. 2001) to that of dwarf galaxies.

MORPHOLOGY

At redshift $z \sim 3$, cameras on board HST can resolve spatial scales of $\sim 0.5 h^{-1}$ kpc, sufficient to resolve the size of individual starburst regions (Kennicutt 1989, 1998) and provide good dynamic range to characterize the overall morphology of LBGs, e.g., ≈ 500 resolution elements for an L^* LBG in HDF-like images. Initial HST works consisted of optical imaging sampling the far-UV morphology of the galaxies. After the installation of the NICMOS instrument on HST the optical morphology has also been studied with near-IR imaging. The samples included galaxies from the ground-based survey (Giavalisco et al. 1995, 1996a, 1996c) and the HDF itself (Steidel et al. 1996a; Abraham et al. 1996; Lowenthal et al. 1997; Dickinson 1998, 2000), approximately covering the redshift range $2 \lesssim z \lesssim 4$. Other studies included HST imaging of Ly α galaxies (Pascarelle et al. 1996a,b) at similar redshifts.

These works found that whereas LBGs are characterized by a relatively wide dispersion of morphological properties, there are also a number of common

features that seem to be typical of the population. These galaxies generally are smaller, more compact and more irregular than local galaxies of comparable *B*-band luminosity, and they have comparatively bluer integrated colors than the local mix, with UV to optical SED similar to that of the Irregular Hubble types (Papovich et al. 2001). Although color gradients are clearly observed within the galaxies, their morphology depends mildly on the wavelength, remaining essentially unchanged from the far-UV to the optical window. In general, their morphology cannot be classified in terms of the traditional Hubble types (other than pointing to a generic similarity with Ellipticals or Irregular types for some of them), because the structural components of bulge, disk, spiral arms, and bars are not identified in these galaxies.

The mix of morphologies ranges from relatively regular systems to irregular to fragmented and multiple systems, and both the UV and optical images show typical half-light radii in the range $r_{1/2} \sim 3\text{--}5 h^{-1}$ kpc. Such sizes are significantly larger than those of dwarf galaxies, and similar to those of large bulges and elliptical galaxies of intermediate luminosity in the local universe. (See, for example, the compilation of data on the structural parameters of spheroids by Bender et al. 1992.) In a number of cases, the isophotal analysis reveals a relatively smooth morphology with either an $r^{1/4}$ or exponential profile and an overall appearance reminiscent of an elliptical galaxy or a spiral one. Figure 10 shows two such examples selected from the ground-based survey at both UV and optical rest-frame wavelengths. In a few cases there are tentative detections of rotation curves from spectroscopy of the optical nebular lines (Pettini et al. 2001, Moorwood et al. 2000), suggesting that rotationally supported disks might be present among LBGs. Unfortunately, no spectra have been taken yet of those galaxies for which existing HST imaging suggests a disk-like morphology. Thus, it is quite possible that the unknown inclination of the disk and the lack of alignment with the major axis have resulted in underestimating both the amount of rotation and the spatial extent of the rotation curve. Also, note that in other cases, deep spectroscopy of LBGs with an apparent edge-on disk-like morphology failed to reveal any evidence of rotation (H. Spinrad, private communication).

More frequently, however, the galaxies have disturbed or fragmented morphologies, with one bright core or multiple knots embedded in diffuse nebulosity, reminiscent of merging events or interactions. Diffuse, low-surface brightness galaxies seem to be comparatively rare, even though the HST images have enough sensitivity to detect them if they were present. Also rare are highly elongated galaxies, e.g., like the chain galaxies found by Cowie et al. (1995b), which seem to suggest that overall LBGs are characterized by a relatively high degree of spherical symmetry (Giavalisco et al. 1996c). Figure 11 shows color images of LBGs from the HDF at both UV and optical rest-frame wavelengths and illustrates both their morphological diversity and the weak dependence of morphology on wavelength. Regardless of the underlying (unknown) kinematics of the galaxies, it is interesting to observe that very often the bulk of the light of LBGs, including both the single galaxies and multiple ones (Giavalisco et al. 1996c, Steidel et al.

1996a), come from compact structures, suggesting that the sites of the most intense star formation in these galaxies are dense, virialized structures.

Based on their morphology and size, the closest counterparts to most LBGs in the local universe are either late-type spiral and irregular galaxies or merging systems (Lowenthal et al. 1997, Trager et al. 1997, Sawicki & Yee 1998). However, LBGs have a much higher star-formation activity than local galaxies, and this fact could be responsible, at least in part, for their apparent morphology, since even at rest-frame optical wavelengths the brightest regions of star formation dominate the integrated light. In local galaxies, the morphology of these regions is often different from that of the underlying galaxy, and tend to be fragmented and irregular (Giavalisco et al. 1996b; Hibbard & Vacca 1997; Kuchinski et al. 2001, 2000; Marcum et al. 2001) and in general is not representative of that of the whole structure. Thus, the observed morphology of LBGs could primarily reflect that of their most active regions of star formation, while that of the underlying galaxy remains unconstrained. The weak dependence of the morphology of LBGs on wavelength is generally consistent with this interpretation. We note, however, that the constraints on the relative proportions of old and young stars in LBGs are rather loose (Papovich et al. 2001), approximately $0 \lesssim m_{old}/m_{new} \lesssim 7$; on average, as much as four times the stellar mass of the forming population could still be present in LBGs and still its morphology be outshined by that of the forming population, thus remaining substantially unobserved in the images.

Finally, we conclude by stressing the importance that morphological studies will have in understanding the mechanisms of star formation in these galaxies when complemented with kinematic information. A key example is testing the occurrence of merging in these systems, which is predicted to be the primary trigger of star formation in systems according to the hierarchical cosmologies (e.g., Somerville et al. 2000, 2001). This requires the study of the kinematics of the apparent fragments that compound the galaxies on scales of a few kiloparsec, and it will be made possible by integral field spectrographs attached to large-aperture space telescopes.

CLUSTERING AND LARGE-SCALE STRUCTURES AT $z \sim 3$

A very important avenue of research opened by the high efficiency of the Lyman-break technique is the possibility of studying galaxy clustering and large-scale structures in the young universe. The large samples yielded by the technique have well-controlled selection effects, and their redshift distribution function is measured with high accuracy, which makes them well suited for applications such as the correlation function and count statistics.

The strength of the spatial clustering of LBGs has been measured at $z \sim 3$ and 4 in a number of works, generally finding consistent results. Early reports of strong spatial clustering came from Giavalisco et al. (1994b) who observed a concentration of LBG candidates around the $z = 3.39$ damped Ly α absorber of

quasar Q000–2619 and estimated a spatial correlation length of $\sim 2.5 h^{-1}$ Mpc. Steidel et al. (1998) reported strong clustering in redshift space of spectroscopically confirmed LBGs and noticed a large spike of LBGs at $z \sim 3.01$ in one of their survey areas (the SSA22a field), which they suggested is likely a protocluster or possibly even a supercluster. Giavalisco et al. (1998) and Giavalisco & Dickinson (2001) measured the angular correlation function from a sample of ~ 1000 U -band dropouts from the ground-based survey and inverted it using the Limber transform (Peebles 1980, Efstathiou et al. 1991) to derive the spatial one, finding a correlation length $r_0 \sim 4 h^{-1}$ Mpc. This method is particularly efficient and accurate when, as in the case of the U -band dropouts, the redshift distribution function of the sample is known and the contamination by interlopers is essentially negligible. In this case, one can use the photometric samples, i.e., galaxies with and without spectroscopic redshifts, and take advantage of the larger numbers. Connolly et al. (1998) and Arnouts et al. (1999) used the same technique with samples from the HDF selected by photometric redshifts and reported strong clustering at $z > 2$. Adelberger et al. (1998) derived the spatial correlation length from the fluctuations of the number counts in spatial cells and found $r_0 \sim 6 h^{-1}$ Mpc, higher than the value derived from the angular clustering, but consistent within the errors [a new application of the technique to a larger sample yielded $r \sim 4 h^{-1}$ Mpc, (K.L. Adelberger, private communication)]. This method has the advantage of including the information on the clustering along the radial (redshift) direction, which is lost in the angular projection, but it requires the knowledge of the redshift of the individual galaxies and hence it relies on smaller samples. More recently, Ouchi et al. (2001) extended these studies to redshift $z \sim 4$ using a sample of ≈ 1200 B -band dropouts from deep imaging with the Subaru telescope, and found a correlation length $r_0 \sim 3 h^{-1}$ Mpc.

Although the size of current LBGs samples is such that clustering measures could actually be made, these samples are still small in absolute terms. For example, the sample used by Giavalisco et al. (1998) only covers ~ 0.3 square degrees; in comparison, local samples are two orders of magnitude larger (e.g., 2dF). As a consequence, large fluctuations of volume density are still observed from sample to sample (e.g., Adelberger et al. 1998, Porciani & Giavalisco 2002). This means that the average volume density of LBGs is only broadly known, and the measure of the correlation is affected by bias, because its strength is normalized to the observed volume density and not to the true one, which is unknown. The direction of this integral constraint bias, which is notoriously difficult to estimate, is that the observed correlation is lower than the true one (Hamilton 1988). Porciani & Giavalisco (2002) carried out numerical simulations to test for the presence of the bias in the current samples and concluded that the measures are affected at least at the 15% level. Because the bias also affects the shape of the correlation (its slope, in the case of the power law model), detailed comparisons with the theory require larger samples. Another consequence of the relatively small samples is that the traditional statistics used in these works could yield crude measures of the shape of the correlation function, i.e., simultaneously give r_0 and the slope γ in the traditional power law approximation $\xi(r) = (r/r_0)^{-\gamma}$ (Peebles 1980).

Although the measure of r_0 was found to be robust, with a relative error $\sim 30\%$ (Giavalisco et al. 1998), the slope was much more loosely constrained, $\gamma = 2.0 \pm 0.7$ (Giavalisco et al. 1998, Giavalisco & Dickinson 2001) to compare with the local value $\gamma = 1.77 \pm 0.3$ (from 2dF). Porciani & Giavalisco (2002) use statistics based on the counts of galaxies in angular cells to minimize the effects of the shot noise. They again find $r_0 \sim 4 h^{-1}$ Mpc but, more importantly, also find evidence that a power law correlation function is a good approximation for the LBGs and estimate the slope to be $\gamma = 1.5 \pm 0.3$, apparently shallower than the local one.

Regardless of these problems, however, because the effect of the integral constraint is to bias the measures toward lower values, the conclusion that LBGs have strong spatial clustering seems a robust one. A correlation length $r_0 \sim 4 h^{-1}$ Mpc or higher at $z \sim 3$ directly compares with that found in local surveys, $r_0 = 5.7 h^{-1}$ Mpc (e.g., the SDSS measure). This cannot be explained in terms of the gravitational evolution of clustering alone in any reasonable cosmology that is normalized to reproduce the clustering of galaxies and clusters at $z = 0$ (e.g., Eke et al. 1996). This conclusion does not strongly depend on the shape of the power spectrum used to calculate the evolution or on the adopted cosmology; it is simply a direct consequence of the assumption that gravity drove the formation of structure. To reconcile the weak clustering of the mass predicted at $z \sim 3$ by the gravitational instability and the cluster normalization with the observed correlation function of LBGs, one has to conclude that the spatial distribution of LBGs is biased with respect to that of the mass, namely they preferentially trace regions of the mass-density distribution that are significantly more clustered than the average.

This conclusion has profound physical implications, because the theory predicts that such biased regions are collapsed perturbations of the mass-density field, or halos (Kaiser 1984, Bardeen et al. 1986). Thus, the strong clustering would imply a direct association between the most active regions of star formations and the halos, and this conclusion is solely based on the assumption of gravity as the primary physical interaction responsible for the formation of cosmic structures and on the empirical evidence that LBGs are strongly clustered in space.

The key paradigm behind our understanding of galaxy formation is that they form within dark matter halos when gas condenses and cools in the bottom of their potential well and is converted into stars (White & Rees 1978). The strong clustering observed among LBGs suggests that this paradigm can be tested, at least in broad lines, on empirical grounds. In the local universe the test is difficult, because the effects of bias are not very pronounced and the galaxies are evolved. For example, values of the bias estimated for the local mix of galaxies are in the range $b \sim 1-1.5$ (Peacock et al. 2001, Hamilton & Tegmark 2000), although galaxies of different type and luminosity cluster differently, with earlier type and more luminous galaxies being in general more clustered than later type and fainter ones. At high redshifts, the bias is much stronger and the galaxies are observed during a relatively early phase of formation, and measuring the clustering properties of LBGs offers the opportunity of testing fundamental ideas of galaxy formation.

The clustering properties of the dark matter are well understood from the theoretical point of view and the clustering and abundance of halos are relatively easily calculated, given a cosmological model, namely a power spectrum and the cosmological parameters (Mo & Fukugita 1996, Mo & White 1996, Kauffmann et al. 1997, Jing & Suto 1998, Governato et al. 1998, Baugh et al. 1999). The problem is that predicting the properties of the observable halos, namely the galaxies, is still highly uncertain, because it requires assumptions on the poorly understood mechanisms of star formation.

Some general features of the theory can be tested without modeling star formation, or with only very general assumptions. For example, Adelberger et al. (1998) showed that volume density and clustering strength of LBGs are very similar to those predicted for massive Cold Dark Matter (CDM) halos, roughly with $M > 10^{11} M_{\odot}$. Giavalisco & Dickinson (2001) found that fainter samples of LBGs (i.e., with fainter UV luminosity) cluster less strongly than brighter ones, and explored the scaling relationship between volume density and clustering strength, finding it to be in good agreement with that of the halos. This scaling law depends very weakly on the details of the relationship between star-formation activity and the properties of the halos, if the scatter between UV luminosity and total mass is small. Thus, this finding seems to imply that (a) LBGs trace the halos very closely, i.e., star formation occurs with high efficiency in collapsed structures; and (b) the star-formation rate is, on average, regulated by the mass of the galaxy, because less massive halos correlate less strongly than more massive ones. A further implication is that the mass spectrum of the observed samples of LBGs is approximately 10^{10} – $10^{12} M_{\odot}$. These conclusions, however, are all based on the evidence that the faint HDF sample of LBGs is less strongly clustered than the brighter ground-based one, with a correlation length ~ 3 times smaller. The HDF sample covers a volume of space nearly two orders of magnitude smaller than that of the ground-based survey, and although numerical simulations suggest that the detection of such weak clustering is significant at the $\sim 96\%$ confidence level, it needs confirmation with new observations.

More detailed comparisons require more sophisticated modeling of the star formation in the forming galaxies. In general, both N-body simulations that include the gas hydrodynamics (Katz et al. 1999) and semianalytical models (Governato et al. 1998, Baugh et al. 1998, Somerville et al. 2001, Wechsler et al. 2001) can successfully reproduce both the strong clustering and volume density of LBGs, suggesting that the paradigm of galaxy formation is correct in its broad lines. Differences mostly arise in the predictions of the mass spectrum of the galaxies, and these are clearly due to the different assumptions of the mechanisms of star formation. Semianalytical models that require merging as the primary trigger of star formation (Somerville et al. 2001, Wechsler et al. 2001, Mustakas & Somerville 2002) generally predict that the visible galaxies are systems of small mass that are substructures of more massive halos. N-body simulations where star formation is described in terms of the hydrodynamics of the baryonic gas tend to predict a larger mass spectrum, but the robustness of this prediction depends on the mass

resolution, which is still relatively poor. Some of these properties can, in principle, be tested by the observations, but the current samples are still too small for this. For example, the merging models predict a relatively high abundance of galaxies with close separations (Wechsler et al. 2001, Bullock et al. 2002) and a very mild dependence of the clustering strength with luminosity, whereas the observations are still too uncertain. Porciani & Giavalisco (2002) find a deficiency of close pairs (at the 98% level), at $z \sim 3$ that they interpret as evidence of the physical size of halos, whereas Ouchi et al. (2001) find an excess of pairs at $z \sim 4$; Giavalisco & Dickinson (2001) find weak clustering of faint LBGs, whereas Arnouts et al. (1999) claim the detection of strong clustering at $z > 2$ in the HDF, although based on a very small sample of 39 photometric redshifts.

It is also of interest to compare the high bias inferred for LBGs to that of the “faint blue galaxies” at $0.5 \lesssim z \lesssim 1$ (Efstathiou et al. 1991, Efstathiou 1995; see also Ellis 1997, Le Fevre et al. 1996, Carlberg et al. 1997). These galaxies, which as the LBGs host the bulk of the cosmic star-formation activity (as traced by the UV light) at their epoch (Lilly et al. 1995, Madau et al. 1996), have correlation lengths comparable to that of LBGs and about one half that of the local galaxies. However, because the clustering of the mass at $z \sim 1$ is larger than at $z \sim 3$, their bias is smaller than that of the LBGs by approximately a factor of 2. In the local universe, the average bias is estimated to be in the range 1 to 1.5 (Peacock et al. 2001, Peacock 1997, Katz et al. 1999, Hamilton & Tegmark 2000). Thus, the bias of galaxies that host most of the star formation at their epoch appears to be decreasing in going from high to low redshift, in qualitative agreement with the predictions of biased galaxy formation that galaxies form first and more efficiently in the denser and more massive peaks of the mass-density field. Star formation then propagates to the less dense and less massive halos during the course of evolution.

Clusters at High Redshifts?

A number of groups have reported detection of concentrations of galaxy-size objects at $z > 2$ that could be young clusters of galaxies observed at an early stage of evolution. Most of these detections come from narrow-band imaging targeting Ly α emission from companions of known high-redshift objects such as QSO, QSO absorbers, and radio galaxies (see, among others, Pascarelle et al. 1996a,b, 1998; Campos et al. 1999; Carilli et al. 1998a,b; Pentericci et al. 2000; Francis et al. 1997; see also Dickinson 1997, 2000). Lyman-break galaxy surveys have also returned candidate protoclusters, observed as marked overdensities, or spikes, in the redshift distribution of the galaxies in a given field. Virtually every field has yielded at least one such detection (Steidel et al. 1998, Adelberger et al. 1998).

One of the most conspicuous of these candidate protoclusters or superclusters of LBGs, located at $z = 3.09$, has been studied in greater detail. The structure extends spatially over several h^{-1} Mpc (comoving) and, down to a flux limit of $\mathcal{R} = 25.5$, includes 67 LBGs. Follow-up narrow-band imaging of the cluster that targets the Ly α emission of its galaxies revealed many more members, and showed

that it possibly contains two substructures. These are physically coincident with two sources of very large ($\sim 100 h^{-1}$ kpc), diffuse Ly α emission. One of these hosts a source that is very red and very faint in the rest-frame UV and optical wavelengths (Steidel et al. 2000) but rather bright at submillimeter wavelength (Chapman et al. 2001) consistent with a massive proto elliptical galaxy.

THE MASS SPECTRUM

A key measure in galaxy evolution is the evolution of the mass spectrum. As is the case at any redshift, measuring the mass of galaxies is affected by large uncertainties, and at $z \sim 3$ the situation is made worse by the generally increased difficulty of carrying out the relevant observations. Currently, there are no robust constraints to the mass spectrum or even individual masses of LBGs from direct measures. Crude estimates of mass for a few LBGs are available from the kinematic of optical nebular emission lines, and from the measure of the stellar mass under the assumption of the stellar-to-total mass ratio. Other crude estimates of the mass spectrum come from the observed spatial clustering.

Line Emission Kinematics and the Total Mass

A number of groups (Pettini et al. 1998, 2001; Kobulnicky & Koo 2000; Teplitz et al. 2000a,b; Moorwood et al. 2000) observed the optical emission lines of [OII], H β , and [OIII] with near-IR spectroscopy for about 20 LBGs with the goal of deriving dynamical information on these galaxies from their kinematics. The lines have been resolved in every case, and all groups report values of the FWHM of the lines in the range 200–400 km s $^{-1}$, which if interpreted as due to rotation, corresponds to rotation velocity in the range of 60–120 km s $^{-1}$ (similar values are obtained if the linewidth is interpreted as due to velocity dispersion). Pettini et al. (2001) and Moorwood et al. (2000) also find possible evidence of rotation curves in the spatially resolved spectra of two of their galaxies.

Images at rest-frame optical wavelengths of LBGs taken with HST/NICMOS show that this velocity comes from radii of a few kpc, implying that it is smaller than the rotation velocity of local bright galaxies at similar radii (e.g., Sofue & Rubin 2001). Assuming that the line broadening is due to ordered gravitational motions, either due to rotation or velocity dispersion, and using the observed size of LBGs from HST imaging, all groups derived virial mass $M_{vir} = v^2 \times r_{1/2} / G$ in the range 10^{10} to $10^{11} M_{\odot}$. This is between 1/10 and 1/100 of the total mass within the optical diameter of a typical L^* galaxy in the local universe and compares to the mass of the bulge of a bright spiral (e.g., Dwek et al. 1995, Sofue & Rubin 2001) and low- to intermediate-luminosity ellipticals (Bender et al. 1992).

It is important to realize that these measures are very likely affected by large and uncontrolled systematics, and must be used with caution. For example, if LBGs are rotation-supported disks, the limited dynamic range in surface brightness of these spectra due to the $(1+z)^4$ dimming would result in only the central part

of the rotation curve being reasonably well observed. Because the spectra are spatially only partially resolved, the total flux is dominated by the central regions of the galaxy. Thus, the velocity width is effectively luminosity-weighted, and dominated by the brightest regions. The derived rotation velocity, therefore, will be systematically lower than its true value. Furthermore, to measure the rotation velocity one needs to align the spectrograph's slit with the semi-major axis of the galaxy and also to estimate the inclination of the disk on the plane of the sky, otherwise the observed velocity is underestimated. This requires morphological information from suitable high-resolution imaging, e.g., HST that was not available for any but one of the galaxies observed by Pettini et al. (2001) and Kobulnicky & Koo (2000), and in both cases, no clear evidence of a disk-like morphology was found.

Another serious problem is that it is unknown if nebular emission lines can be used as dynamical indicators in starburst galaxies. One source of uncertainty is the extent to which the brightest emitting HII regions trace the dynamics of the whole structure. If they segregate in the central regions, this leads to underestimating the rotation velocity and hence the mass. Another problem is the kinematic structure of the HII gas, namely the relative importance of integrated ordered motions of gravitational origin vs. nongravitational motions and turbulence generated by the activity of star formation, such as super-winds and SNe ejecta. If nongravitational motions significantly contribute to the observed linewidth, they lead to overestimation of the rotation velocity. Weedman (1983) noted that the width of emission lines in starburst nuclei were small compared to expectations for gas in virial equilibrium in the bulge of spiral galaxies. Lehnert & Heckman (1996) also found no correlation between the FWHM of the linewidths measured from the nuclear spectra and the galaxy rotations in a sample of IR-selected edge-on starburst galaxies and conclude that the narrow nuclear lines arise because the gas in nuclei where most of the starburst activity takes place does not sample the full range of the rotation curves. On the one hand, Kobulnicky & Gebhardt (2000) find that gaseous and stellar kinematic tracers in a sample of local late-type galaxies with ongoing star formation have comparable line broadening. In particular, they find the [OII] λ 3727 and the HI 21-cm emission line to have the same width, with an observed dispersion of only $\sim 20 \text{ km s}^{-1}$. Pisano et al. (2001), on the other hand, find that in nearby compact blue galaxies the linewidth of the [OII] line is systematically narrower than that of the HI line, with the ratio of the two widths being on average $W_{[\text{OII}]} / W_{\text{HI}} \sim 0.6$. By comparing HI and H α kinematics, Barton & van Zee (2001) showed that the optical line grossly underestimates the rotation velocity of galaxies with centrally concentrated starbursts. They also showed that even the spatial size is usually underestimated in these systems, which together with the measure of the velocity, leads to grossly underestimating the mass.

Overall, all these works suggest that, at least in local galaxies, nebular line kinematics tends to underestimate the virial mass, and that there is no evidence that strong nongravitational motions contribute to the kinematics of the lines. Whether this condition applies to LBGs as well is not known. Pettini et al. (2001) compared

the redshifts of interstellar gas, HII gas, and Ly α of LBGs and concluded that large-scale outflows of several hundreds km s⁻¹ exist in these systems. However, it is not known what this implies for the kinematics of the nebular gas.

For pressure-supported systems, projection and slit alignment are not factors. Unfortunately though, virtually nothing is known about the kinematics of the HII gas in these systems. Because the gas is highly collisional, for example, it is not inconceivable that cloud-cloud collisions in the dense central regions shock the HII gas and bring it to high temperature ($T \sim 10^6$ K), resulting in depressed line emission in the core of the galaxies. In this case, the observed linewidth would only carry information on the dynamics of the less dense and more external regions, where the stellar velocities are smaller, biasing the measure of the velocity dispersion toward low values. Both the observed rest-frame UV (Giavalisco et al. 1996b,c Steidel et al. 1996a, Lowenthal et al. 1997, Dickinson 1998) and optical (Calzetti & Giavalisco 2001) images taken with HST show light profiles and morphology that are consistent with spheroids in some cases or disks in others. However, often the morphology is simply irregular and fragmented, essentially offering no clues as to the dynamical status of the galaxies. In one case, spectroscopy of a bright galaxy with an apparent edge-on, disk-like morphology (HDF 4-555, Spinrad et al. 1999; H. Spinrad, private communication) failed to return conclusive results.

Stellar Mass and Total Mass

Crude estimates of the total mass of individual LBGs can be obtained from the measure of stellar mass discussed above (Papovich et al. 2001, Shapley et al. 2001), with assumptions of the stellar-to-total mass ratio (shown here as m_{s2t}). An L^* galaxy in the local universe contains $M_{star} \sim 10^{11} M_{\odot}$ worth of stars (Cole et al. 2001) and has a total mass around $M_{tot} \sim 10^{12} M_{\odot}$, although the latter is known only approximately. It actually depends on the radius within which the mass is being measured, because most rotation curves are nearly flat up to the largest observed radii. For example, the Milky Way has a total mass of $\sim 10^{11} M_{\odot}$ interior to the orbit of the Sun (Sofue & Rubin (2001) and $\approx 6 \times 10^{11} M_{\odot}$ interior to the distance of the LMC (Wilkinson & Evans 1999). Rotation curves of galaxies of similar luminosity give comparable mass values (Sofue & Rubin 2001). Measures based on weak lensing (Fischer et al. 2000) probe the mass within a few hundred kpc radii and yield larger values, $\approx 3 \times 10^{12} M_{\odot}$ for an L^* galaxy (Smith et al. 2001, Wilson et al. 2001a,b), which is consistent with estimates of the Galaxy mass based on its satellite galaxies (Zaritsky & White 1994).

Thus, local galaxies have stellar-to-total mass ratios in the range $m_{s2t} \approx 10$ –30, depending on the radial distance that the specific technique targets.⁴ Assuming

⁴An upper limit to this number can be set from the ratio of the cosmic mass density $\Omega_m \sim 0.3$ to the baryon density $\Omega_b \sim 0.03$ (e.g., Balbi et al. 2000, 2001) multiplied by the fraction of baryons locked in star $f_b \sim 17\%$ (Fukugita et al. 1998), which yields $m_{s2t} \approx f_s \times \Omega_m / \Omega_b = 60$.

$m_{s2t} = 10$, namely the value found within the optical diameter of local galaxies, the stellar mass fits by Papovich et al. (2001) and by Shapley et al. (2001) translate into a total mass of LBGs in the range 10^{10} to $10^{12} M_{\odot}$.

Measures of the total mass-to-light ratio at large radial distances ($r \lesssim 260$ kpc) for galaxies at moderate redshifts as a function of luminosity and galaxy type have become recently available from weak lensing observations (McKay et al. 2001). In the (rest-frame) B and V bands, this ratio depends on the galaxy type, and it increases toward earlier types. However, at wavelengths larger than about 6000 \AA , it appears to reach a minimum at ≈ 100 (in solar units) and to be independent of the galaxy type, indicating that variations of stellar population composition have become negligible. LBGs, however, are forming stars at higher rates than starburst galaxies at moderate redshift (Madau et al. 1996, Steidel et al. 1999) and have a lower stellar mass-to-light ratio than local spirals and irregulars, approximately by a factor of 2 (see Figure 12). In other words, they are on average twice as luminous for a given amount of stellar mass. Thus, an estimate of the total mass-to-light ratio for these galaxies is derived by dividing by 2 the value 100 at 6000 \AA discussed above, namely ~ 50 (in solar units). The total mass is then estimated by multiplying this number by the observed rest-frame B -band luminosity reported by Papovich et al. (2001) and Shapley et al. (2001). The mass found in this way is in the range $10^{11} < M_T < 10^{13} M_{\odot}$ (see Figure 13), significantly larger than the estimates of dynamical mass discussed above. In the local universe, this mass range is typical of relatively massive galaxies.

Spatial Clustering and the Mass Spectrum

Another crude estimate of the mass spectrum of LBGs comes from their spatial clustering. This estimate relies on the interpretation that the observed large correlation length of LBGs at $z \sim 3$ and $z \sim 4$ (Steidel et al. 1998, Giavalisco et al. 1998, Adelberger et al. 1998, Arnouts et al. 1999, Giavalisco & Dickinson 2001, Porciani & Giavalisco 2002, Ouchi et al. 2001) is due to the clustering bias of collapsed structures (halos) relative to the average mass density distribution (Mo & White 1996, Jing & Suto 1998, Governato et al. 1998, Somerville et al. 2001). As we discussed in “Clustering and Large-Scale Structures at $z \sim 3$,” above, for a given power spectrum, the volume density, and the spatial correlation length of the halos, to first order, are only a function of the mass of the halos (Press & Schechter 1974, Mo & White 1996). The estimate is done by solving for the mass spectrum of halos that simultaneously reproduces the observed volume density (corrected for incompleteness) and correlation length of LBGs (Giavalisco et al. 1998, Adelberger et al. 1998, Bullock et al. 2002, Giavalisco & Dickinson 2001, Porciani & Giavalisco 2002). For the U -band dropouts of the ground-based and HDF surveys, it is found approximately $5 \times 10^{10} < M < 5 \times 10^{12} M_{\odot}$. This is in broad agreement with the mass derived from the stellar mass distribution, and therefore, in disagreement with that derived from the dynamical measures.

Key elements in this derivation are robust measures of the spatial correlation length and volume density, and also knowledge of how many LBGs are observed,

on average, in each halo, i.e., the amount of substructure (one LBG per halo was assumed above). This last parameter is important, because significant substructure means that many LBGs are bound satellites of massive halos. In such a case, whereas such halos still have to be rather massive to satisfy the observed strong clustering ($M \gtrsim 10^{11} M_{\odot}$), the implied mass of the individual galaxies is generally small, e.g., $\gtrsim 10^9 M_{\odot}$ (Kolatt et al. 1999, Somerville et al. 2001, Wechsler et al. 2001, Bullock et al. 2002, Moustakas & Somerville 2002). Currently, the amount of substructure is poorly constrained. Porciani & Giavalisco (2002) report the possible deficiency of close pairs of LBGs of the ground-based sample, which would imply that bright LBGs have no multiplicity. However, Ouchi et al. (2001) report an excess of close pairs at $z \sim 4$, which would imply the opposite conclusion. The multiplicity will be quantified as a function of luminosity in the upcoming large-area surveys of LBGs from HST. This will considerably help reconstruct the mechanisms of formation of massive galaxies, i.e., whether a significant fraction of the stellar and total mass were already in place at $z \sim 3$ or whether the total mass was but the stellar mass was not and it accreted later by hierarchical merging of small satellites.

LOOKING AT THE BIG PICTURE

The large samples afforded by the Lyman-break technique have given us the first systematic and quantitative picture of normal galaxies in the high-redshift universe, selected because they are forming stars and not by properties related to their nuclear activity. Sources selected by their prominent Ly α or submillimeter emission also include normal galaxies in this sense. However, except for a handful of cases, their continuum emission is too faint or their optical counterparts too uncertain to allow us to study their properties at the same level of detail that has been possible to do with LBGs.

We have seen that normal galaxies at high redshifts look very different from the normal galaxies of the present-day universe, and the question is which evolutionary path, if any, links these two distant populations together. In this regard, one thing to keep in mind is that stars that have formed at $z > 2$ are, by necessity, very old today. If we see them in today's normal galaxies, they must be part of the oldest stellar populations, and hence be the components of the spheroids (elliptical and S0 galaxies, and bulges) as well as of the disks of early spiral galaxies (Dressler & Gunn 1992; Wyse et al. 1998; Renzini 1998, 1999). Today, between 50% and 70% of all the stars are in spheroids and the remainder in the disks of spirals and in later-type galaxies (Schechter & Dressler 1987, Persic & Salucci 1992, Fukugita et al. 1998). Thus, if the association between LBGs and today's old stellar populations is correct, LBGs must have hosted a large fraction of the star formation that took place at their epoch. The flatness of the Madau diagram (Madau et al. 1998, Steidel et al. 1999) or even its possible increase toward the highest observed redshifts (Lanzetta et al. 2001), implies that LBGs at $z > 2$ are responsible for a large fraction, between ≈ 30 and 60% depending on the uncertain corrections of dust obscuration, of all the cosmic star formation that can be observed through its UV emission. What

needs to be established to test the consistency of this picture is how much star formation at high redshift remains undetected with UV observations because it is hidden by large amounts of dust.

Powerful starburst galaxies such as Arp 220 and other ULIRGs, for example, would not be observed as LBGs if placed at $z > 2$, because their UV-spectral energy distribution is too reddened and obscured by dust to satisfy the color selection criteria. At submillimeter wavelengths, they can be observed up to redshift $z \sim 10$ or so. In the local universe, galaxies such as Arp 220 contribute only a small fraction of the total stellar production, which is dominated by starburst galaxies, spirals, and other later types. These galaxies were evolving very rapidly in the past, however, and their volume density, and correspondingly, their contribution to the cosmic star-formation density increased by almost a factor 10^3 from $z = 0$ to $z \sim 2$, as illustrated in Figure 7, reproduced from Barger et al. (2000). Whereas UV-bright starburst galaxies also show considerable evolution over the same epoch (Madau et al. 1996, Steidel et al. 1999), this is not as strong as that of the ULIRGs, because the star-formation density traced by the UV light increases about 10 times from $z = 0$ to $z \sim 1$. Thus, it is not completely clear which of the two species of star-forming galaxies has given the largest contribution to the cosmic star-formation activity.

As we discussed in “Other Starburst Galaxies at High Redshifts,” if the measure of the submillimeter background and of the faint SCUBA number counts, and if the correction for dust obscuration of LBGs are not all grossly wrong, faint SCUBA galaxies and LBGs seem to trace the same population of star-forming galaxies. At the highest submillimeter flux (> 6 mJy), a large fraction of the sources are ULIRGs, hence very faint (and red) in the UV and not detected as LBGs because of the extreme dust obscuration. At fainter flux (approximately > 2 mJy), the fraction of ULIRGs decreases and some UV-bright starbursts appear among the SCUBA counts, while at faint flux (< 2 mJy), the counts are dominated by UV-bright starbursts observed as LBGs. The data, however, are hardly accurate enough to accept or reject such an interpretation with high confidence. Others have proposed that the SCUBA sources include a population of heavily obscured powerful starburst galaxies at high redshift that are not significantly present in the UV-selected surveys. These high-redshift ULIRGs would be responsible for the submillimeter background and hosted the bulk of star formation at their epoch. They would be the progenitors of the massive spheroids (Barger et al. 1998; Lilly et al. 1999; Smail et al. 1999, 2000) that formed either during the monolithic collapse of a massive structure or during a major merging event. In comparison, LBGs would be the sites of more quiescent and prolonged star formation that would lead to spheroids of smaller mass and to the old stellar populations presently observed in disks. Progress in this area will have to wait for new submillimeter facilities of increased sensitivity and angular resolution.

The morphology of LBGs only offers limited clues to discriminate between these two scenarios, but it is not inconsistent with either. The sizes of the galaxies are consistent with the interpretation that they have formed the central regions

of today's bright galaxies, particularly considering that they are very likely lower limits of the true ones owing to the large $(1+z)^4$ surface brightness dimming. Light profiles that, in some cases, are reminiscent of elliptical galaxies, and in other cases, of exponential disks (see Figure 10), with possible evidence of rotation curves are also broadly consistent with this scenario. More generally, however, these galaxies show a fragmented and irregular morphology (Giavalisco et al. 1996c, Steidel et al. 1996a) that cannot be classified in terms of the Hubble sequence. This is in line with the general result that, at any redshift, the morphology of starburst galaxies (or at least of the starbursting stellar population that dominated the UV/optical luminosity) is considerably more fragmented and less regular than the underlying optical morphology (Giavalisco et al. 1996b; Hibbard & Vacca 1997; Kuchinski et al. 2001, 2000; Marcum et al. 2001) and is not very useful to constrain their subsequent evolution. It does tell, however, that the morphological differentiation of galaxies into the Hubble sequence occurred later than the epochs at which LBGs are being observed, which are still poorly studied from an empirical point of view.

The estimate of the spectrum of stellar mass (Shapley et al. 2001, Papovich et al. 2001) implies that a significant fraction of LBGs, already at $z \sim 3$, have stellar masses not much smaller than those found in today's bright galaxies, such as large bulges or elliptical galaxies of intermediate luminosity (see Figure 10). Combining the stellar mass distribution with the estimate of the rest-frame B -band luminosity function (Shapley et al. 2001) shows that a substantial number of stars have assembled in LBGs at $z > 2$, which supports the notion of an evolutionary link between LBGs and today's spheroids. Dickinson et al. (2002, submitted) estimate that between $\approx 1/10$ and $\approx 1/3$ of the current cosmic stellar mass density has been assembled in LBGs at $z > 2$. The suggestion is that the most massive LBGs could have already assembled the bulk of the stellar mass and the body of the final structure at $z \sim 3$, and have evolved almost passively from then. This is consistent with the discovery of passively evolving old galaxies at redshift as high as $z \sim 1.6$ (Cimatti et al. 2002) and with the observation that some LBGs have the star-formation history and metal enrichment pattern of massive bursts of star formation (Pettini et al. 2002). The less massive LBGs can have either given origin to today's smaller galaxies or merged into larger systems. Recall, however, that the frequent occurrence of fragmented morphology among LBGs does not necessarily imply that they are starbursts triggered by merging and interactions, although this can be true in some cases. The fragments that are often observed in the images of LBGs, which are compact star-forming regions that segregate a considerable fraction of the total star-formation rate of the galaxy (Giavalisco et al. 1996c, Steidel et al. 1996a), are virtually always observed on spatial scales of a few kiloparsec, corresponding to less than an arcsec in the images. Models of merging-triggered starbursts for LBGs predict an excess of galaxy pairs over tens to hundreds kiloparsec (Bullock et al. 2002), i.e., over tens of arcsec, but there is no clear evidence that this is observed in the data. Porciani & Giavalisco (2002) claim a deficiency of pairs of U -band dropouts over these scales relative to the

small-scale extrapolation of the angular correlation function, whereas Ouchi et al. (2001) claim an excess of pairs of B -band dropouts.

The estimate of the total mass (baryonic plus nonbaryonic) remains highly uncertain. Taken at face value, measures of the dynamical mass from the kinematics of optical emission lines yield small values, between 10^9 to $10^{10} M_{\odot}$, or about 1/1000 to 1/100 that of present-day L^* galaxies, and comparable to the stellar mass of bulges. However, it is unknown if the optical nebular lines can be used as reliable dynamical indicators in these galaxies, and the few works that have explored this issue in local star-forming spiral galaxies have shown that these spectral features generally underestimate the magnitude of the rotation traced by the HI gas. Furthermore, because of the lack of morphological information on the galaxies for which dynamical measures have been attempted, the estimates of the mass are only lower limits.

The clustering properties imply a larger mass range, in the range $10^{11} < M < 10^{13} M_{\odot}$, about a factor of 100 larger than the dynamical estimates (Giavalisco & Dickinson 2001, Porciani & Giavalisco 2002, Wechsler et al. 2002, Bullock et al., Moustakas & Somerville 2002). This conclusion, however, depends on the assumption that there is essentially a one-to-one correspondence between LBGs and dark matter halos, at least at the observed luminosity. If more substructure is present, i.e., if more LBGs are associated with the same halo, the above mass range is only valid for the halos, whereas the visible galaxies (which are bound satellites of the massive halos) would be considerably less massive, e.g., $M \gtrsim 10^9 M_{\odot}$ (Somerville et al. 2001, Wechsler et al. 2001, Bullock et al. 2002, Somerville & Moustakas 2002). These conclusions seem robust, regardless of the specific assumptions on star-formation activity and the properties of the halos. Whereas current direct constraints to the amount of substructure are not conclusive (Porciani & Giavalisco 2002, Ouchi et al. 2001, Bullock et al. 2002), this situation should rapidly improve with upcoming new surveys. Regardless however, the conclusion that the clustering properties of LBGs imply that the bulk of star formation at $z \sim 3$ has occurred in association with relatively massive systems seems to hold. Finally, despite the large uncertainty involved, the spectrum of total mass inferred from the stellar mass (under assumptions of M/L ratio) is comparable to that derived from the clustering properties (see Figure 13).

Although estimates of the age of the stellar populations from fitting star-formation history are highly uncertain (Casey et al. 2001, Shapley et al. 2001), the range of values that has been found is generally consistent (given the observed star-formation rates) with both the presence of massive galaxies, and with the presence of smaller galaxies or even subgalactic fragments that will merge into large systems. The claim by Shapley et al. (2001) of a correlation between age, star-formation rate, and obscuration is in qualitative agreement with this picture. According to this interpretation, galaxies undergo an initial phase of very intense but short-lived star formation where their UV radiation is relatively highly obscured by large amounts of dust, and then they enter a phase with lower—but still high in absolute terms—star-formation rates that lasts for $\sim 10^9$ yr and is characterized by lower dust obscuration. This is consistent with the assembly of the spheroidal

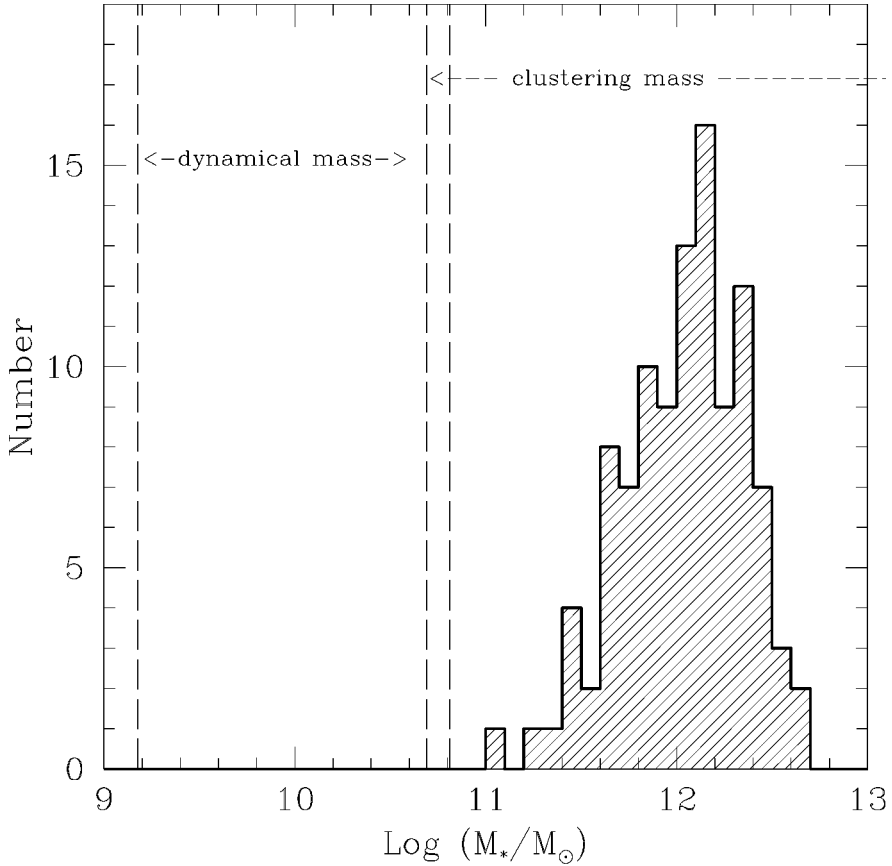


Figure 13 Histogram of the total mass of LBGs derived from the total mass-to-light ratio of field galaxies observed from weak gravitational lensing experiments (McKey et al. 2002) corrected by the ratio of the stellar mass-to-light ratio of LBGs to that of irregular galaxies (see text). Also shown are the range of dynamical mass derived from the kinematics of the optical nebular emission lines and the range of mass derived from the clustering properties.

component of spiral galaxies and the subsequent formation of the disk (Eggen et al. 1962). The crude estimate of metallicity currently available for LBGs are also qualitatively consistent with a large fraction of the stellar mass of the oldest populations of present-day galaxies being assembled at $z > 2$.

A rather important point is that the current data indicate that the UV-luminous galaxies at $z \sim 4$ are similar to those at $z \sim 3$. Whereas there is not a large wavelength basis for measuring the UV continua of the $z \gtrsim 4$ galaxies, the assumption that they have the same distribution of intrinsic SED observed at $z \sim 3$ results in a predicted redshift and luminosity distribution that are consistent with the spectroscopic redshifts and the observed luminosity function. Thus, there is no empirical

ground to support a decline of the star-formation activity for redshifts $z > 1$, a fact that pushes the detection of the onset of the dark age of the universe at $z > 5$, in qualitative agreement with the recent suggestion based on the Gunn-Peterson (1965) troughs of distant QSO that the reionization might have happened at $z > 6$ (Becker et al. 2001, Djorgovsky et al. 2001).

Another very important result is the strong spatial clustering of LBGs. This has provided empirical evidence of the general robustness of one of the fundamental ideas about galaxy formation, namely the association between massive virialized structures (the halos) and the activity of star formation, by showing evidence of the reality of galaxy biasing. This is much more difficult to test in the local universe, where the light on average traces the distribution of mass (Peacock et al. 2001). A key observation in this regard is the report that the clustering strength of LBGs scales with their UV luminosity (Giavalisco & Dickinson 2001), which seems to show that the scaling law of the clustering strength and volume density of the galaxies is similar to that predicted for the halos by the gravitational instability theory. It also implies that, on average, the star-formation rate of the galaxies depends more strongly on their total mass, namely on the local gravity, than it does on external accidents such as interactions and merging. Currently, this evidence is based on the measure of the spatial correlation function of the HDF sample, which is small and has an associated large uncertainty. Given its importance, it will be the subject of a careful test during upcoming, much larger surveys from the ground and HST.

Surveys of LBGs have finally opened a wide window on the universe of galaxies, covering most (if not all) of the cosmic time where galaxies are plausibly expected to exist, and have demonstrated that at least our basic ideas about how galaxies form are holding up reasonably well. There is enormous potential for progress in the area of understanding galaxy and structure formation in extending these surveys with larger samples, thus reducing the effects of cosmic variance that still makes many of the results that we have been discussing uncertain, and covering a larger redshift range to study their evolution. Detector technology is maturing to the point where a systematic exploration of the redshift range $1 < z < 10$ is becoming realistic, and telescopes and instrumentation, either space-borne or ground-based, seem to promise to let us do just this with less effort than it took us to confirm the first color-selected galaxy at redshift ~ 3.5 not even ten years ago.

**The Annual Review of Astronomy and Astrophysics is online at
<http://astro.annualreviews.org>**

LITERATURE CITED

- Abraham RG, Merrifield MR, Ellis RS, Tanvir NR, Brinchmann J. 1999. *MNRAS* 308:569
- Abraham RG, Van Der Bergh S, Glazebrook K, Ellis RS, Santiago X, et al. 1996. *Ap. J. Suppl.* 107:1
- Adelberger KL, Steidel CC. 2000. *Ap. J.* 544: 218
- Adelberger KL, Steidel CC, Giavalisco M, Dickinson M, Pettini M, Kellogg M. 1998. *Ap. J.* 505:18

- Alonso-Herrero A, Engelbracht CW, Rieke MJ, Rieke GH, Quillen AC. 2001. *Ap. J.* 546:952
- Arnouts S, Cristiani S, Moscardini L, Matarrese S, Lucchin F, et al. 1999. *MNRAS* 310:540
- Baade W. 1958. In *Stellar Populations*, ed. DJK O'Connell, p. 3. Amsterdam: North Holland
- Balbi A, Ade P, Bock J, Borrill J, Boscaleri A, et al. 2000. *Ap. J.* 545:1
- Balbi A, Ade P, Bock J, Borrill J, De Bernardis P, et al. 2001. *Ap. J.* 558:145
- Bardeen JM, Bond JR, Kaiser N, Szalay AS. 1986. *Ap. J.* 304:15
- Barger AJ, Aragon-Salamanca A, Smail I, Ellis RS, Couch WJ, et al. 1998. *Ap. J.* 501:522
- Barger AJ, Cowie LL, Richards EA. 2000. *Astron. J.* 119:2092
- Barger AJ, Cowie LL, Sanders DB. 1999a. *Ap. J.* 518:5
- Barger AJ, Cowie LL, Smail I, Ivison RJ, Blain AW, Kneib JP. 1999b. *Astron. J.* 117:2656
- Barton EJ, van Zee L. 2001. *Ap. J.* 550:35
- Baugh CM, Benson AJ, Cole S, Frenk CS, Lacey CG. 1999. *MNRAS* 305:21
- Baugh CM, Cole S, Frenk CS, Lacey CG. 1998. *Ap. J.* 498:504
- Becker RH, Fan XH, White RL, Strauss MA, Narayanan VK, et al. 2001. *Astron. J.* 122:2850
- Beckwith SV, Thompson D, Mannucci F, Djorgovski SG. 1998. *Astron. J.* 116:1591
- Bender R, Burnstein D, Faber SM. 1992. *Ap. J.* 399:462
- Blain AW, Ivison RJ, Smail I. 1998. *MNRAS* 296:29
- Blain AW, Smail I, Ivison RJ, Kneib JP. 1999a. *MNRAS* 302:632
- Blain AW, Smail I, Ivison RJ, Kneib JP. 1999b. *Ap. J.* 512:87
- Brinchmann J, Abraham R, Schade D, Tresse L, Ellis RS, et al. 1998. *Ap. J.* 499:112
- Brinchmann J, Ellis RS. 2000. *Ap. J.* 536:L77
- Broadhurst TJ, Ellis RS, Shanks T. 1988. *MNRAS* 235:827
- Bruzual G, Charlot S. 1993. *Ap. J.* 405:538
- Buat V. 1989. *Astron. Astrophys.* 220:49
- Bullock JS, Wechsler RH, Somerville RS. 2002. *MNRAS* 329:246
- Calzetti D. 1997. *Astron. J.* 113:162
- Calzetti D. 2001. *Publ. Astron. Soc. Pac.* 113:1449
- Calzetti D, Armus L, Bohlin RC, Kinney AL, Korneef J, Storchi-Bergmann T. 2000. *Ap. J.* 533:682
- Calzetti D, Giavalisco M. 2001. *Ap. Space Sci.* 277:609
- Calzetti D, Kinney AL, Storchi-Bergmann T. 1994. *Ap. J.* 429:582
- Campos A, Yahil A, Windhorst RA, Richards EA, Pascarelle S, et al. 1999. *Ap. J.* 511:1
- Carilli CL, Harris DE, Pentericci L, Rottgering HJA, Miley GK, Bremer MN. 1998a. *Ap. J.* 496:57
- Carilli CL, Harris DE, Pentericci L, Rottgering HJA, Miley GK, Bremer MN. 1998b. *Ap. J.* 494:143
- Carlberg RG, Cowie LL, Songaila A, Hu EM. 1997. *Ap. J.* 484:538
- Casertano S, de Mello D, Dickinson M, Ferguson HC, Fruchter AS, et al. 2000. *Astron. J.* 120:2747
- Chambers KC, Miley GK, van Breugel W. 1990. *Ap. J.* 363:21
- Chambers KC, Miley GK, van Breugel W. 1988. *Ap. J.* 327:47
- Chapman SC, Lewis GF, Scott D, Richards E, Borys C, et al. 2001. *Ap. J.* 548:17
- Chapman SC, Scott D, Steidel CC, Borys C, Halpern M, et al. 2000. *MNRAS* 319:318
- Charlot S, Fall SM. 1991. *Ap. J.* 378:471
- Charlot S, Fall SM. 1993. *Ap. J.* 415:580
- Chen H-W, Lanzetta KM, Pascarelle S. 1999. *Nature* 398:586
- Chen H-W, Lanzetta KM, Pascarelle S, Yahota N. 2000. *Nature* 408:6812
- Cimatti A, Daddi E, Mignoli M, Pozzetti L, Renzini A, et al. 2002. *Astron. Astrophys.* 381:L68
- Cohen JG, Blandford R, Hogg DW, Pahre MA, Shopbell PL. 1999. *Ap. J.* 512:30
- Cohen JG, Cowie LL, Hogg DW, Songaila A, Blandford R, et al. 1996. *Ap. J.* 471:5
- Cohen JG, Hogg DW, Blandford R, Cowie LL, Hu E, et al. 2000. *Ap. J.* 538:29
- Cole S, Norberg P, Baugh C, Frenk CS, Bland-Hawthorn J, et al. 2001. *MNRAS* 326:55

- Colless M, Ellis RS, Broadhurst TJ, Taylor K, Peterson BA. 1993. *MNRAS* 261:19
- Colless M, Ellis RS, Shaw G, Taylor K. 1991. *MNRAS* 253:686
- Colless M, Schade D, Ellis RS, Broadhurst TJ. 1994. *MNRAS* 267:1108
- Connolly AJ, Szalay AS, Brunner RJ. 1998. *Ap. J.* 499:125
- Connolly AJ, Szalay AS, Dickinson M, Subbarao MU, Brunner RJ. 1997. *Ap. J.* 486:11
- Cowie LL, Gardner JP, Hu HM, Songaila A, Hodapp KW, Wainscoat RJ. 1994. *Ap. J.* 434:11
- Cowie LL, Hu EM. 1998. *Astron. J.* 115:1319
- Cowie LL, Hu EM, Songaila A. 1995a. *Nature* 377:603
- Cowie LL, Hu EM, Songaila A. 1995b. *Astron. J.* 110:1576
- Cowie LL, Hu EM, Songaila A, Egami E. 1997. *Ap. J.* 481:9
- Cowie LL, Songaila A, Hu EM, Cohen JG. 1996. *Astron. J.* 112:839
- Cristiani S, Appenzeller I, Arnouts S, Nonino M, Aragon-Salamanca A, et al. 2000. *Astron. Astrophys.* 359:489
- Davis M, Wilkinson DT. 1974. *Ap. J.* 192:251
- Deharveng JM, Bowyer S, Buat V. 1990. *Astron. Astrophys.* 236:351
- Deharveng JM, Sassen TP, Buat V, Bowyer S, Lampton M, Wu X. 1994. *Astron. Astrophys.* 289:715
- De Propris R, Pritchett CJ, Hartwick FDA, Hickson P. 1993. *Astron. J.* 105:1243
- Dey A, Graham JR, Ivison RJ, Smail I, Wright GS, Liu MC. 1999. *Ap. J.* 519:610
- Dey A, Spinrad H, Stern D, Graham JR, Chaffee FH. 1998. *Ap. J.* 498:93
- Dey A, Van Breugel W, Vacca WD, Antonucci R. 1997. *Ap. J.* 490:698
- Dickinson M. 1997. In *The Early Universe with the VLT*, ed. J Bergeron, p. 274. Berlin: Springer-Verlag
- Dickinson M. 1998. STScI May Symp. Ser. 11, p. 219. New York: Cambridge Univ. Press
- Dickinson M. 2000. *Philos. Trans. R. Astron. Soc. London Ser. A* 358(1772):2001
- Dickinson M. 2000. In *Constructing the Universe with Clusters of Galaxies*, ed. F Durret, D Gerbal. Paris: IAP
- Dickinson M, Hanley C, Elston R, Eisenhardt PR, Stanford SA, et al. 2000. *Ap. J.* 531:624
- Djorgovski SG, Castro S, Stern D, Mahabal AA. 2001. *Ap. J.* 560:5
- Djorgovski SG, Pahre MA, Bechtold J, Elston R. 1996. *Nature* 382:234
- Djorgovski SG, Spinrad H, McCarthy P. 1985. *Ap. J.* 299:1
- Djorgovski SG, Strauss MA, Spinrad H, McCarthy PJ, Perley RA. 1987. *Astron. J.* 93:1318
- Djorgovski SG, Thompson DJ. 1992. *IAU Symp. No. 149*, p. 337. Dordrecht: Kluwer
- Dressler A, Gunn JE. 1992. *Ap. J. Suppl.* 78:1
- Driver SP, Fernandez-Soto A, Couch WJ, Odewahn SC, Windhorst RA, et al. 1998. *Ap. J.* 496:93
- Driver SP, Windhorst RA, Griffiths RE. 1995a. *Ap. J.* 543:48
- Driver SP, Windhorst RA, Ostrander EJ, Keel WC, Griffiths RE, Ratnatunga KU. 1995b. *Ap. J.* 449:23
- Dwek E, Arendt RG, Hauser MG, Kelsall T, Lisse CM, et al. 1995. *Ap. J.* 445:716
- Eales SA, Lilly S, Gear W, Dunne L, Bond JR, et al. 1999. *Ap. J.* 515:518
- Eales SA, Rawlings S. 1990. *MNRAS* 243:1
- Eales SA, Rawlings S. 1993. *Ap. J.* 411:67
- Eales SA, Rawlings S, Dickinson M, Spinrad H, Hill G, Lacy M. 1993a. *Ap. J.* 409:578
- Eales SA, Rawlings S, Puxley P, Rocca-Volmerange B, Kunth K. 1993b. *Nature* 363:140
- Efstathiou G. 1995. *MNRAS* 272:L25
- Efstathiou G, Bernstein G, Katz N, Tyson AJ, Guhathakurta P. 1991. *Ap. J.* 380:L47
- Eggen OJ, Lynden-Bell D, Sandage AR. 1962. *Ap. J.* 136:748
- Eke VR, Cole S, Frenk CS. 1996. *MNRAS* 282:263
- Ellis RS. 1997. *Annu. Rev. Astron. Astrophys.* 35:389
- Ellis RS. 1998. *Nature* 395:3
- Ellis RS, Colles M, Broadhurst T, Heyl J, Glazebrook K. 1996. *MNRAS* 280:235
- Ellis RS, Smail I, Dressler A, Couch WJ, Oemler A Jr, et al. 1997. *Ap. J.* 483:582

- Ferguson HC, Dickinson M, Williams R. 2000. *Annu. Rev. Astron. Astrophys.* 38:667
- Fernandez-Soto A, Lanzetta KM, Yahil A. 1999. *Ap. J.* 513:34
- Fischer P, McKay TA, Sheldon E, Connolly A, Stebbins A, et al. 2000. *Astron. J.* 120:1198
- Fixsen DJ, Dwek E, Mather JC, Bennett CL, Shafer RA. 1998. *Ap. J.* 508:123
- Folkes S, Ronen S, Price I, Lahav O, Colless M, et al. 1999. *MNRAS* 308:459
- Foltz CB, Chafee FH, Weymann RJ. 1986. *Astron. J.* 92:247
- Forster-Schreiber NM, Genzel R, Lutz D, Kunze D, Stemberg A. 2001. *Ap. J.* 552:544
- Francis PJ, Woodgate BE, Warren S, Moller P, Mazzolini M, et al. 1996. *Ap. J.* 457:490
- Francis PJ, Williger GM, Collins NR, Palunas P, Malumuth EM, et al. 2001. *Ap. J.* 554:1001
- Francis PJ, Woodgate BE, Danks AC. 1997. *Ap. J.* 482:25
- Frayser DT, Ivison RJ, Smail I, Yun MS, Armus L. 1999. *Astron. J.* 118:139
- Frayser DT, Smail I, Ivison RJ, Scoville NZ. 2000. *Astron. J.* 120:1668
- Frye B, Broadhurst TJ, Benitez N. 2002. *Ap. J.* 568:558
- Fukugita M, Hogan CJ, Peebles PJE. 1998. *Ap. J.* 503:518
- Fynbo JU, Moller P, Warren SJ. 1999. *MNRAS* 305:849
- Gallego J, Zamorano J, Aragon-Salamanca A, Rego M. 1995. *Ap. J.* 455:L1
- Genzel R, Lutz D, Sturm E, Egami E, Kunze D, et al. 1998. *Ap. J.* 498:579
- Giavalisco M, Dickinson M. 2001. *Ap. J.* 550:177
- Giavalisco M, Koratkar A, Calzetti D. 1996a. *Ap. J.* 466:831
- Giavalisco M, Livio M, Bohlin R, Macchetto F, Stecher T. 1996b. *Astron. J.* 112:369
- Giavalisco M, Macchetto FD, Madau P, Sparks WB. 1995. *Ap. J.* 441:L13
- Giavalisco M, Macchetto FD, Sparks WB. 1994a. *Astron. Astrophys.* 288:103
- Giavalisco M, Steidel CC, Adelberger KL, Dickinson ME, Pettini M, Kellogg M. 1998. *Ap. J.* 503:543
- Giavalisco M, Steidel CC, Macchetto FD. 1996c. *Ap. J.* 470:189
- Giavalisco M, Steidel CC, Szalay AS. 1994b. *Ap. J.* 425:5
- Glazebrook K, Abraham R, Santiago B, Ellis R, Griffiths R. 1998. *MNRAS* 297:885
- Glazebrook K, Ellis R, Colles M, Broadhurst T, Allington-Smith J, Tanvir N. 1995a. *MNRAS* 273:157
- Glazebrook K, Ellis R, Santiago B, Griffiths R. 1995b. *MNRAS* 275:19
- Goldader JD, Meurer G, Heckman TM, Seibert M, Sanders DB, et al. 2002. *Ap. J.* 568:651
- Governato F, Baugh CM, Frenk CS, Cole S, Lacey CG, et al. 1998. *Nature* 392:359
- Guhathakurta P, Tyson JA, Majewski SR. 1990. *Ap. J.* 357:9
- Gunn JE, Peterson BA. 1965. *Ap. J.* 142:1633
- Hamilton AJ. 1988. *Ap. J.* 331:L59
- Hamilton AJ, Tegmark M. 2000. *MNRAS* 312:28
- Hauser M, Arendt R, Kelsall T, Dwek E, Odegard N, et al. 1998. *Ap. J.* 508:25
- Heckman TM. 1996. In *The Interplay Between Star Formation the ISM and Galaxy Evolution*, ed. D Kunth, B Guiderdoni, M Heydari-Malayeri, T Xu Thuan, p. 159. Paris: Editions Frontieres
- Heckman TM. 2000. *Philos. Trans. R. Astron. Soc. London Ser. A* 358(1772):2077
- Heckman TM, Lehnert MD, Miley GK, van Breugel W. 1991a. *Ap. J.* 381:373
- Heckman TM, Miley GK, Lehnert MD, van Breugel W. 1991b. *Ap. J.* 370:78
- Heckman TM, Robert C, Leitherer C, Garnett DR, Van der Rydt F. 1998. *Ap. J.* 503:646
- Helou G. 1986. *Ap. J.* 311:L33
- Heyl J, Colless M, Ellis R, Broadhurst T. 1997. *MNRAS* 285:613
- Hibbard JE, Vacca WD. 1997. *Astron. J.* 114:1741
- Hogg DW, Cohen JG, Blandford R, Pahre MA. 1998. *Ap. J.* 504:622
- Hu EM, Cowie LL. 1987. *Ap. J.* 317:L7
- Hu EM, Cowie LL, McMahan RG. 1998. *Ap. J.* 502:99
- Hu EM, McMahan RG. 1996. *Nature* 382:281

- Hu EM, McMahon RG, Cowie LL. 1999. *Ap. J.* 522:9
- Hu EM, McMahon RG, Egami E. 1996. *Ap. J.* 459:53
- Hughes DH, Serjeant S, Dunlop J, Rowan-Robinson M, Blain A, et al. 1998. *Nature* 394:241
- Hunstead RW, Fletcher AB, Pettini M. 1990. *Ap. J.* 356:23
- Hurwitz M, Jelinsky P, Dixon WVD. 1997. *Ap. J.* 481:31
- Iverson RJ, Dunlop JS, Hughes DH, Archibald EN, Stevens JA, et al. 1998. *Ap. J.* 494:211
- Iverson RJ, Smail I, Barger AJ, Kneib JP, Blain AW, et al. 2000. *MNRAS* 315:209
- Jing YP, Suto Y. 1998. *Ap. J.* 494:5
- Kaiser N. 1984. *Ap. J.* 284:9
- Katz N, Hernquist L, Weinberg DH. 1999. *Ap. J.* 523:463
- Kauffmann G, Nusser A, Steinmetz M. 1997. *MNRAS* 286:795
- Kennicutt RC. 1989. *Ap. J.* 344:685
- Kennicutt RC. 1998. *Annu. Rev. Astron. Astrophys.* 36:189
- Kobulnicky HA, Gebhardt K. 2000. *Astron. J.* 119:1608
- Kobulnicky HA, Kennicutt RC, Pizagno JL. 1999. *Ap. J.* 514:544
- Kobulnicky HA, Koo DC. 2000. *Ap. J.* 545:712
- Kolatt TS, Bullock JS, Somerville RS, Sigad Y, Jonsson P, et al. 1999. *Ap. J.* 523:109
- Koo DC, Kron RG. 1980. *Publ. Astron. Soc. Pac.* 545:537
- Kuchinski LE, Freedman WL, Madou BF, Trewheella M, Bohlin RC, et al. 2000. *Ap. J. Suppl.* 131:441
- Kuchinski LE, Madore BF, Freedman WL, Trewheella M. 2001. *Astron. J.* 122:729
- Kudritzki RP, Mendez RH, Feldmeier JJ, Ciardulo R, Jacoby GH, et al. 2000. *Ap. J.* 536:19
- Lacy M, Miley G, Rawlings S, Sauders R, Dickinson M, et al. 1994. *MNRAS* 271:504
- Lanzetta KM, Wolfe AM, Turnshek DA, Lu L, McMahon RG, Hazard C. 1991. *Ap. J. Suppl.* 77:1
- Lanzetta KM, Yahata N, Pascarelle S, Chen H-W, Fernandez-Soto A. 2002. *Ap. J.* 570:492
- Lanzetta KM, Yahil A, Fernandez-Soto A. 1998. *Astron. J.* 116:1066
- Le Fèvre O, Hudon D, Lilly SJ, Crampton D, Hammer F, Tresse L. 1996. *Ap. J.* 461:534
- Lehnert MD, Heckman TM. 1996. *Ap. J.* 472:546
- Leitherer C, Ferguson HC, Heckman TM, Lowenthal JD. 1995. *Ap. J.* 454:19
- Leitherer C, Heckman TM. 1995. *Ap. J. Suppl.* 96:9
- Leitherer C, Vacca W, William D, Conti PS, Filippenko AV, et al. 1996. *Ap. J.* 465:717
- Lilly SJ. 1988. *Ap. J.* 333:161
- Lilly SJ, Cowie LL, Gardner JP. 1991. *Ap. J.* 369:79
- Lilly SJ, Eales SA, Gear WKP, Hammers F, Le Fèvre O, et al. 1999. *Ap. J.* 518:641
- Lilly SJ, Le Fèvre O, Hammer F, Crampton D. 1996. *Ap. J.* 460:1
- Lilly SJ, Schade D, Ellis R, Le Fèvre O, Brinchmann J, et al. 1998. *Ap. J.* 500:75
- Lilly SJ, Tresse L, Hammer F, Crampton D, Le Fèvre O. 1995. *Ap. J.* 455:108
- Lowenthal JD, Hogan CJ, Leach RW, Schmidt GD, Foltz CB. 1990. *Ap. J.* 357:3
- Lowenthal JD, Koo DC, Guzman R, Gallego J, Phillips AC, et al. 1997. *Ap. J.* 481:673
- Macchetto F, Lipari S, Giavalisco M, Turnshek D, Sparks WB. 1993. *Ap. J.* 404:51
- Madau P. 1995. *Ap. J.* 441:18
- Madau P, Ferguson HC, Dickinson ME, Giavalisco M, Steidel CC, Fruchter A. 1996. *MNRAS* 283:1388
- Madau P, Pozzetti L, Dickinson M. 1998. *Ap. J.* 498:106
- Malhotra S, Rhoads J. 2002. *Ap. J.* 565:71
- Marcum PM, O'Connell RW, Fanelli MN, Cornett RH, Waller WH, et al. 2001. *Ap. J. Suppl.* 132:129
- Matarrese S, Coles P, Lucchin F, Moscardini L. 1997. *MNRAS* 286:115
- McCarthy PJ. 1991. *Astron. J.* 102:518
- McCarthy PJ. 1993. *Annu. Rev. Astron. Astrophys.* 31:639
- McCarthy PJ, Carlberg RG, Chen HW, Marzke RO, Firth AE, et al. 2001. *Ap. J.* 560:131
- McCarthy PJ, Kapahi VK, van Breugel W, Subrahmanya CR. 1990. *Astron. J.* 100:1014

- McCarthy PJ, Persson SE, West SC. 1992. 386:52
- McCarthy PJ, van Breugel W, Kapahi VK, Subrahmanya CR. 1991. *Astron. J.* 102:522
- McGaugh SS. 1991. *Ap. J.* 380:140
- McKay TA, Sheldon ES, Racusin J, Fischer P, Seljak V, et al. 2002. *Ap. J.* In press. astro-ph/0108013
- Meier DL. 1976a. *Ap. J.* 207:343
- Meier DL. 1976b. *Ap. J.* 203:103
- Meier DL, Terlevich R. 1981. *Ap. J.* 246:L109
- Meurer GR, Heckman TM, Calzetti D. 1999. *Ap. J.* 521:64
- Meurer GR, Heckman TM, Lehnert MD, Leitherer C, Lowenthal J. 1997. *Astron. J.* 114:54
- Meurer GR, Heckman TM, Leitherer C, Kinney AL, Robert C, Garnett DR. 1995. *Astron. J.* 110:2665
- Miley G, Chambers KC, van Breugel W, Macchetto F. 1992. *Ap. J.* 401:69
- Mo HJ, Fukugita M. 1996. *Ap. J.* 467:L9
- Mo HJ, White SDM. 1996. *MNRAS* 282:347
- Moller P, Warren S. 1993. *Astron. Astrophys.* 270:43
- Moorwood AFM, van der Werf PP, Cuby JG, Oliva E. 2000. *Astron. Astrophys.* 362:9
- Moustakas LA, Somerville RS. 2002. *Ap. J.* In press. astro-ph/0110584
- Neufeld DA. 1991. *Ap. J.* 370:85
- Oke JB, Cohen JG, Carr M, Cromez J, Dinzgizian A, et al. 1995. *Publ. Astron. Soc. Pac.* 107:3750
- Oke JB, Gunn JE. 1983. *Ap. J.* 266:713
- Ouchi M, Shimasaku K, Akamura S, Doi M, Fuzusawa H, et al. 2001. *Ap. J.* 558:83
- Pagel BEJ. 1986. *Publ. Astron. Soc. Pac.* 98:1009
- Pahre MA, Djorgovski GS. 1995. *Ap. J.* 449:1
- Papovich C, Dickinson M, Ferguson HC. 2001. *Ap. J.* 559:620
- Partridge RB. 1974. *Ap. J.* 192:241
- Partridge RB, Peebles PJE. 1967a. *Ap. J.* 148:377
- Partridge RB, Peebles PJE. 1967b. *Ap. J.* 147:868
- Pascarelle SM, Windhorst RA, Driver SP, Ostrander EJ, Keel WC. 1996a. *Ap. J.* 456:21
- Pascarelle SM, Windhorst RA, Keel WC. 1998. *Astron. J.* 116:2659
- Pascarelle SM, Windhorst RA, Keel WC, Odewan SC. 1996b. *Nature* 383:45
- Peacock JA. 1997. *MNRAS* 284:885
- Peacock JA, Cole S, Norberg P, Baugh CM, Bland-Hawthorn J, et al. 2001. *Nature* 410:169
- Peacock JA, Rowan-Robinson M, Blain AW, Dunlop JS, Efstathiou A, et al. 2000. *MNRAS* 318:535
- Peebles PJE. 1971. *Physical Cosmology*. Princeton: Princeton Univ. Press
- Peebles PJE. 1980. *The Large-Scale Structure of the Universe*. Princeton: Princeton Univ. Press
- Pentericci L, Kurk JD, Röttgering HJ, Miley GK, van Breugel W, et al. 2000. *Astron. Astrophys.* 361:25
- Persic M, Salucci P. 1992. *MNRAS* 258:14
- Pettini M, Kellogg M, Steidel CC, Dickinson M, Adelberger KL, Giavalisco M. 1998. *Ap. J.* 508:539
- Pettini M, Lipman K. 1995. *Astron. Astrophys.* 297:63
- Pettini M, Rix SA, Steidel CC, Adelberger KL, Hunt MP, Shapley A. 2002. *Ap. J.* 569:742
- Pettini M, Shapley AE, Steidel CC, Cuby J-G, Dickinson M, et al. 2001. *Ap. J.* 554:981
- Pettini M, Steidel CC, Adelberger KL, Dickinson M, Giavalisco M. 2000. *Ap. J.* 528:96
- Pisano DJ, Kobulnicky HA, Guzman R, Gallego J, Bershady MA. 2001. *Astron. J.* 122:1194
- Porciani C, Giavalisco M. 2002. *Ap. J.* 565:24
- Pozzetti L, Madau P, Zamorani G, Ferguson HC, Bruzual GA. 1998. *MNRAS* 298:1133
- Press WH, Schechter P. 1974. *Ap. J.* 187:425
- Pritchett CJ, Hartwick FDA. 1990. *Ap. J.* 355:11
- Puget J-L, Abergel A, Bernard J-P, Boulanger F, Burton WB, et al. 1996. *Astron. Astrophys.* 308:5
- Quirk WJ, Tinsley BM. 1973. *Ap. J.* 179:69
- Rawlings S, Eales S, Warren S. 1990. *MNRAS* 243:14
- Renzini A. 1998. *Astron. J.* 115:2459
- Renzini A. 1999. *Ap. Space Sci.* 267:357

- Rhoads JE, Malhotra S. 2001. *Ap. J.* 563:L5
- Rhoads JE, Malhotra S, Dey A, Stern D, Spinrad H, Jannuzi BT. 2000. *Ap. J.* 545:L85
- Salpeter EE. 1995. *The Physics of the Interstellar Medium and Intergalactic Medium, ASP Conf. Ser.*, ed. A Ferrara, CF McKee, PR Shapiro, 80:264. San Francisco: Publ. Astron. Soc. Pac.
- Sandage A, Freeman KC, Stokes NR. 1970. *Ap. J.* 160:831
- Sanders DB, Mirabel IF. 1996. *Annu. Rev. Astron. Astrophys.* 34:749
- Sargent WLW, Young PJ, Boksemberg A, Tytler D. 1980. *Ap. J. Suppl.* 42:41
- Sawicki M. 2001. *Astron. J.* 121:240
- Sawicki M, Yee HKC. 1998. *Astron. J.* 115:1329
- Schade D, Lilly SJ, Crampton D, Ellis R, Le Fèvre O, et al. 1999. *Ap. J.* 525:31
- Schade D, Lilly SJ, Crampton D, Hammer F, Le Fèvre O, Tresse L. 1995. *Ap. J.* 451:L1
- Schechter P. 1976. *Ap. J.* 203:297
- Schechter PL, Dressler A. 1987. *Astron. J.* 94:563
- Schlegel D, Finkbeiner D, Davis M. 1998. *Ap. J.* 500:525
- Schneider D, Gunn J, Turner E, Lawrence C, Hewitt J, et al. 1986. *Astron. J.* 91:991
- Scott D, Lagache G, Borys C, Chapman SC, Halpern M, et al. 2000. *Astron. Astrophys.* 357:5
- Sellgren K. 1984. *Ap. J.* 277:623
- Shapley AE, Steidel CC, Adelberger KL, Dickinson M, Giavalisco M, Pettini M. 2001. *Ap. J.* 562:95
- Smail I, Ivison RJ, Blain AW. 1997. *Ap. J.* 490:5
- Smail I, Ivison RJ, Blain AW, Kneib JP. 1998. *Ap. J.* 507:21
- Smail I, Ivison RJ, Kneib JP, Cowie LL, Blain AW, et al. 1999. *MNRAS* 308:1061
- Smail I, Ivison RJ, Owen FN, Blain AW, Kneib JP. 2000. *Ap. J.* 528:612
- Smith DR, Bernstein GM, Fischer P, Jarvis M. 2001. *Ap. J.* 551:643
- Smith HE, Cohen RD, Burns JE, Moore DJ, Uchida BA. 1989. *Ap. J.* 347:87
- Sofue Y, Rubin V. 2001. *Annu. Rev. Astron. Astrophys.* 39:137
- Somerville RS, Lemson G, Kolatt TS, Dekel A. 2000. *MNRAS* 316:479
- Somerville RS, Primack JR, Faber SM. 2001. *MNRAS* 320:504
- Spinrad H. 1989. In *The Epoch of Galaxy Formation, ASI Ser. C*, 264:39. Dordrecht: Kluwer
- Spinrad H, Dey A, Graham JR. 1995. *Ap. J.* 438:51
- Spinrad H, Dey A, Stern D, Bunker A. 1999. In *The Most Distant Galaxies*, ed. HJA Rottgering, PN Best, MD Lehnert, p. 257. Amsterdam: Neth. R. Acad. Arts Sci.
- Spinrad H, Djorgovski S. 1984a. *Ap. J.* 285:49
- Spinrad H, Djorgovski S. 1984b. *Publ. Astron. Soc. Pac.* 96:795
- Spinrad H, Filippenko AV, Wyckoff S, Stocke JT, Wagner MR, Lawrie DG. 1985. *Ap. J.* 299:L7
- Spinrad H, Stern D, Bunker A, Dey A, Lanzetta K, et al. 1998. *Astron. J.* 116:2617
- Steidel CC, Adelberger KL, Dickinson ME, Giavalisco M, Pettini M, Kellogg M. 1998. *Ap. J.* 492:428
- Steidel CC, Adelberger KL, Giavalisco M, Dickinson ME, Pettini M. 1999. *Ap. J.* 519:1
- Steidel CC, Adelberger KL, Shapley AE, Pettini M, Dickinson M, Giavalisco M. 2000. *Ap. J.* 532:170
- Steidel CC, Dickinson M, Persson SE. 1994. *Ap. J.* 437:75
- Steidel CC, Dickinson M, Sargent WLW. 1991. *Astron. J.* 101:1187
- Steidel CC, Giavalisco M, Dickinson M, Adelberger KL. 1996a. *Astron. J.* 112:352
- Steidel CC, Giavalisco M, Pettini M, Dickinson M, Adelberger K. 1996b. *Ap. J.* 462:17
- Steidel CC, Hamilton D. 1992. *Astron. J.* 104:941
- Steidel CC, Hamilton D. 1993. *Astron. J.* 105:2017
- Steidel CC, Pettini M, Adelberger KL. 2001. *Ap. J.* 546:665
- Steidel CC, Pettini M, Hamilton D. 1995. *Astron. J.* 110:2519
- Stern D, Spinrad H. 1999. *Publ. Astron. Soc. Pac.* 111:1475
- Stiavelli M, Scarlatta C, Panagia N, Treu T,

- Bertin G, Bertola F. 2001. *Ap. J.* 561: 37
- Sullivan M, Treyer M, Ellis RS, Bridges TJ, Milliard B, Donas J. 2000. *MNRAS* 312:442
- Tegmark M, Zaldarriaga M. 2000. *Ap. J.* 544:30
- Teplitz HI, Malkan MA, Steidel CC, McLean IS, Becklin EE, et al. 2000a. *Ap. J.* 542:18
- Teplitz HI, McLean IS, Becklin EE, Figer DF, Gilbert AM, et al. 2000b. *Ap. J.* 533:65
- Teplitz HI, Malkan MA, McLean IS. 1999. *Ap. J.* 514:33
- Teplitz HI, Malkan MA, McLean IS. 1998. *Ap. J.* 506:519
- Thommes E, Meisenheimer K, Fockenbrock R, Hippelein H, Roeser H-J, Beckwith S. 1998. *MNRAS* 293:L6
- Thompson D, Djorgovski SG. 1995. *Astron. J.* 110:982
- Thompson D, Djorgovski S, Beckwith SV. 1994. *Astron. J.* 107:1
- Thompson D, Djorgovski SG, Trauger J. 1995. *Astron. J.* 110:963
- Thompson D, Mannucci F, Beckwith SV. 1996. *Astron. J.* 112:1794
- Tinsley BM. 1972a. *Ap. J.* 178:319
- Tinsley BM. 1972b. *Astron. Astrophys.* 20:383
- Tinsley BM. 1973a. *Ap. J.* 186:35
- Tinsley BM. 1973b. *Astron. Astrophys.* 24:89
- Tinsley BM, Gunn JE. 1976. *Ap. J.* 302:52
- Trager SC, Faber SM, Dressler A, Oemler A. 1997. *Ap. J.* 485:92
- Tremonti CA, Calzetti D, Leitherer C, Heckman TM. 2001. *Ap. J.* 555:322
- Tresse L, Maddox SJ. 1998. *Ap. J.* 495:691
- Turner M. 2001. *Publ. Astron. Soc. Pac.* 113: 653
- Turnshek DA, Wolfe AM, Lanzetta KM, Briggs FH, Cohen RD, et al. 1989. *Ap. J.* 344:567
- Tyson JA. 1988. *Ap. J.* 96:1
- Van Breugel W, De Breuck C, Stanford SA, Stern D, Rottgering H, Miley G. 1999. *Ap. J.* 518:61
- van der Werf PP, Kraiberg Knudsen K, Labbe I, Franx M. 2002. In *The Far-Infrared and Submillimeter Spectral Energy Distribution of Active and Starburst Galaxies*, ed. P Barthel, B Wilkes, I Van Bemmel. Amsterdam: Elsevier. In press
- Walborn NR, Lennon DJ, Haser SM, Kudritzki RP, Voles SA. 1995. *Publ. Astron. Soc. Pac.* 107:104
- Warren SJ, Moller P. 1996. *Astron. Astrophys.* 311:25
- Wechsler RH, Somerville RS, Bullock JS, Kollatt TS, Primack JR, et al. 2001. *Ap. J.* 554:85
- Weedman DW. 1983. *Ap. J.* 266:479
- Weymann RJ, Stern D, Bunker A, Spinrad H, Chaffee FH, et al. 1998. *Ap. J.* 505:95
- White SM, Rees MJ. 1978. *MNRAS* 183:341
- Wilkinson MI, Evans NW. 1999. *MNRAS* 310:645
- Williams RE, Blacker B, Dickinson M, Dixon W, Ferguson HC, et al. 1996. *Astron. J.* 112: 1335
- Williams RE, Baum S, Bergeron L, Bernstein N, Blacker B, et al. 2000. *Astron. J.* 120:2735
- Wilson G, Kaiser N, Luppino G. 2001a. *Ap. J.* 556:601
- Wilson G, Kaiser N, Luppino G, Cowie LL. 2001b. *Ap. J.* 555:572
- Windhorst R, Burstein D, Mathis DF, Neuschaefer LW, Bertola F, et al. 1991. *Ap. J.* 380:362
- Windhorst R, Mathis DF, Keel WC. 1992. *Ap. J.* 400:1
- Wolfe AM. 1989. *NATO Adv. Res. Workshop, ASI Ser. C* 264:101. Dordrecht: Kluwer
- Wolfe AM, Lanzetta KM, Turnshek DA, Oke JB. 1992. *Ap. J.* 385:151
- Wolfe AM, Prochaska JX. 2000a. *Ap. J.* 545: 603
- Wolfe AM, Prochaska JX. 2000b. *Ap. J.* 545: 591
- Wolfe AM, Turnshek DA, Lanzetta KM, Lu L. 1993. *Ap. J.* 404:480
- Wolfe AM, Turnshek DA, Smith HE, Cohen RD. 1986. *Ap. J. Suppl.* 61:249
- Wyse RFG, Gilmore G, Franz M. 1997. *Annu. Rev. Astron. Astrophys.* 35:637
- Young PJ, Sargent WLW, Boksemberg A. 1982. *Ap. J. Suppl.* 48:455
- Zaritsky D, White SDM. 1994. *Ap. J.* 435:599

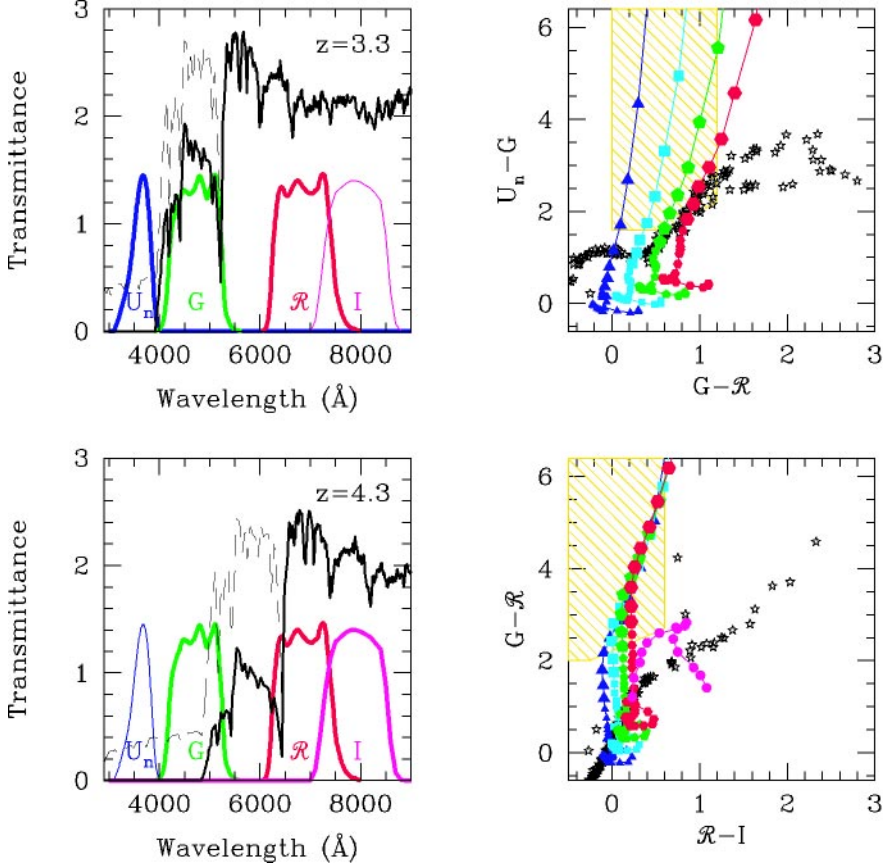


Figure 1 The idea behind the Lyman-break technique. Star-forming galaxies at high redshifts are identified by the colors of the spectral region around the 912 \AA continuum discontinuity obtained through a suitable set of filters (shown here is the U_nGRI set used for the ground-based survey). Redshifted synthetic model spectra of continuous star formation (Bruzual & Charlot 1993), which include the effects of cosmic opacity (Madau 1995), are plotted together with the filters' transmittance (*left panels*). The two upper panels show the U -band dropouts at $z \sim 3$, defined with the U_nGR filters; the lower ones the G -band dropouts at $z \sim 4$, defined through the GRI set. The candidates are selected from their position in the color-color space, as shown in the right panels. The curves represent galaxies placed at progressively higher redshifts, starting at $z = 0.5$ with step $\Delta z = 0.1$. The case of continuous star formation is used, and the four tracks correspond to different amounts of dust obscuration, namely $E(B - V) = 0$, i.e., no dust (*triangles*); $E(B - V) = 0.15$ (*squares*); $E(B - V) = 0.3$ (*pentagons*); $E(B - V) = 0.45$ (*hexagons*). In all cases, the starburst attenuation law by Calzetti et al. (1997) is used. Larger symbols denote the two redshift intervals $2.6 < z < 3.5$ and $3.8 < z < 5$. The locus of stellar colors is also shown. The shaded areas correspond to Equation 3.2 and 3.3, respectively.

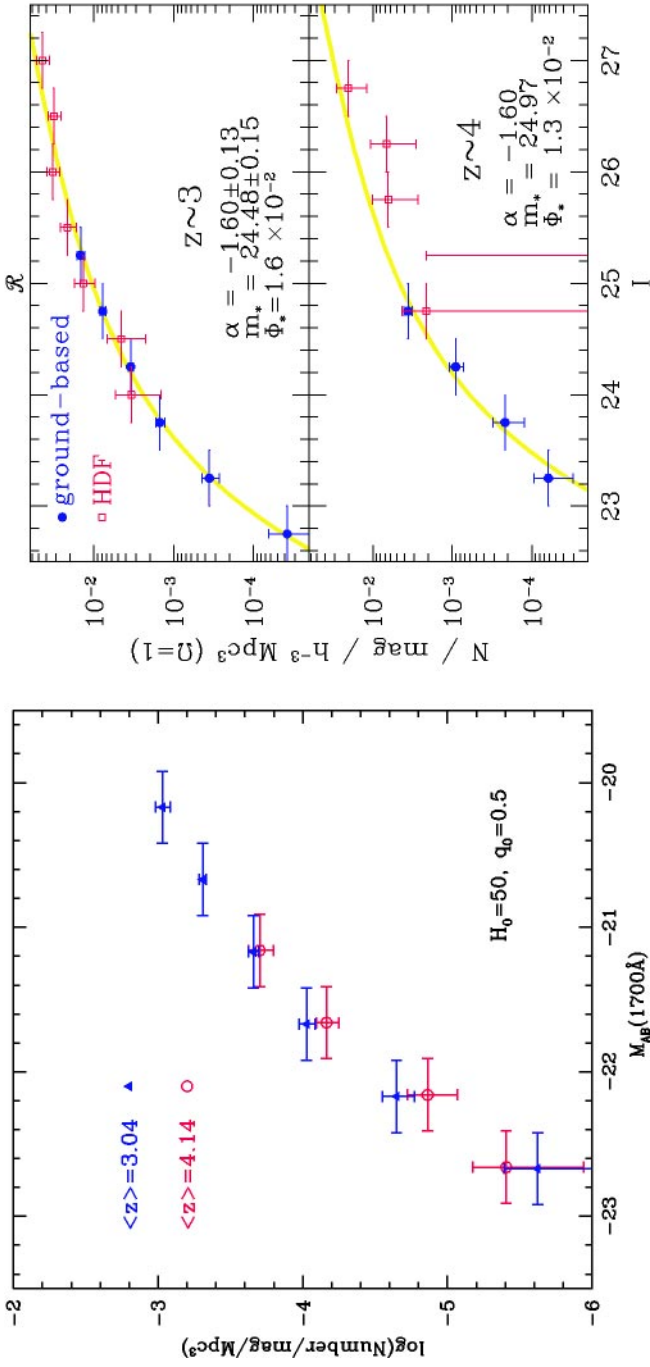


Figure 3 The luminosity function of U -band (*upper panel*) and G -band dropouts (*lower panel*). Because of the relatively narrow range of luminosity distance spanned by the samples of LBGs, apparent magnitudes can be used as proxy of absolute ones. The data points, which range over 4.5 magnitudes, are derived from the ground-based and HDF surveys, as indicated in the figure. For the U -band dropouts the figure also shows the best Schechter-function fit to the data and its parameters. At $z \sim 4$ the data are not good enough for a fit, and in this case the $z \sim 3$ best-fit luminosity function has been “redshifted” and overimposed to the data (see text for the procedure). The apparent shallower low-luminosity end is very likely the effect of cosmic variance fluctuations in the small HDF sample. In fact, the comparison shows no significant evidence of evolution in the luminosity function of Lyman-break galaxies between $z \sim 3$ and $z \sim 4$ (reproduced from Steidel et al. 1999).

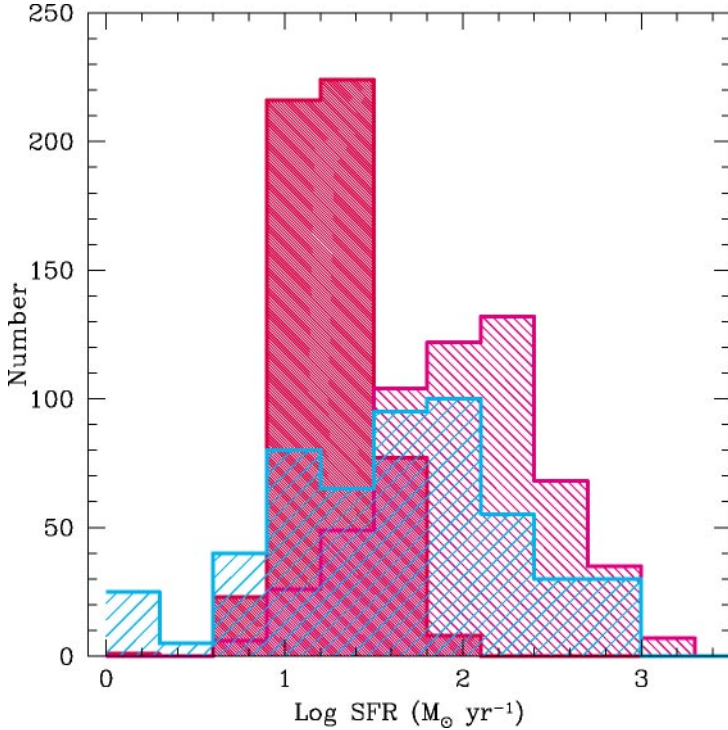


Figure 6 Distributions of the star formation rates of U -band dropouts from both the ground-based and HDF surveys normalized on arbitrary scales. The dark-shaded histogram shows the rates calculated from the UV luminosity without any correction for dust obscuration. The medium-shaded histogram shows the rates corrected for dust obscuration assuming a continuous star formation with age $T = 0.1$ Gyr as the underlying spectral energy distribution and the starburst obscuration law with the value of $E(B - V)$ determined by comparing the observed colors with the predicted ones. The light-shaded histogram shows the rates derived from the fitting procedures by Papovich, Dickinson & Ferguson (2001) and Shapley et al. (2001), as described in the text. In all cases the Madau’s (1995) cosmic opacity was used in the calculation. There is broad agreement between the two techniques. Note that the corrected rates are distributed over three orders of magnitude, including galaxies that form stars as slowly as the Milky Way or as rapidly as required to put together the stellar mass of an L^* galaxy in 1 Gyr or less.

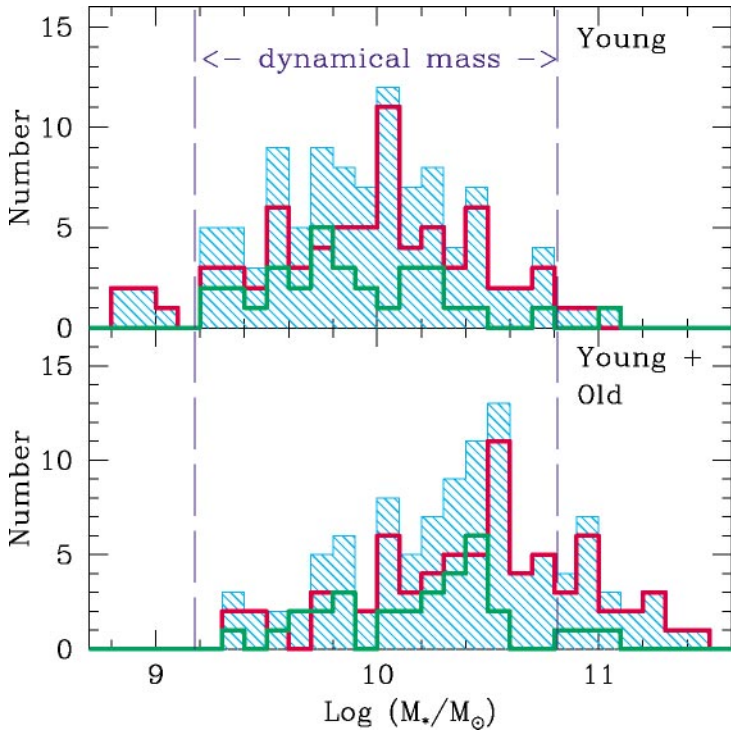


Figure 9 (Top) Histogram of the fits of stellar mass of LBGs. The dark gray curve is the ground-based sample, the light gray curve the HDF, while the shaded histogram is the sum of the two. (Bottom) Histogram of the sum of the young stellar mass plus the old one (see text) with the same coding as above. The 2-population fit has only been done for the HDF sample; for the ground-based sample the mass of the old population has been taken equal to 4 times that of the young population, the average value found in the HDF. Also shown is the range of values of dynamical mass derived from the kinematics of the optical nebular emission lines (see text).

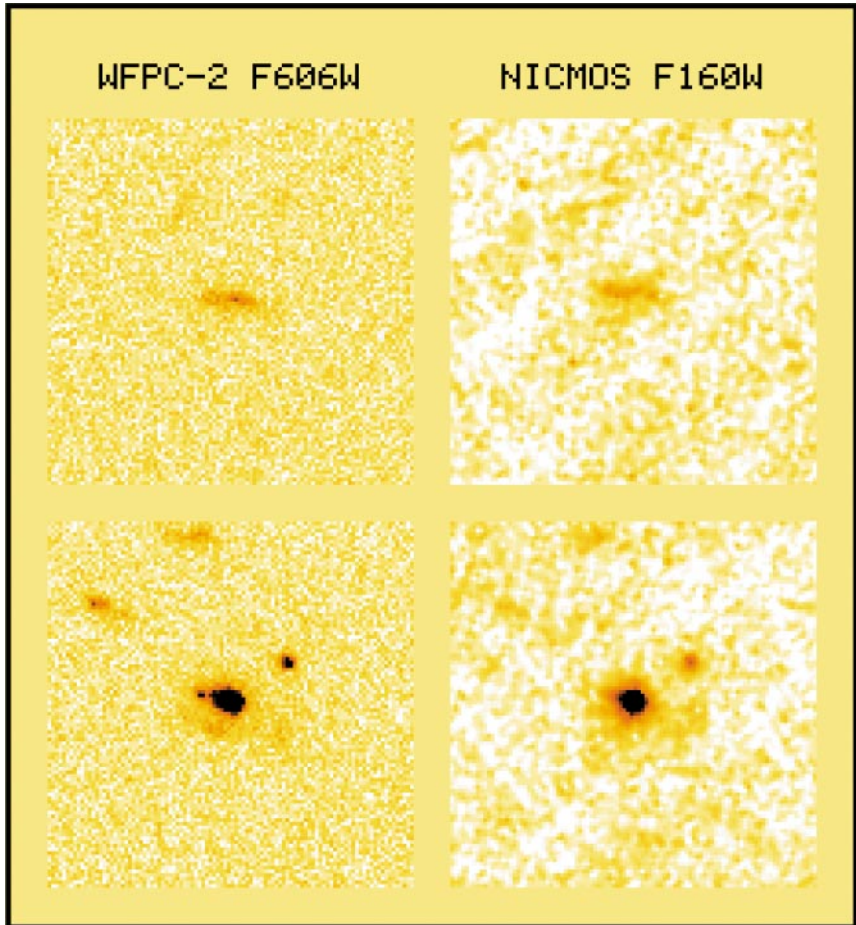


Figure 10 Two examples of regular morphology encountered among LBGs of the ground-based sample observed with *HST*. In each case the left panel shows optical images taken with WFPC2 in the F702W filter, corresponding roughly to the rest-frame UV at $\lambda = 1700 \text{ \AA}$; the right panel shows near-IR images in the *H* band (F160W) taken with NICMOS, and corresponding to rest-frame $\lambda = 4000 \text{ \AA}$. (*Top*) A disk-like galaxy at $z = 3.23$ with $R = 25.2$. (*Bottom*) A spheroid-like galaxy, with an $r^{1/4}$ profile and relatively compact and regular morphology, at $z = 2.96$ with $R = 22.8$. Note that the morphology is essentially independent on the wavelength.

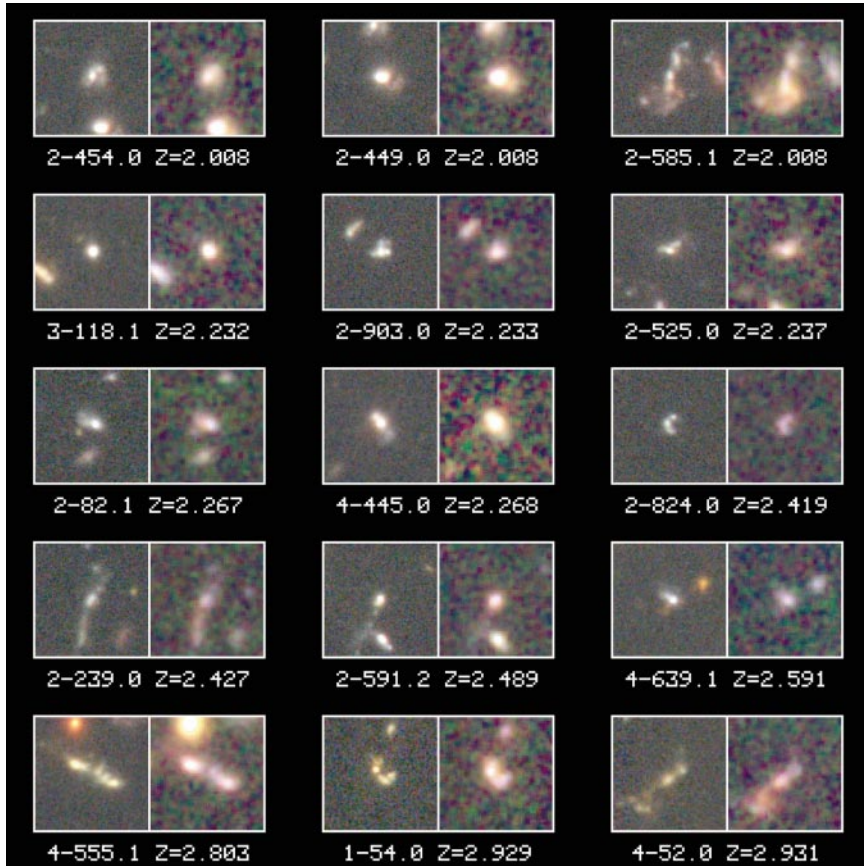


Figure 11 *HST* images of LBGs from the HDF sample. On the left of each panel is an optical *BVI* (F450W, F606W and F814W) color image observed with WFPC2, while on the right there is the corresponding near-IR *IJH* (F814W, F125W and F160W) taken with NICMOS. Note that in almost all cases the morphology is independent on wavelength. Also note that no Hubble types can be recognized in these images, which, on the other hand, show a remarkable variety, from small compact and relatively regular objects to highly fragmented, diffuse and irregular ones (reproduced from Dickinson 1998).

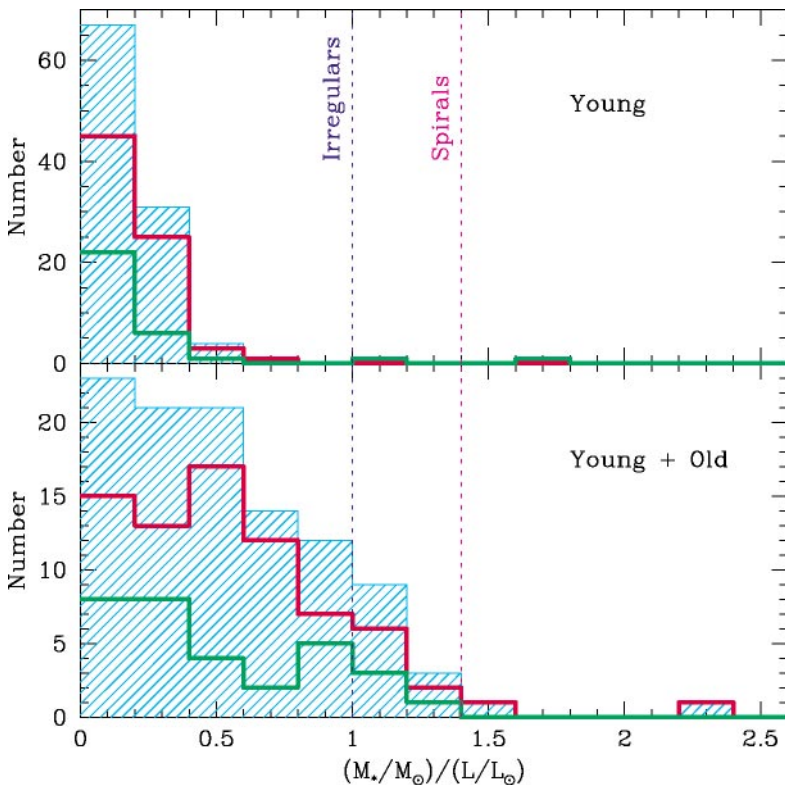


Figure 12 Histogram of the stellar mass-to-light ratio (rest-frame B band) of LBGs derived from the fitting procedure described in the text. The green histogram represents the ground-based sample, the red histogram the HDF one, and the shaded histogram the sum of the two samples. Also plot is the typical value for Irregular and Spiral galaxies from Fukugita, Hogan & Peebles (1998). Note the LBGs have smaller stellar mass-to-light ratio than local late type galaxies.

Copyright of *Annual Review of Astronomy & Astrophysics* is the property of Annual Reviews Inc. and its content may not be copied or emailed to multiple sites or posted to a listserv without the copyright holder's express written permission. However, users may print, download, or email articles for individual use.